

BIOSYNTHESIS OF BENZOATE-DERIVED BIPHENYL PHYTOALEXINS IN CELL CULTURES OF *Pyrus pyrifolia*

Ph.D THESIS

by

SHASHANK SAGAR SAINI



**DEPARTMENT OF BIOTECHNOLOGY
INDIAN INSTITUTE OF TECHNOLOGY, ROORKEE
ROORKEE-247667, INDIA
SEPTEMBER, 2017**

BIOSYNTHESIS OF BENZOATE-DERIVED BIPHENYL PHYTOALEXINS IN CELL CULTURES OF *Pyrus pyrifolia*

A THESIS

*Submitted in partial fulfilment of the
requirements for the award of the degree*

of

DOCTOR OF PHILOSOPHY

In

BIOTECHNOLOGY

by

SHASHANK SAGAR SAINI



**DEPARTMENT OF BIOTECHNOLOGY
INDIAN INSTITUTE OF TECHNOLOGY, ROORKEE
ROORKEE-247667, INDIA
SEPTEMBER, 2017**



**©INDIAN INSTITUTE OF TECHNOLOGY ROORKEE, ROORKEE- 2017
ALL RIGHTS RESERVED**



ABSTRACT

Pear is an important fruit crop, known for its beautiful texture and high nutritional value. In comparison to European pears (*Pyrus communis*), Asian pears (*Pyrus pyrifolia*) exhibit higher ontogenic resistance, thereby they are less susceptible to the scab disease caused by the fungus *Venturia pirina*. To date, the scab-resistance mechanisms in pear are not well understood. The present study investigates the comparative basal metabolomics profile of immature and mature healthy leaves of *P. pyrifolia* and *P. communis* with aim to identify defense responsive metabolites in these two plant groups. Gas chromatography–mass spectrometry (GC-MS) coupled with multivariate analysis were applied to analyze the metabolite profiles in both the pear species between immature and mature leaves. Using non-targeted comparative metabolomics a total of 30 differentially accumulating metabolites were identified in both the pear species, out of which phenolic accumulation were significantly higher in *P. pyrifolia* leaves.

Benzoic acid is an important plant natural product which serves as precursor for biosynthesis of an array of the other economically important secondary metabolites. In pears, benzoic acid serves as the precursor for biphenyl biosynthesis, which serves as defense metabolite protecting against pathogen infection. Till date, the biosynthesis of benzoic acid is poorly understood in pears. Therefore this thesis further aims at exploring the enzymatic route of benzoic acid formation in cell cultures of Asian pear (*P. pyrifolia*). Pear cell cultures responded to yeast-extract elicitor treatment by producing two biphenyls, the aucuparin and the noraucuparin. Cell free extract / partially purified proteins prepared from these elicited cell cultures were used to elucidate the enzymatic route of benzoic acid formation. A novel C₂-chain cleavage enzyme, benzaldehyde synthase (BS), has been detected and characterized first time from these cell cultures. BS catalyzed the formation of benzaldehyde from cinnamic acid. The next step of the biosynthetic pathway was catalyzed by a NAD⁺-dependent benzaldehyde dehydrogenase (BD) which catalyzed the conversion of benzaldehyde into benzoic acid. The next step was detection and characterization of benzoate-CoA-ligase (BZL) activity catalyzing conversion of benzoic acid into benzoyl-CoA. Finally benzoyl-CoA enters into the biphenyl biosynthesis using biphenyl synthase (BIS) enzyme. The properties of BS, BD and BZL were biochemically characterized. Upon YE treatment BS, BD, BZL and BIS activities were coordinately induced. In conclusion, biosynthesis of benzoic acid in elicited cell cultures of *P. pyrifolia* was found to proceed *via* CoA-independent and non- β -oxidative route.

Keywords: Asian pear; benzaldehyde synthase; benzaldehyde dehydrogenase; benzoate-CoA ligase; cell culture; metabolomics; *Pyrus communis*; *Pyrus pyrifolia*.

Acknowledgements

Thanks to Braham Swarup Almighty, the creator of universe and source of all knowledge for his divine sanction on me and allowing me to see immensity in his creatures.

I take immense pleasure in expressing my deep sense of gratitude to my supervisor and mentor **Dr. Debabrata Sircar** for giving me the opportunity to join his research laboratory. His trust in me and constant supervision has been a constant source of positive energy for me. He has patiently listened and accordingly supervised and supported me throughout my Ph.D. His enthusiasm and profound concern for my success has made this journey a joyous one. It has been a great privilege and honour to work and study under his precious guidance. His sincerity, dynamism, vision and motivation deeply inspired me to learn new things. Along with academic support his affectionate behaviour and moral support also helped me through the rough road to finish my thesis. I express my wholehearted indebtedness to him.

I would also like to express my profound gratitude to **Prof. Partha Roy**, Head of Department of Biotechnology for providing the basic infrastructural facilities in the department that allowed me to successfully complete my Ph.D. I'm thankful to him for giving me access to his laboratory instrumentation. His punctuality and sense of duty have been a source of motivation. His expert advices and jovial nature have encouraged me all along the path to success.

Besides, I would like to thank the Department of Biotechnology, and Institute Instrumentation Centre (IIC), IIT Roorkee for instrument facilities to carry out the research work. I am also grateful to my SRC committee members: **Dr. Bijan Choudhury, Dr. Paravindar Kumar and Dr. P. Gopinath**; DRC chairman: **Prof. Vikas Pruthi** for their continuous advice and kind support.

I also express my sincere gratitude towards **Dr. Harsh Chauhan** and **Dr. Sri Ram Yadav** for their kind and valuable suggestions and other faculty members of Department of Biotechnology during my PhD.

My warmest thanks to my colleagues in my lab and in my department who made this study a successful experience. I especially thank Ms. Deepa Teotia for her timeless support and constructive ideas. I was lucky to work with a kind and helpful colleague Mr. Amol Sarkate.

I am thankful to Ms. Kriti Juneja, Mr. Ashwani Kumar, Mr. Mukund Kumar, Ms. Varsha Tomar, Mr. Bhairavnath Waghmode and Ms. Komal Kushwaha for the pleasant working environment and companionship during laboratory works.

I am also thankful to the office staff, Department of Biotechnology especially Mr. Veadpal Saini for their kind help and support, campus administration and workers team of my hostel, Azad Bhawan, their hard work made my stay comfortable in campus.

A special note of thanks to my friends in IIT Roorkee namely Mr. Yogesh Sariya, Mr. Vijay Sharma, Mr. Ragvender Singh, Mr. Somesh Baneerjee, Mr. Swapneel Jaiswal, Mr. Sunil Sharma and Mr. Harvijay Singh for their encouragement, support and giving unforgettable moments during my stay in IIT and in my life.

I would also like to express my deep gratitude to Mrs. Rakhi Sircar and two little angels Ishika and Annie for their moral support, kind blessings and for letting me feel like home during my stay in IIT Roorkee.

Finally, my sincere thanks to my Father, Mother and Brother for standing with me in every situation of my life. Special thanks to my Father for teaching and integrating spirituality in my life style and to teach me for being calm in every situation of life.

Shashank Sagar Saini

LIST OF ABBREVIATIONS

ATP	Adenosine triphosphate
AlCl ₃	Aluminum chloride
AOX	Alternate oxidase
BA	Benzoate or benzoic acid
BD	Benzaldehyde dehydrogenase
BS	Benzaldehyde synthase
BIS	Biphenyl synthase
BZL	Benzoate-CoA-ligase
CoA	Coenzyme A
C4H	Cinnamate -4-hydroxylase
4CL	4-Coumarate CoA-ligase
CNL	Cinnamate CoA-ligase
CHD	Cinnamic acid CoA- hydratase / dehydrogenase
CHY	3-hydroxyisobutyryl CoA- hydrolase
DMSO	Dimethyl sulfoxide
2,4-D	2,4-Dichlorophenoxyacetic acid
DTT	Dithiothreitol
ESI-MS	Electro-spray-ionization mass spectrometry
E	Elicited
EDTA	Ethylene di amine tetra acetic acid
FAD	Flavin adenine dinucleotide
FMN	Flavin mononucleotide
F3H	Flavanone-3-hydroxylase
GC-MS	Gas chromatography- mass spectrometry
HBD	4-Hydroxybenzaldehyde dehydrogenase
HBS	4-Hydroxybenzaldehyde synthase
HPLC	High-performance liquid chromatography
HBA	Hydroxybenzoate or hydroxybenzoic acid
HCHL	Hydroxycinnamoyl-CoA hydratase/lyase
4-HBA	4-Hydroxybenzoic acid
IFS	Isoflavone synthase

LIST OF ABBREVIATIONS

IAA	Indole-3-acetic acid
KAT	3-ketoacyl thiolase
L	Line
MeOH	Methanol
MEOX	Methoxime
MeBA	Methyl-benzoate
MW	Molecular weight
MS	Murashige and Skoog
MDCA	3,4-methylenedioxy cinnamic acid
MSTFA	N-methyl-N-(trimethylsilyl) trifluoroacetamide
NAD	Nicotinamide adenine dinucleotide
NADP	Nicotinamide adenine dinucleotide phosphate
NE	Non-elicited
NaOH	Sodium hydroxide
PAL	Phenylalanine ammonia-lyase
PP	<i>Pyrus pyrifolia</i>
PC	<i>Pyrus communis</i>
PVPP	Polyvinyl poly pyrrolidone
PPIL	<i>Pyrus pyrifolia</i> immature leaves
PPML	<i>Pyrus pyrifolia</i> mature leaves
PCIL	<i>Pyrus communis</i> immature leaves
PCML	<i>Pyrus communis</i> mature leaves
PCR	Polymerase chain reaction
RT	Retention time
SAS	Salicylic aldehyde synthase
SDS	Sodium dodecyl sulfate
TIC	Total ion current
TMS	Tri-methyl-silylation
YE	Yeast-extract



CONTENTS

	Page No	
Title page	(i)	
Declaration	(iv)	
Certificate		
Abstract	(v)	
Acknowledgement	(vi-vii)	
List of Abbreviations	(viii-ix)	
Contents	(xi-xviii)	
List of Figures	(xix-xxii)	
List of Tables	(xxiii-xxv)	
Chapter 1	Introduction and Literature Review	1 - 31
	1.1: The Rosaceae family	1-2
	1.2: The sub-tribe Malinae of Rosaceae family	3-4
	1.3: The origin, distribution and taxonomy of pear (<i>Pyrus species</i>)	5 - 8
	1.4: The pear genome sequence	9-9
	1.5: The pear production	10-11
	1.6: The nutritional value of pears and its health benefits	11-12
	1.7: Bioactive metabolites from pear	12-13
	1.8: Major diseases of pear	13-16
	1.8.1: Pear scab disease	13-15
	1.8.2: Fire-blight disease of pear	15-16

1.9:	Metabolomics of pear: A new tool to understand plant's disease resistance mechanism	16-17
1.10:	Defense metabolites / phytoalexins of pear and other members of Malinae	17-20
1.10.1:	Pre-formed defense metabolites.	17-18
1.10.2:	Inducible defense metabolites of Maliane: the biphenyls and the dibenzofurans	19-20
1.11:	Biosynthesis of the biphenyl and the dibenzofuran	21-23
1.12:	Benzoic acid biosynthesis in plants	24-28
1.12.1:	CoA-dependent and β -oxidative route of benzoic acid biosynthesis	25-25
1.12.2:	CoA-dependent and non β -oxidative route of benzoic acid biosynthesis	26-26
1.12.3:	CoA-independent and non β -oxidative route of benzoic acid biosynthesis	26-28
1.13:	Benzoate-CoA ligase (BZL) activity	29-29
1.14:	Benzoic acid biosynthesis in Pear	29-30
1.15:	Understanding of benzoic acid biosynthesis in pear is important: Why?	30-31
1.16:	Aim of the work	31-31
1.17:	Objectives	31-31

Chapter 2

Materials and Methods 33-60

2.1:	Chemicals	33-35
2.1.1.1:	Chemicals used for callus induction and maintenance of suspension culture	33-33
2.1.1.2:	Metabolite standards	34-34
2.1.1.3:	Enzyme assay / purification	35-35

2.1.1.4: Elicitor used	35-35
2.2: Solvents & reagents	36-36
2.3: Reagents for GC-MS analysis	36-36
2.4: Equipments	37-37
2.5: Nutrient media for plant tissue culture	38-38
2.6: Buffers and solutions for enzyme assay	39-41
2.6.1: Buffer for enzyme extraction	39-39
2.6.2: Buffer used for enzyme assay	40-40
2.6.3: Reagents used for protein estimation	41-41
2.6.4: Solution for regeneration of PD ₁₀ column	41-41
2.7: Reagents and enzymes used for molecular biology	42-43
2.7.1: mRNA extraction, cDNA synthesis and real-time PCR reagents	42-42
2.7.2: Buffer for DNA gel electrophoresis	42-42
2.7.3: Primers for real-time PCR analysis	43-43
2.8: Plant material	43-43
2.9: Comparative metabolomics of leaves of <i>P. pyrifolia</i> and <i>P. communis</i> by GC-MS based metabolomics approach	44-49
2.9.1: Plant material and chemicals	44-44
2.9.2: Extraction and sample preparation for GC-MS analysis of polar metabolites	44-45
2.9.3: GC-MS analysis	45-45
2.9.4: Metabolite identification	45-46
2.9.5: Metabolite data pre-processing and statistical analysis	46-46
2.9.6: Quantitative real-time PCR	46-47
2.9.7: Estimation of total phenolics content (TPC)	48-48

2.9.8:	Estimation of total flavonoids content (TFC)	48-49
2.9.9:	Free radical scavenging activity (FRSA)	49-49
2.10:	Chemical synthesis of aucuparin and noraucuparin	49-50
2.11:	Callus induction and establishment of cell suspension cultures	50-50
2.12:	Elicitor treatment	50-51
2.13:	Extraction and HPLC analysis of phytoalexins	51-51
2.14:	Detection and characterization of benzaldehyde synthase (BS) activity from YE-treated cell suspension culture of <i>P. pyrifolia</i>	51-54
2.14.1:	Cell culture condition and elicitation	51-51
2.14.2:	Precursor feeding experiments	51-52
2.14.3:	Preparation of crude and partially purified enzyme extracts for benzaldehyde synthase (BS) assay	52-52
2.14.4:	Assay of benzaldehyde synthase (BS)	52-53
2.14.5:	Analysis of BS catalyzed reaction by HPLC-DAD and GC-MS	53-54
2.14.6:	Determination of kinetic parameters	54-54
2.15:	Detection and characterization of benzaldehyde dehydrogenase (BD) activity from YE-treated cell suspension culture of <i>P. pyrifolia</i>	54-57
2.15.1:	Cell culture condition and elicitation	54-54
2.15.2:	Precursor feeding experiments	54-55
2.15.3:	Preparation of cell-free extracts for benzaldehyde dehydrogenase (BD) assay	55-55
2.15.4:	Benzaldehyde dehydrogenase (BD) assay	55-56

2.15.5:	Analysis of BD enzymatic products by HPLC-DAD	56-56
2.15.6:	Determination of kinetic parameters	56-56
2.15.7:	Identification of putative benzaldehyde dehydrogenase (<i>BD</i>) gene candidates in the pear genome	57-57
2.16:	Identification and characterization of novel benzoate-CoA ligase (BZL) activity from YE-treated cell suspension culture of <i>P. pyrifolia</i>	57-59
2.16.1:	Cell culture condition and elicitation	57-57
2.16.2:	Preparation of cell-free extracts for benzoate-CoA ligase (BZL) assay	57-58
2.16.3:	Assay of benzoate-CoA ligase (BZL)	58-58
2.16.4:	Analysis of BZL catalyzed reaction by HPLC-DAD and ESI-MS	58-59
2.16.5:	Substrate specificity test for BZL	59-59
2.17:	Detection of biphenyl synthase (BIS) activity from YE-treated cell suspension culture of <i>P. pyrifolia</i>	60-60
2.17.1:	Cell culture condition and elicitation	60-60
2.17.2:	Preparation of cell-free extracts for biphenyl synthase (BIS) assay	60-60
2.17.3:	Biphenyl synthase (BIS) assay	60-60
2.17.4:	Analysis of BIS reaction product by HPLC-DAD	61-61
2.18:	Detection of phenylalanine ammonia-lyase (PAL) activity from YE-treated cell suspension culture of <i>P. pyrifolia</i>	61-61
2.18.1:	Cell culture condition and elicitation	61-61
2.18.2:	Preparation of cell-free extract and	61-61

assay of phenylalanine ammonia-lyase
(PAL)

Chapter 3	Results	63-111
3.1:	Comparative leaf metabolomics of two pear species at young and mature stage	63-73
3.1.1:	Amino acids (04)	69-69
3.1.2:	Sugar alcohols (04)	69-69
3.1.3:	Sugars (04)	70-70
3.1.4:	Organic acids (06)	70-70
3.1.5:	Vitamins (02)	70-70
3.1.6:	Phenolics (10)	72-73
3.2:	Principal component analysis (PCA) reveals changes in leaf metabolite profile between two pear species	73-74
3.3:	Hierarchical clustering analysis of the metabolite profiles	74-75
3.4:	Changes in metabolic pathways: metabolic pathway network	76-77
3.5:	Expression analysis of phenyl propanoid biosynthetic genes in the leaves of both <i>Pyrus</i> species	78-79
3.6:	Total phenolics (TPC), total flavonoid (TFC) and free radical scavenging activity (FRSA)	80-80
3.7:	Chemical synthesis of aucuparin and noraucuparin	80-81
3.8:	Development of callus and cell-suspension culture of <i>Pyrus pyrifolia</i>	82-83
3.9:	Time-course study of biphenyl-phytoalexin accumulation in the cell cultures of <i>Pyrus pyrifolia</i>	84-85
3.10:	Biochemical investigation of benzoic acid biosynthesis in the cell cultures of <i>Pyrus pyrifolia</i>	85-111

3.10.1:	Detection and characterization of benzaldehyde synthase (BS) activity from yeast-extract (YE)-treated cell suspension culture of <i>Pyrus pyrifolia</i>	87-95
3.10.1.1:	Effects of precursor feeding (<i>trans</i> -cinnamic acid) on biphenyl phytoalexin accumulation	87-87
3.10.1.2:	<i>In vitro</i> conversion of <i>trans</i> -cinnamic acid to benzaldehyde	88-90
3.10.1.3:	Elicitor induced changes in BS activity	90-91
3.10.1.4:	Characterization of BS	91-95
3.10.2:	Detection and characterization of benzaldehyde dehydrogenase (BD) activity from YE-treated cell suspension culture of <i>Pyrus pyrifolia</i>	95-103
3.10.2.1:	Effects of precursor feeding (benzaldehyde) on biphenyl phytoalexin accumulation	95-96
3.10.2.2:	Detection of benzaldehyde dehydrogenase (BD) activity from elicitor-treated cell suspension culture of <i>P. pyrifolia</i>	96-97
3.10.2.3:	YE-induced changes in BD activity	98-98
3.10.2.4:	Characterization of BD	98-102
3.10.2.5:	Putative BD gene candidates in pear genome	102-103
3.10.3:	Detection and characterization of benzoate-CoA ligase (BZL) activity from YE-treated cell suspension culture of <i>Pyrus pyrifolia</i>	104-109
3.10.3.1:	Detection of Benzoate-CoA ligase (BZL) activity from elicitor-treated	104-105

	cell suspension cultures of <i>P. pyrifolia</i>	
	3.10.3.2: Yeast-extract elicitor -induced changes in BZL activity	105-106
	3.10.3.3: Characterization of BZL	106-109
	3.10.4: Detection of biphenyl synthase (BIS) activity from YE-treated cell suspension culture of <i>Pyrus pyrifolia</i>	109-110
	3.10.4.1: Yeast extract elicitor-induced changes in BIS activity	110-110
	3.10.5 Time course changes in the phenylalanine ammonia-lyase (PAL) activity from YE-treated cell suspension culture of <i>P. pyrifolia</i>	110-111
Chapter 4	Discussion	113-124
Chapter 5	Summary, Conclusion and Future scopes	125-129
	5.1: Summary	125-126
	5.2: Conclusion	127-128
	5.3: Future scopes	128-129
Chapter 6	References	131-148
Chapter 7	Publications	149-150

LIST OF FIGURES

Figure No.		Page No.
1.1:	Cladogram of Rosales (based on rbcL sequence analyses of Rosaceae).	1
1.2:	Geographical distribution of world pear production	10
1.3:	Symptoms of the pear scab disease on infected fruits (A), leaves (B) and stem (C).	14
1.4:	Life cycle of pear scab disease caused by fungus <i>V. pirina</i>	15
1.5:	Life cycle of <i>Erwinia amylovora</i> , causing fire-blight disease in pears	16
1.6:	Major preformed defense metabolites detected from Malinae	18
1.7a:	Structures of biphenyl-derivatives (1-10) recorded from Malinae	20
1.7b:	Structures of dibenzofuran-derivatives (1-17) recorded from Malinae	20
1.8:	Proposed biosynthetic pathway of biphenyl and dibenzofuran formation in Malinae	22
1.9:	Regioselective intra-molecular cyclizations of 2,3',4,6-tetrahydroxybenzophenone to isomeric xanthones in cell cultures of <i>C. erythraea</i> and <i>H. androsaemum</i>	23
1.10:	Possible routes of benzoic acid biosynthesis in plants	24
1.11:	CoA-dependent and β -oxidative route of benzoic acid biosynthesis in plants	25
1.12:	CoA-dependent and non β -oxidative route of benzoic acid biosynthesis in plants	26

1.13:	CoA-independent and non β -oxidative route of benzoic acid biosynthesis in plants	27
1.14:	Biosynthetic pathway for C ₂ -chain cleavage and subsequent formation of 4-hydroxybenzoic acid	28
1.15:	Biosynthetic pathway for C ₂ -chain cleavage and subsequent formation of salicylaldehyde.	28
1.16:	Biosynthetic pathway for C ₂ -chain cleavage reaction in vanillin biosynthesis	28
1.17:	BZL catalyzed conversion of benzoyl-CoA from benzoic acid	29
2.1:	Chemical synthesis of aucuparin and noraucuparin	49
3.1:	Experimental design of pear leaves at two stages: immature and mature. The pictures were taken at the time of leaf sampling	62
3.2:	Typical GC-MS chromatograms (TIC)	63
3.3:	Fragmentation pattern of major identified metabolites from pear leaves	65-66
3.4:	Pie diagram showing distribution of 30 identified pear leaf metabolites within each metabolite class	67
3.5:	Leaf metabolites showing significant differences among <i>P. pyrifolia</i> and <i>P. communis</i>	69
3.6:	Differential accumulation of phenolics in the leaves of <i>P. pyrifolia</i> and <i>P. communis</i>	70
3.7:	Scores plot (A) and loading plots (B) of principal components (PC1) and (PC2) from the PCA results obtained from 30 identified metabolite data for different types of <i>Pyrus</i> leaves	72
3.8:	Hierarchical clustering analyses of 30 detected metabolites from <i>P. pyrifolia</i> and <i>P. communis</i> leaves at immature and mature stage	73
3.9:	The proposed metabolic pathways networks of pear leaves	75

3.10:	Expression levels of selected phenylpropanoid and flavonoid biosynthetic genes in the immature and mature leaves of <i>P. pyrifolia</i> and <i>P. communis</i>	77
3.11:	TIC and mass-spectrum (GC-MS) of chemically synthesized aucuparin (A) and nor-aucuparin (B).	79
3.12:	Friable callus induced from the leaves of <i>Pyrus pyrifolia</i>	80
3.13:	Cell suspension culture of <i>Pyrus pyrifolia</i> derived from the friable callus	81
3.14:	Phytoalexin accumulation in yeast extract-treated cell cultures of <i>P. pyrifolia</i>	82
3.15:	Time-course accumulation of noraucuparin and aucuparin in the yeast extract-treated cell cultures of <i>P. pyrifolia</i>	83
3.16:	Predicted biosynthetic pathway of benzoic acid and benzoyl-CoA in pear	84
3.17:	Effect of feeding <i>trans</i> -cinnamic acid on aucuparin and noraucuparin accumulation in yeast extract-treated cell cultures of <i>P. pyrifolia</i>	85
3.18:	HPLC chromatograms showing benzaldehyde synthase activity from yeast extract-treated cell cultures of pear	86
3.19:	GC-MS chromatogram showing the detection of product of benzaldehyde synthase reaction	87
3.20:	Time-course changes in the benzaldehyde synthase activity from yeast extract-treated cell cultures of <i>P. pyrifolia</i>	89
3.21:	Apparent K_m value of BS enzyme for <i>trans</i> -cinnamic acid (substrate of BS) determined from Hanes plots (Hyper 32).	90
3.22:	pH (A) and temperature (B) optimum for benzaldehyde synthase activity from <i>P. pyrifolia</i> .	91
3.23:	Proposed mechanism of benzaldehyde synthase mediated C ₂ -chain cleavage of <i>trans</i> -cinnamic acid to yield benzaldehyde	93
3.24:	Effect of feeding benzaldehyde on phytoalexin accumulation in YE-treated cell cultures of <i>P. pyrifolia</i>	94

3.25:	HPLC chromatograms showing benzaldehyde dehydrogenase activity	95
3.26:	Time-course changes in the benzaldehyde dehydrogenase (BD) activities in yeast extract-treated cell cultures of <i>P. pyrifolia</i>	96
3.27:	Apparent <i>K_m</i> values for benzaldehyde (a) and NAD ⁺ (b) from Hanes plots (Hyper 32).	97
3.28:	pH (a) and temperature (b) optimum for benzaldehyde synthase (BS) activity from <i>P. pyrifolia</i>	98
3.29:	Proposed mechanism of benzaldehyde dehydrogenase (BD) reaction	100
3.30:	HPLC chromatograms showing BZL activity	102
3.31:	Negative mode LC-ESI-MS of BZL-catalyzed formation of benzoyl-CoA	103
3.32:	Time-course changes in the benzoate-CoA ligase (BZL) activities in yeast extract-treated cell cultures of <i>P. pyrifolia</i>	104
3.33:	Substrate specificity of <i>P. pyrifolia</i> BZL determined by luciferase-based assay.	105
3.34:	pH (a) and temperature (b) optimum for benzoate-CoA ligase (BZL) activity from <i>P. pyrifolia</i>	106
3.35:	Apparent BZL <i>K_m</i> value for benzoic acid from Hanes plots (Hyper 32). Inserts show the Michaelis–Menten kinetics	107
3.36:	Time-course changes in the biphenyl synthase (BIS) activities in yeast extract-treated cell cultures of <i>P. pyrifolia</i>	108
3.37:	Time-course changes in the phenylalanine ammonia-lyase (PAL) activities in yeast extract-treated cell cultures of <i>P. pyrifolia</i>	109
4.1:	Enzymatic route of benzoate-derived phytoalexin biosynthesis in pear.	115

LIST OF TABLES

Table No.		Page No.
1.1:	Commercially important fruit-bearing and ornamental plants of the Rosaceae family.	2
1.2:	Classification of Malinae	3
1.3:	The genera included within the sub-tribe Malinae. Bold marks represent commercially relevant fruit producing genera	4
1.4:	Site of origin of some important <i>Pyrus</i> species	6-8
1.5:	Summary of gene prediction for <i>Pyrus communis</i> based on pear genome sequence	9
1.6:	World-wide production of pears and area under cultivation among ten most pear producing countries	10
1.7:	Indian pear production and percentage share among ten top pear producing states	11
2.1:	Chemicals used for callus induction and suspension culture	32
2.2:	Metabolite standards	33
2.3:	Chemicals used for enzyme assay / partial purification	34
2.4:	Elicitors used	34
2.5:	Solvents and reagents	35
2.6:	Solvents and reagents used for GC-MS analysis	35


















2.7:	Equipment used	36
2.8:	Media composition for callus and suspension culture	37
2.9:	Buffer used for enzyme extraction	38
2.10:	Buffer used for enzyme assay	39
2.11:	Composition of Bradford reagent	40
2.12:	Composition of solution for washing and regenerating PD ₁₀ column	40
2.13:	Enzyme and reagents used in molecular biology	41
2.14:	Composition of 50 X TAE buffer	41
2.15:	Primers used in real time PCR analysis	42
2.16a:	Composition of qPCR reaction	46
2.16b:	qPCR reaction program	47
3.1:	List of 30 identified metabolites from pear leaves. The peak area of the quantification ion was used for comparative quantification	64
3.2:	Efficiency test for qPCR reactions	76
3.3:	Total phenolics (TPC), total flavonoid (TFC) and DPPH free radical scavenging activity (FRSA) of pear leaves	78
3.4:	Changes in the benzaldehyde synthase (BS) activity in presence of various reducing agent	88
3.5:	Substrate specificity studies of benzaldehyde synthase (BS) from yeast extract-treated cell cultures of <i>P. pyrifolia</i>	92

- 3.6:** Substrate specificity studies of benzaldehyde dehydrogenase (BD) from yeast-extract-treated cell cultures of *P. pyrifolia* 99-100
- 3.7:** Putative benzaldehyde dehydrogenase unigenes detected in the pear genome via *in silico* analyses 101





Table1.1: Commercially important fruit-bearing and ornamental plants of the Rosaceae family.

Common name	Scientific name	Plant type	Fruit / flower shape
Asian pear	<i>Pyrus pyrifolia</i>	Fruit producing	
European pear	<i>Pyrus communis</i>	Fruit producing	
Peach	<i>Prunus persica</i>	Fruit producing	
Apple	<i>Malus domestica</i>	Fruit producing	
Raspberry	<i>Rubus occidentalis</i>	Fruit producing	
Plum	<i>Prunus domestica</i> <i>Prunus salicina</i>	Fruit producing	
Cherry	<i>Prunus avium</i> <i>Prunus cerasus</i>	Fruit producing	
Apricot	<i>Prunus armeniaca</i>	Fruit producing	
Almond	<i>Prunus dulcis</i>	Fruit producing	
Quince	<i>Cydonia oblonga</i>	Fruit producing	
Strawberry	<i>Fragaria ananassa</i>	Fruit producing	
Loquat	<i>Eriobotrya japonica</i>	Fruit producing	
Rose	<i>Rosa species</i>	Ornamental	
Hawthorn	<i>Crataegus species</i>	Ornamental	
Firethorn	<i>Pyracantha species</i>	Ornamental	
Mountain ash	<i>Sorbus aucuparia</i>	Ornamental	
Meadowsweets	<i>Filipendula ulmaria</i>	Ornamental	

1.2. The sub-tribe Malinae of Rosaceae family:

The Rosaceae family is known to bear a number of pome-fruit bearing tree species. Since long time these pome bearing tree species were kept into the sub family Maloideae, however, recently the Maloideae subfamily was re-classified as the subtribe Malinae of Amygdaloideae subfamily (Reveal, 2012) (Table 1.2). Previously members of Malinae were wrongly put into the sub-tribe Pyrinae (Campbell et al., 2007). The Malinae is well known for bearing several economically important fruit plants such as apple and pear. Till now, the Malinae comprises of approximately 30 genera and about 1000 species distributed throughout the world (Chizzali and Beerhues, 2012 a). Some important edible fruit bearing genus of the Malinae are listed in Table 1.3. The members of this sub-tribe mostly bear pome fruits, which is not a common feature of other members of Rosaceae. The basal chromosome number of the Maline is $n = 17$, whereas in other Rosaceae members, basal chromosome number varies ($x = 8$ or 9). This sub-tribe Malinae is further characterized by its ability to produce two special classes of defense metabolites, the biphenyls and the dibenzofurans, upon pathogen infection. Till date, the biosynthesis of these biphenyls and dibenzofurans are not well understood. The *Pyrus* is one of the most important fruit producing plants of the Malinae. The *Pyrus* species produces economically important pear fruits. Pear fruits are well known for their beautiful texture, high nutrition value and pleasant taste.

Table1.2: Classification of Malinae (Reveal, 2012):

Kingdom:	Plantae
Order:	Rosales
Family:	Rosaceae
Subfamily:	Amygdaloideae
Tribe:	Maleae Small
Subtribe:	Malinae Reveal

Table1.3: The genera included within the sub-tribe Malinae. Bold marks represent commercially relevant fruit producing genera

S.No	Genus
1	<i>Aria</i>
2	<i>Amelanchier</i> [chokeberry fruit]
3	<i>Aronia</i>
4	<i>Chaenomeles</i>
5	<i>Chamaemeles</i>
6	<i>Chamaemespilus</i>
7	<i>Cotoneaster</i>
8	<i>Cormus</i>
9	<i>Crataegus</i>
10	<i>Cydonia</i> [loquat fruit]
11	<i>Dichotomanthes</i>
12	<i>Docynia</i>
13	<i>Docyniopsis</i>
14	<i>Eriobotrya</i>
15	<i>Eriolobus</i>
16	<i>Hesperomeles</i>
17	<i>Heteromeles</i>
18	<i>Malacomeles</i>
19	<i>Malus</i> [apple fruits]
20	<i>Mespilus</i>
21	<i>Osteomeles</i>
22	<i>Peraphyllum</i>
23	<i>Photinia</i>
24	<i>Pseudocydonia</i> [chinese quince]
25	<i>Pyracantha</i>
26	<i>Pyrus</i> [pear fruit]
27	<i>Rhaphiolepis</i>
28	<i>Sorbus</i>
29	<i>Stranvaesia</i>
30	<i>Torminalis</i>

1.3. The origin, distribution and taxonomy of pear (*Pyrus species*):

The genus *Pyrus* represents one of the most economically important deciduous fruit producing members of the sub-tribe Malinae. The genus *Pyrus* produces pear fruits. The genus *Pyrus* consists of 24 species which include up to three artificial hybrids, six natural interspecific hybrids and several landraces (Fotirić Akšić et al., 2015). Pears seem to be originated during tertiary period (65-55 million years ago) in the China along the south-western mountain ranges (Katayama et al., 2016). Pear fruits are widely cultivated in China, India and many other Asian countries, United States and Western Europe (USDA, 2012). As per other members of sub-tribe Malinae, pear bears seventeen chromosomes ($n = 17$), where is in other members of Rosaceae family, the basic chromosome number is either $n = 8$ or $n = 9$. The best possible hypothesis for the origin of $x = 17$ in the pears and other members of Malinae was given by (Sax, 1931). This theory suggests the origin of $n = 17$ as allotetraploid or allopolyploid by fusion between two primitive families of Rosaceae, Spiraeoideae with $n = 9$ and the Prunoideae with $n = 8$. Abundance of many unpaired chromosomes during meiosis as well as isozyme studies strongly supports this theory (Weeden and Lamb, 1987; Silva et al., 2014). Most of the pear cultivars are diploid ($2n = 34$), whereas some cultivars such as *Pyrus* × *bretschneideri* are polyploids. Throughout the world, two domestication centers and primary origin point is located for the genus *Pyrus*. The first domestication center located in the China, second one located in the Asia Minor to the Middle East and in the Central Asia, a third secondary center is located (Vavilov, 1951).

Based on fruit size and numbers of carpel, pears are categorized into three groups: small fruits with two carpels (group 1, mostly Asian pears); large fruit size with five numbers of carpels (group 2, mostly European pears) and a third group bearing hybrids between group 1 and group 2, with three to four carpels and moderate fruit size. European pear has soft and juicy texture, elongated body with pleasant aroma, while Asian pear has crisp & granular texture with round shape (Silva et al., 2014). Because of this grainy texture Asian pear is also known as sand pear. This characteristic grainy texture is due to presence of stone cells in the peel of pear fruit. The genus *Pyrus* is represented by several species and many artificial hybrids and interspecific hybrids. Some important pear species and their site of origin are mentioned in Table 1.4. Throughout the world, most popularly grown pear species are *Pyrus communis* L, commonly known as European pear and *Pyrus pyrifolia* (Burm.) Nak, popularly known as Asian pear (Hancock, 2008; Silva et al., 2014).

Table1.4: Site of origin of some important *Pyrus* species

Pear species	Site of Origin
A. Asian	
<i>Pyrus alnifolia</i>	Russian Far East, China, Japan, Korea, Taiwan,
<i>Pyrus baccata</i>	Russia, Korea , Mongolia, China,
<i>Pyrus baccatavar</i>	China, Bhutan, India , Nepal
<i>Pyrus betulifolia</i>	China, Laos
<i>Pyrus</i> × <i>bretschneideri</i>	China
<i>Pyrus calleryana</i>	China, Korea, Taiwan, Vietnam
<i>Pyrus cathayensis</i>	China
<i>Pyrus delavayi</i>	China
<i>Pyrus discolor</i>	China
<i>Pyrus doumeri</i>	China, Taiwan, Laos, Vietnam
<i>Pyrus folgner</i>	China
<i>Pyrus foliolosa</i>	Burma, Bhutan, India , Nepal, China
<i>Pyrus glabra</i>	Iran
<i>Pyrus gracilis</i>	Japan
<i>Pyrus harrowiana</i>	China, India , Nepal, Burma
<i>Pyrus heterophylla</i>	Kyrgyzstan, Tajikistan, China
<i>Pyrus hondoensis</i>	Japan
<i>Pyrus</i> × <i>hopeiensis</i>	China
<i>Pyrus hupehensis</i>	China, Taiwan
<i>Pyrus indica</i>	South Asia and Far East Asia
<i>Pyrus japonica</i>	Japan
<i>Pyrus keissleri</i>	China, Myanmar
<i>Pyrus kansuensis</i>	China
<i>Pyrus lanata</i>	Afghanistan, India , Pakistan
<i>Pyrus matsumurana</i>	Japan
<i>Pyrus nussia</i>	Far East, South Asia
<i>Pyrus</i> × <i>phaeocarpa</i>	China
<i>Pyrus pohuashanensis</i>	Russia, China, Korea
<i>Pyrus prattii</i>	China
<i>Pyrus prunifolia</i>	China
<i>Pyrus pseudopashia</i>	China
<i>Pyrus pyrifolia</i>	China, India , Laos, Vietnam
<i>Pyrus ringo</i>	China, Korea
<i>Pyrus ringo</i>	China
<i>Pyrus scabrifolia</i>	China
<i>Pyrus scalaris</i>	China
<i>Pyrus</i> × <i>serrulata</i>	China
<i>Pyrus sieboldii</i>	China, Japan

<i>Pyrus sikkimensis</i>	China, Bhutan, India
<i>Pyrus sinensis</i>	Korea
<i>Pyrus</i> × <i>sinkiangensis</i>	China
<i>Pyrus spectabilis</i>	China
<i>Pyrus taiwanensis</i>	Taiwan
<i>Pyrus ussuriensis</i>	Russia, China, Japan, Korea, Brazil
<i>Pyrus</i> × <i>uyematsuana</i>	Japan, Korea
<i>Pyrus vestita</i>	China, Bhutan, India , Nepal,
<i>Pyrus vilmorinii</i>	China
<i>Pyrus xerophila</i>	China
<i>Pyrus yunnanensis</i>	China, Myanmar
<i>Pyrus zahlbruckneri</i>	China
<i>Pyrus tschonoskii</i>	Japan
<i>Pyrus cydonia</i>	Iran, Armenia, Azerbaijan, Russia, Turkmenistan
<i>Pyrus germanica</i>	Middle East and Northern Asia
<i>Pyrus korshinskyi</i>	Afghanistan, Tajikistan, Uzbekistan
<i>Pyrus kumaoni</i>	Middle East, Far East and South Asia
<i>Pyrus salicifolia</i>	Iran, Armenia, Turkey, Arzerbaij̃ao
<i>Pyrus trilobata</i>	Israel, Lebanon, Turkey, Bulgaria, Greece
<i>Pyrus turkestanica</i>	Kyrgyzstan, Tajikistan, Turkmenistan, Afghanistan
B. Europe and Africa	
<i>Pyrus aria</i>	Canary Islands, North Africa, All of Europe
<i>Pyrus ariacretica</i>	Africa, Middle East, Central Europe, Oriental and Southern and Turkmenistan
<i>Pyrus aucuparia</i>	All Europe
<i>Pyrus boissieriana</i>	Azerbaijan, Turkmenistan, Iran
<i>Pyrus korshinskyi</i>	Former Soviet Union
<i>Pyrus bulgarica</i>	Western Europe, Central Eastern and Southern
<i>Pyrus caucasica</i>	Eastern Europe and Central Greece
<i>Pyrus chamaemespilus</i>	Western Europe, Central Eastern and Southern
<i>Pyrus communis</i>	All Europe
<i>Pyrus communis</i>	UK, Portugal, Spain, France
<i>Pyrus communis</i>	Algeria, Morocco
<i>Pyrus communis</i>	Morocco
<i>Pyrus communis</i>	Western Europe, Central Eastern, and Southern Europe
<i>Pyrus</i> × <i>complexa</i>	Former Soviet Union
<i>Pyrus cossonii</i>	Algeria
<i>Pyrus crataegifolia</i>	Turkey, Albania, Serbia, Greece, Italy, Macedonia
<i>Pyrus cuneifolia</i>	Central Eastern Europe, South and Central Europe
<i>Pyrus decipiens</i>	All Europe and North Africa
<i>Pyrus domestica</i>	Algeria, Cyprus, Eastern Europe, Central West and Meridional

<i>Pyrus elaeagrifolia</i>	Turkey, Ukraine, Albania, Bulgaria, Greece, Romania
<i>Pyrus elaeagrifolia</i>	Turkey
<i>Pyrus germanica</i>	Middle East, Eastern Europe, Central, Southern and Northern Asia
<i>Pyrus gharbiana</i>	Algeria, Morocco
<i>Pyrus intermedia</i>	All Europe
<i>Pyrus minima</i>	UK
<i>Pyrus nebrodensis</i>	Italy - Sicily
<i>Pyrus pinnatifida</i>	All Europe
<i>Pyrus praemorsa</i>	South of Italy, France
<i>Pyrus sachokiana</i>	Georgia
<i>Pyrus spinosa</i>	Central Eastern Europe, South, and Central
<i>Pyrus sudetica</i>	Western Europe, Central Eastern, and Southern
<i>Pyrus syriaca</i>	Caucasus and Middle East Region
<i>Pyrus torminalis</i>	North Africa, Middle East,
<i>Pyrus trilobata</i>	Turkey, Bulgaria, Greece, Israel, Lebanon
America	
<i>Pyrus americana</i>	Greenland, USA, Canada
<i>Pyrus angustifolia</i>	USA, Canada
<i>Pyrus arbutifolia</i>	USA
<i>Pyrus arbutifolia</i>	USA
<i>Pyrus coronaria</i>	Canada, USA
<i>Pyrus diversifolia</i>	USA, Canada
<i>Pyrus floribunda</i>	USA, Canada
<i>Pyrus fusca</i>	USA, Canada
<i>Pyrus sanguinea</i>	Canada, USA

1.4. The pear genome sequence:

Recently, pear genome was sequenced and made publically available [Genome Data base of Rosaceae (GDR) www.rosaceae.org]. The whole genome sequence of European pear (*P. communis*), Bartlett (Chagné et al., 2014) showed 171 MD anchored to high density genetic map. There are 43,419 putative gene models and a total of 5,350 protein clusters. A total of 3,893,643 putative SNPs were identified, where 7.53% and 6.37% SNPs were located within 1,000 bases of a predicted gene model, either upstream or downstream. Summary of gene prediction for *Pyrus communis* and comparison with *P. bretschneideri* and *Malus domestica* (apple) was given in Table 1.5. Availability of pear genome sequence will be beneficial for studying fruit and plant characteristics and developing new traits. Furthermore, pear genome sequence provides the better chance to understand pear taxonomy as well as provide the opportunity to perform functional genomics and marker / genome assisted breeding.

Table 1.5: Summary of gene prediction for *Pyrus communis* based on pear genome sequence adopted from (Chagné et al., 2014).

Parameters	<i>P. communis</i>	<i>P. bretschneideri</i>	<i>M. domestica</i>
Predicted genes	43,419	42,812	54,921
Average gene length (including introns)	3,320 nt	2,776 nt	2,802 nt
Average CDS length	1,209 nt	1,172 nt	1,155 nt
Exons	221,804	202,169	273,206
Average exon length	237 nt	248 nt	273 nt
Single exon genes	10,909	12,310	10,378
Introns	178,385	159,357	218,353
Average intron length	398 nt	386 nt	491 nt
Genes per 100 Kb	7.5	8.4	7.3



The total annual pear production in India is approximately 31,6700 tones with a total land area under cultivation of 4,2280 ha. According to National Horticulture Board data (2014-15), among Indian states, Uttarakhand is the largest producer of the pear sharing 33.7% of total Indian production followed by Punjab and Jammu and Kashmir (Table 1.7)

Table 1.7: Indian pear production and percentage share among ten top pear producing states (source: APEDA Agri Exchange data 2014).

Position	State	Production in kilo tones	Percentage Share
1	Uttarakhand	104.01	34.37
2	Punjab	68.29	22.56
3	Jammu & Kashmir	65.41	21.61
4	Tamil Nadu	32.23	10.65
5	Himachal Pradesh	20.22	6.68
6	Chattisgarh	5.04	1.67
7	Haryana	4.34	1.43
8	Nagaland	3.10	1.02
9	Mizoram	0.10	< 1
10	Sikkim	0.10	< 1

1.6. The nutritional value of pears and its health benefits:

The pear fruits are consumed throughout the world for its high nutritional values. Pears are consumes as raw fresh fruits, or as processed fruit products such as jam, candy, juice etc. Pear fruits are rich source of many health protective nutrients. The fruit contains fibers, ascorbic acid (vitamin C), potassium, phenolics, and flavonoids, with negligible amount of saturated fat, cholesterol and sodium. Peel of pear fruit contain high amount of Vitamin C (7 mg per fruit), fiber (6 g per fruit) and potassium (180 mg per fruit) (Reiland and Slavin, 2015). Compared to other pome fruits, pears contain high amount of sugars such as fructose (4.5%), glucose (4.2%), sucrose (2.5%) and sorbitol (2.5%). As compared to apples, pear has higher fructose level (Fourie et al., 1991; Jovanovic-Malinovska et al., 2014). Pears fruit have very high antioxidant properties and even under storage conditions for more than 8 months, pear can retain its antioxidant properties (Leontowicz et al., 2002). High antioxidant value mostly results from high phenolics acid contents such as caffeic acid, ferulic acid, *p*-coumaric acid, chlorogenic acid etc. Examination of polyphenol contents of ten pear cultivars revealed that pears are rich in

phenolics, tri-terpenes, flavonoids, mainly concentrated in the fruit peel. Major phenolics detected in pears are caffeic acid, catechin, epicatechin, arbutin, quercetin, rutin, ursolic acid and chlorogenic acid (Li et al., 2014). Pears are very high in methylated phenolic acids content; approximately 70% of the phenolic acids are being dimethylated to give heal-promoting phenolics such as, syringic and sinapic acid. As compared to any other fruits, values of these methylated-phenolics are almost 23% higher in pears (Russell et al., 2009). These methylated-phenolics are easily broken down by the gut bacteria, resulting into smooth function of gut. Pear fruits exhibited high anti-inflammatory activity, which is closely associated with its high phenolics and anthocyanin contents (Li et al., 2014). Consumption of pear is also related to lowering of cholesterol level in blood (Leontowicz et al., 2002). Bunzel and Ralph. (2006) have shown that pear fruits contain lignin fibers, which are bio-transformed into lignans by the gut-bacteria, resulting into good gut health. Barbosa et al. (2013) showed high anti-diabetic properties of pear fruits against type 2 diabetes. Proanthocyanidin extracts from pear fruit showed excellent anti-ulcer activity based on experiments in animal model (Hamauzu et al., 2007). Moreover, malaxinic acid [4-(O- β -D-glucopyranosyl)-3-(3'-methyl-2'-butenyl) benzoic acid, isolated from pear fruits showed anticancer drug like properties (Lee et al., 2013). Pear fruit extracts are also known to possess significant antimicrobial activity (Güven et al., 2006). All these data exhibited that pear fruits are rich source of many health-promoting metabolites and anti-oxidants.

1.7. Bioactive metabolites from pear:

Pears contain an array of natural bioactive compounds which make it phytochemically and ethno-medicinally important plant. In the “Indian materia medica” pear is called as ‘Amrit phale’ because of its bioactive constituents which have positive effect on human health care (Ranjeet Kaur and Arya, 2012). As a rich source of phenolics compound the leaves of pear contain arbutin and arbutin-derivatives, hydroxy-cinnamic acid, ursolic acid and astragalol (Fotirić Akšić et al., 2015). Because to high content of arbutin, the pear leaves are used in skin whitening treatments. Arbutin also acts as anti-bacterial agent. Fruit and leaves of pear also contain flavonoids such as derivatives of β -ring di hydroxylated flavanol (isorhamnetin and quercetin), catechin, epicatechin, caffeic acid, chlorogenic acid, sinapic acid, syringic acid, rutin and pro anthocyanidins (Lee et al., 2013). Tannins and phloridzins are dominant in roots. Fruits contain phenolic compounds comprising of various flavonoid classes (anthocyanins, flavonols, and monomeric catechins), proanthocyanidins, flavanones, hydroxyphenolic acids (mostly hydroxycinnamic acids derived from caffeic acid and *p*-coumaric acids). The bark

contains arbutin, friedelin, triterpenoids and beta-sitosterol (Ranjeet Kaur and Arya, 2012). Apart from these entire bioactive compounds pear can produce certain specialized inducible defense metabolites upon pathogen attack (Chizzali and Beerhues, 2012b). These defense metabolites include a number of biphenyl and dibenzofuran derivatives.

1.8. Major diseases of pear:

The most devastating pear diseases that cause severe loss in the pear production are pear -scab caused by the fungus *Venturia pirina* or *Venturia nashicola* and fire-blight disease caused by the bacterium *Erwinia amylovora* (Saini et al., 2017).

1.8.1 Pear scab disease:

Pear scab infection occurs to both European and Asian pears. This disease causes tremendous loss in the quality and yield of the pear fruits. The pear scab disease is caused by the ascomyceteous fungus *Venturia pirina* to European pear (*P. communis*) (Villalta et al., 2004) and by the *Venturia nashicola* to Asian pear (*P. pyrifolia*) (Abe et al., 2008). Interestingly, Asian and European pear differs in their susceptibility towards scab disease. Mature leaves are less susceptible to scab infection due to higher ontogenic resistance (Baohua and Meiqi, 2001; Brewer et al., 2005). However the mechanism of such ontogenic resistance is not well understood. Therefore, identifying the metabolites involved in scab-resistance in pear and their mechanisms of actions would enable breeders to develop new strategies to enhance scab-resistance in pear cultivars. Nevertheless, there is a wide variability in the pathogenicity of pear scab fungus, such as, Asian pears are very susceptible to *V. nashicola* infection but European pears are less susceptible. Similarly, Asian pears are resistant to infection by *V. pirina* due to non-host resistance, whereas European pears are highly susceptible to the *V. pirina* attack (Brewer et al., 2009). Pear scab fungus infects fruits, leaves and young twigs. Disease symptoms and life cycle of *Venturia* fungus on pear are similar to apple but each *Venturia* species has limited host ranges. For example, apple scab disease caused by fungus *V. inaequalis* shows similar disease symptoms as of pear scab caused by *V. pirina*, however, *V. inaequalis* unable to infect pear due to non-host resistance. Similarly, *V. pirina* cannot infect apples. Upon infection, disease symptoms in fruits and leaves occurs as velvety olive green to dark brown to black circular necrotic or chlorotic lesions (Fig 1.3). Immature fruits may fall-down due to infection or if the fruit is retained till maturity, and as the lesions grow older, the







range of primary metabolites such as amino acids, organic acids, sugar, sugar alcohols, vitamins and secondary metabolites such as phenylpropanoids and flavonoids by employing chemical derivatization of low molecular weight metabolites (Wagner et al., 2003). Consequently, GC- MS has been used to identify and measure metabolites in many plant samples (Bisht et al., 2013; Kumar and Nagar, 2014). To date, metabolomics data from pear is available only from the developing fruits (Oikawa et al., 2015). However, as such, any comprehensive metabolomics data from pear leaves are not available in the literature. Such comparative analyses are essential to get a picture of basal pear leaf metabolism. Metabolomics study is often associated with gene expression analyses (Bera et al., 2017; Kundu et al., 2012; Rajeev Kumar et al., 2014). Mostly, phenylpropanoid biosynthetic genes such as phenylalanine ammonia-lyase (*PAL*), cinnamate-4-hydroxylase (*C4H*), 4-coumarate-CoA-ligase (*4CL*) are up-regulated upon pathogen infection (Mandal, 2010; Mandal et al., 2011; Mukherjee et al., 2016; Sil et al., 2015). Metabolomics also provide clues to clone target genes for developing transgenic plants with higher resistance (Harish et al., 2013).

1.10. Defense metabolites / phytoalexins of pear and other members of Malinae:

The members of Malinae, produces an array of pre-formed and inducible defense metabolites to combat with pathogen attack (Wolska et al., 2010). These metabolites play a crucial role in offering ontogenic and inducible pathogen-resistance to plants.

1.10.1. Pre-formed defense metabolites:

Ontogenic resistance is exhibited by preformed antimicrobial compounds known as phytoanticipins. Phenolic acids and flavon-3-ols, such as quinic acid and its derivatives, epicatechin and catechin play major role as preformed defense metabolites. Phenolic acids like caffeic acid, chlorogenic acid, syringic acid and vanillic acid, Ellagic acid were found to help plant under variable stress condition including pathogen attack (Termentzi et al., 2008; Vasco et al., 2009). It has been found that quinic acid, quercetin-3-O-galactoside, chlorogenic acid present in *Malus* play a crucial role against fungal pathogen, moreover quinic acid also serves as an intermediate of phenylpropanoid pathway (Kanwal et al., 2010) and is transformed into several other secondary metabolites in response to different external stimuli. Quercetin-3-O-galactoside found in leaves and fruits show nonspecific and very potent anti-fungal activity (Kanwal et al., 2010) and was shown to reduce the growth of several fungus up to 99 percent. Chlorogenic acid which is found in high concentration in fruits of *Malinae* reported to help



1.10.2. Inducible defense metabolites of Malinae: the biphenyls and the dibenzofurans

The members of the sub-tribe Malinae can produce two special classes of phytoalexins upon pathogen attack, the biphenyls and the dibenzofurans. The ability to produce these phytoalexins is only confined to this sub-tribe Malinae (Kokubun and Harborne, 1995). The antifungal and antimicrobial activities of biphenyls and dibenzofurans are well demonstrated (Chizzali and Beerhues, 2012a; Hrazdina et al., 1997; Kokubun and Harborne, 1995). Both biphenyls and dibenzofurans inhibited the fungal spore germination and fungal mycelial growth. Earlier, it has been shown that biphenyls and dibenzofurans mainly localized in the sapwood of the plants (Kokubun and Harborne, 1995). These phytoalexins were not found in the leaves, with only exception of *Sorbus aucuparia*, which accumulates aucuparin, a biphenyl-derivative, in the leaves in response to biotic and abiotic elicitor-treatment (Kokubun and Harborne, 1994). Recently, biphenyls and dibenzofurans were found to be absent from the leaves of *Malus domestica* as confirmed by analyzing yeast-extract treated cell cultures and scab (*Venturia inaequalis*) infected leaves of a scab-resistant and a scab-susceptible apple cultivar (Hrazdina, 2003). Until Now, any biphenyl- or dibenzofuran- glycosides have not been identified from any intact plants for Malinae. However, scab-resistant apple cell cultures produced these 2'-glucosyloxyaucuparin (biphenyl-glycoside) and dibenzofuran-glycoside, malusfuran in response to elicitor-treatment (Borejsza-Wysocki et al., 1999; Hrazdina et al., 1997). It has been reported that biphenyls and dibenzofurans do not occur simultaneously (Kokubun and Harborne, 1995), however, yeast extract-treated cell cultures of the scab-resistant apple cultivar Liberty accumulated both biphenyls and dibenzofurans simultaneously, which suggested a biogenic relationship between the two classes of compounds. Recently, elicitor-treated cell cultures of *S. aucuparia* or / *Pyrus pyrifolia* also showed simultaneous accumulation of both the biphenyls and dibenzofuran (Hüttner et al., 2010; Saini et al., 2017). Previously, intact plants of any Malinae members failed to produce these two groups of phytoalexins simultaneously, which questioned a common biosynthetic pathway (Kokubun and Harborne, 1995).

Till date, out of 30 genera in Malinae, 14 have been investigated for the presence of biphenyls and dibenzofurans (Chizzali and Beerhues, 2012a). Ten (10) biphenyls (Fig 1.7 a) and seventeen (17) dibenzofurans (Fig 1.7 b) have been detected so far in Malinae. Most of these biphenyls and dibenzofurans are produced in response to fungal attack (Chizzali and Beerhues, 2012a). Out of total 10 biphenyls, aucuparin is the most widely distributed biphenyl whereas γ -cotonefuran is the most abundant dibenzofuran. Among all detected biphenyls, 3,4,5-tri methoxybiphenyl is unique to *Pyrus* species, similarly among dibenzofurans, α -, β -, and γ -



1.11. Biosynthesis of the biphenyl and the dibenzofuran:

The formation of biphenyl scaffold is known to be catalyzed by a type III polyketide synthase, biphenyl synthase (BIS) (Liu et al., 2007). The BIS enzyme catalyzes the condensation of one molecule of benzoyl-CoA with three molecules of malonyl-CoA to produce one molecule of 3,5-dihydroxybiphenyl, the precursor for other substituted biphenyl phytoalexins (Liu et al., 2004). The complete biosynthesis of biphenyls and dibenzofurans are divided into two parts, the **early benzoic acid pathway** and the **core biphenyl-dibenzofuran biosynthesis pathway**. Both these pathways are not completely deciphered yet. The biosynthesis of benzoic acid and subsequent formation of benzoyl-CoA remains elusive. The starter substrate benzoyl-CoA is either derived from cinnamoyl-CoA (in **β -oxidative pathway**) or from free benzoic acid (**non- β -oxidative pathway**) in a reaction catalyzed by benzoate: CoA ligase (BZL), which promotes thio-esterification of benzoic acid by coenzyme A. BZL activity has been detected in *Clarkia breweri* and *Hypericum androsaemum* (Abd El-Mawla and Beerhues, 2002; Beuerle and Pichersky, 2002a).

Once benzoyl-CoA is formed, it combines with three molecules of malonyl-CoA via iterative condensation to produce one molecule of 3, 5-dihydroxybiphenyl, in a reaction catalyzed by BIS. *BIS* cDNA was cloned and functionally characterized from the *Sorbus aucuparia* cell cultures (Liu et al., 2007). This 3, 5-dihydroxybiphenyl, the starter biphenyl scaffold is further converted into 3-hydroxy-5-methoxy biphenyl in a reaction catalyzed by a *o*-methyl transferase (OMT1) (Khalil et al., 2015). 3-hydroxy-5-methoxybiphenyl is then converted to noraucuparin by a CYP450 monooxygenase, biphenyl-4-hydroxylase (B4H) (Khalil et al., 2013a). Noraucuparin is then transformed into aucuparin by a second *o*-methyltransferase (OMT2) (Khalil et al., 2015). Recently, a cDNA encoding *OMT1*, *OMT2* has been cloned from cell cultures of *S. aucuparia* (Khalil et al., 2015). A *B4H* cDNA has also been cloned from cell cultures of *S. aucuparia* and fire-blight infected *Malus domestica* (Sircar et al., 2015). Till date, enzymes / genes underlying biphenyl to dibenzofurans conversion is not elucidated. However, radio-labeled feeding experiment in cell cultures of *S. aucuparia* demonstrated that dibenzofurans are derived from biphenyl precursors, such as, aucuparin and noraucuparin (Khalil et al., 2015). Two reactions have been postulated for conversion of biphenyl to dibenzofuran, based on detection of various, biphenyl- and dibenzofuran-derivatives at metabolite level. It is likely that noraucuparin or aucuparin first hydroxylated at 2'-position to yield 2'-hydroxy noraucuparin or 2'-hydroxy aucuparin by a CYP450 hydroxylase activity. It is speculated that 2'-hydroxylated noraucuparin or aucuparin undergoes intramolecular



So far, no intra-molecular C-O coupling reaction has been studied at the molecular genetic level. In alkaloid metabolism, an intermolecular C-O coupling reaction giving bisbenzylisoquinoline from (*R*) and (*S*)-methyl coclaurin and an intramolecular C-C coupling reaction yielding salutaridinone from (*R*)-reticuline were investigated (Gerardy and Zenk, 1992; Kraus and Kutchan, 1995; Stadler and Zenk, 1993). A reaction which is likely to proceed in analogy to the intramolecular cyclization of biphenyls is the intramolecular C-O coupling reaction observed in benzophenone metabolism (Peters et al., 1997). 2,3',4,6-Tetrahydroxybenzophenone is regioselectively cyclized to give either 1,3,5- or 1,3,7-trihydroxy xanthenes (Fig 1.9). Recently, (Chizzali et al., 2016), demonstrated that in fire-blight infected *Pyrus communis* (cultivars: Alexander Lucas', 'Conference', and 'Harrow Sweet) a high expression of *BIS2* gene in response to *E. amylovora* infection. In the similar plants, 3,4,5-trimethoxy biphenyl, aucuparin, 2'-hydroxyaucuparin and noreriobofuran were detected upon fire-blight infections. Although, core biphenyl-dibenzofuran biosynthesis is well studied, the early benzoic acid biosynthesis pathway remains poorly studied in Malinae. How benzoic acid and subsequent benzoyl-CoA is formed, what enzymes are involved in the benzoic acid biosynthesis in pears is still elusive.

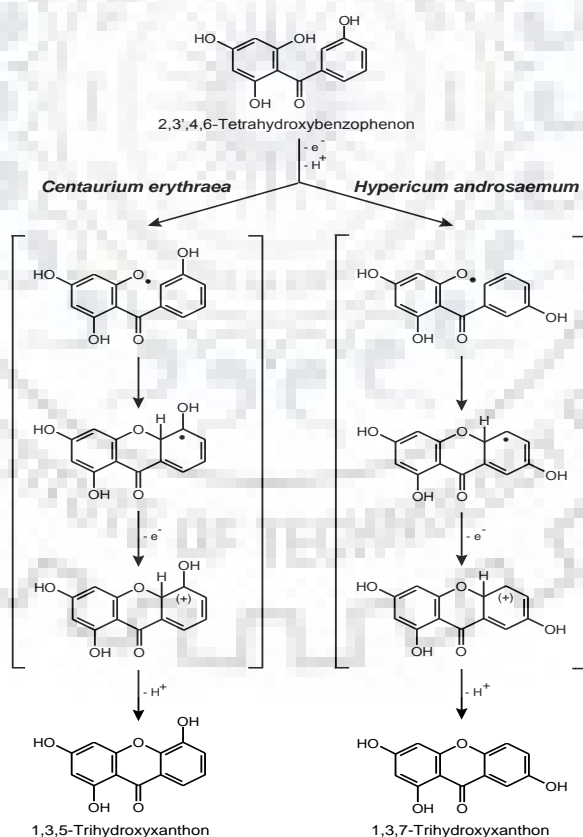


Fig. 1.9: Regioselective intra-molecular cyclizations of 2,3',4,6-tetrahydroxybenzophenone to isomeric xanthenes in cell cultures of *C. erythraea* and *H. androsaemum* (adopted from Peters et al., 1998).

1.12. Benzoic acid biosynthesis in plants:

Benzoic acid and its coenzyme A (CoA) derivative in plants acts as a central molecule for biosynthesis of several plant natural products which play crucial role as plant hormones, defense metabolites, co-factors, attractant for pollinators and seed dispersers (Abd El-Mawla and Beerhues, 2002). Benzoate-derived metabolites have high nutraceutical values for humans. Some of the benzoic acid like salicylic acid, forms volatile methyl esters called as methyl salicylate (MeSA), which serves as an airborne signaling molecules during pathogen attack (Baldwin et al., 2006; Park et al., 2007; Shulaev et al., 1997). Benzoyl-CoA serves as a precursor molecule for the biosynthesis of biphenyl and dibenzofuran class of phytoalexins in the Rosaceous sub-tribe Malinae (Saini et al., 2017).

In plants, benzoic acid is derived from cinnamic acid by C₂ shortening of the propyl side chain. Cinnamic acid, in turn formed from amino acid phenylalanine, in a reaction catalyzed by phenylalanine ammonia-lyase (PAL) (Chakraborty et al., 2009; Mir et al., 2013). PAL catalyzed formation of cinnamic acid is well established in plants (Mir et al., 2010). However, multiple biosynthetic pathways have been reported for C₂ chain shortening of cinnamic acid, proceeding either *via* a (1) CoA-dependent and β -oxidative mechanism; (2) CoA-dependent and non- β -oxidative and (3) CoA-independent and non- β -oxidative mechanism (Fig 1.10).

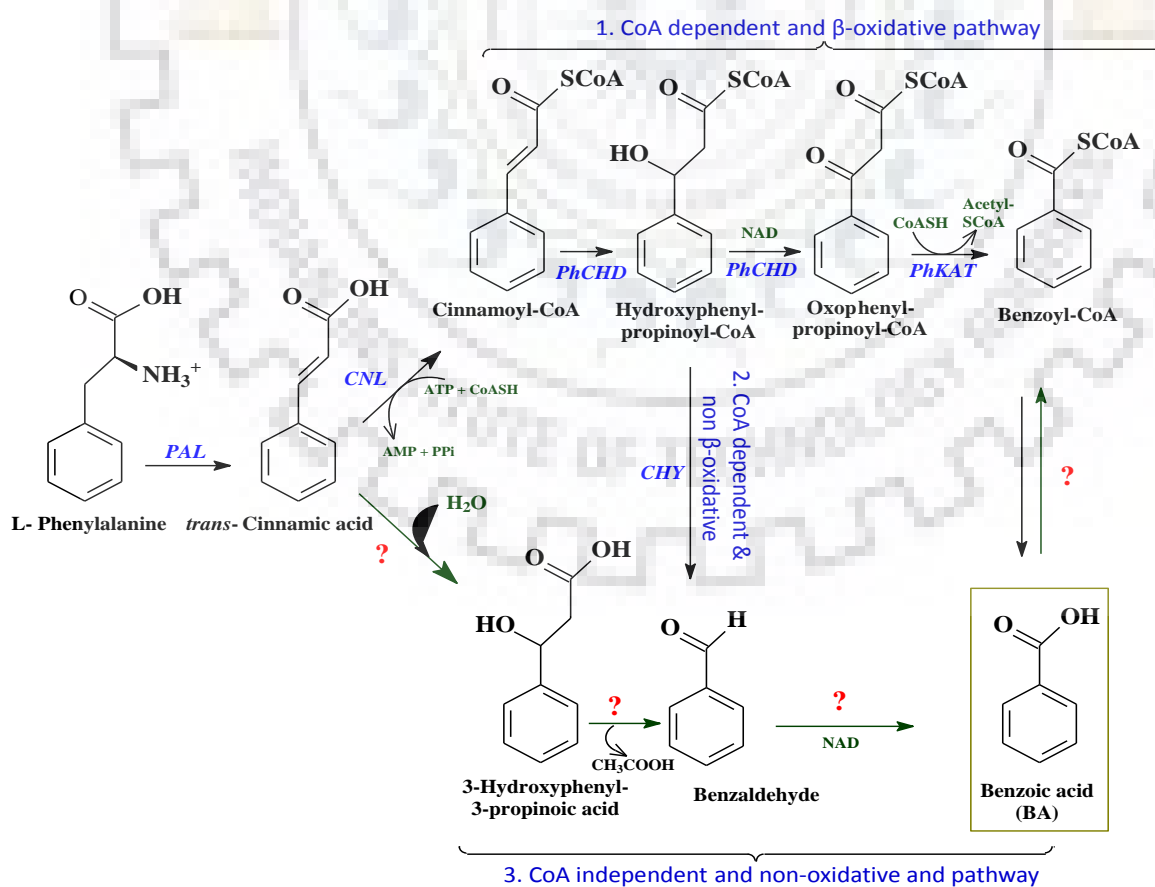


Fig. 1.10: Possible routes of benzoic acid biosynthesis in plants.





to methyl benzoate biosynthesis. Though benzaldehyde dehydrogenase activity has been well characterized in plants, the upstream chain shortening enzyme catalyzing the conversion of *trans*-cinnamic acid into benzaldehyde has not been identified in any plant system so far. Previously, analogous C₂-side chain shortening enzyme activity was previously shown by the 4-hydroxybenzaldehyde synthase (HBS), detected from few plant species. HBS-catalyzed conversion of 4-coumaric acid to 4-hydroxybenzaldehyde was detected in the tubers of *Solanum tuberosum* (French et al., 1976), in the cell cultures of *Lithospermum erythrorhizon* (Yazaki et al., 1991a), in *Daucus carota* (Schnitzler et al., 1992; Sircar and Mitra, 2008) and in the *Vanilla planifolia* cell culture (Podstolski et al., 2002) (Fig 1.14). A similar salicylaldehyde synthase (SAS) activity catalyzing conversion of *o*-coumaric acid to salicylaldehyde has also been observed in the *Nicotiana tabacum* (Fig 1.15) (Malinowski et al., 2007). An analogous pathway for formation of ferulic acid to vanillin by *VpVAN* gene has been cloned from *Vanilla planifolia* (Fig 1.16) (Gallage et al., 2014).

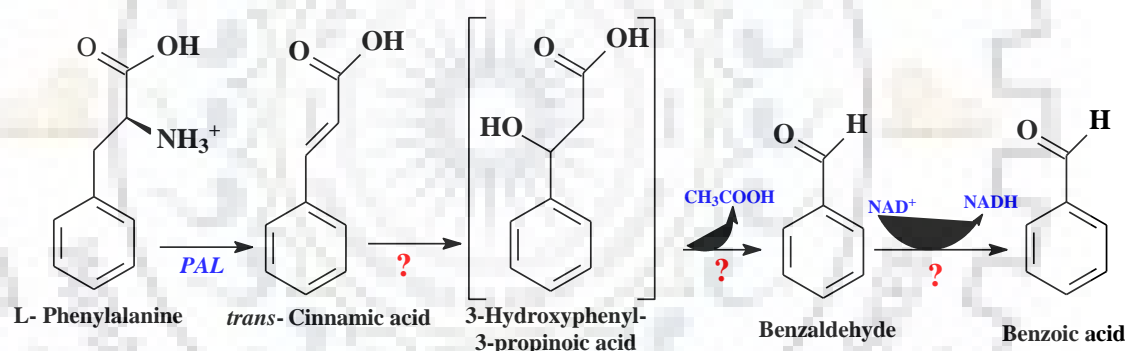


Fig. 1.13: CoA-independent and non β -oxidative route of benzoic acid biosynthesis in plants. [PAL = Phenylalanine ammonia-lyase]. Question marked reaction steps has not been yet identified for benzoic acid biosynthesis in Malinae.





intermediate formation of benzaldehyde. So far there is no information available of the C₂-chain shortening enzyme in this pathway from pear or any other member of Malinae. BZL activity has also not been reported from pear.

1.15. Understanding of benzoic acid biosynthesis in pear is important: Why?

Despite crucial role in biphenyl / dibenzofuran phytoalexin biosynthesis in pear, the enzymatic pathway of benzoic acid biosynthesis and subsequent formation of benzoyl-CoA is still unclear in pear and any other member of Malinae. This apparent complexity is probably due to the simplicity of this molecule and its evolving chemical and functional elaboration (Wildermuth, 2006). Evidence is building to support the idea that benzoic acid could be synthesized in pear from cinnamic acid involving one of the two possible C₂-chain-shortening routes. Till date, no detailed information on the particular enzyme(s) and gene(s) involved in benzoic acid biosynthesis in pear and Malinae is available (Saini et al., 2017). This incomplete knowledge of biosynthetic pathway is a major reason for designing any metabolic engineering strategy for enhancement of benzoic acid-derived phytoalexins. Any successful metabolic engineering venture for a desired natural product (with known structure), requires the following logical steps:

- Up-regulation of a particular natural product biosynthetic pathway by elicitor treatment (preferably) for enhanced production of metabolite of interest
- Identification of active enzymes involved in the biosynthetic pathway using cell free extracts, and their characterization
- Isolation of the corresponding full length cDNA of the target gene(s) usually by homology-based cloning followed by functional characterization of recombinant enzyme
- Metabolic engineering of target plants using target gene(s).

To detect enzyme activity *in vitro*, one needs to know the preferred substrate(s) of that enzyme. A metabolic pathway can be reconstructed by predicting intermediate reactions stepwise in the direction reverse to biosynthesis, from a given secondary compound to a starting basic metabolite. The chemical structures of natural compounds often give a clue to the selection of its precursor(s) and the reaction steps that have to take place to finish with the compound of

interest (Petersen, 2007). Therefore a complete understanding of the enzymes and genes involved in benzoic acid biosynthesis in pear may provide new insights on our understanding about the regulation and function of this important metabolite. This will also help in designing proper strategies for pathway manipulation for fortifying pear defense potential.

1.16. Aim of the work:

Benzoic acid is an important precursor of biphenyl / dibenzofuran biosynthesis in pears and other members of Malinae. However, enzymatic route of benzoic acid biosynthesis in pear is poorly understood, in particular the nature of C₂-side chain-shortening enzyme is enigmatic. The first aim of my doctoral thesis work is to perform a comparative leaf metabolomics of *Pyrus pyrifolia* and *Pyrus communis* to understand the role of basal metabolism in disease resistance. The second aim of my research is to elucidate the enzymatic steps involved in the benzoic acid biosynthesis and subsequent formation of benzoyl-CoA in the elicited cell suspension culture of *Pyrus pyrifolia* (Asian pear). The focus has been set on the detection and biochemical characterization of enzymes that catalyze C₂-side chain cleavage, intermediate dehydrogenation step and final benzoate-CoA ligase activity in benzoic acid biosynthetic pathway. The ultimate aim of this research is to improve our understanding of the benzoic acid biosynthesis in pear, so that metabolic engineering strategies can be successfully applied in the future to fortify disease resistance potential.

1.17. Objectives:

To fulfill described aim of research following objectives were set for present investigation:

1. To perform comparative leaf metabolomics of *Pyrus pyrifolia* and *Pyrus communis* to decipher the metabolites associated with the ontogenic resistance in *P. pyrifolia*.
2. To develop cell suspension culture of *P. pyrifolia*.
3. To study the accumulation pattern of biphenyl phytoalexins in cell cultures of *P. pyrifolia* upon elicitation.
4. To identify and biochemically characterize the enzymes of benzoic acid biosynthesis pathway in elicited cell cultures of *P. pyrifolia*.



Chapter 2

Materials and Methods

2.1. Chemicals:

Commonly used glass wares and chemicals of standard grade were purchased from following brands

Aldrich	Duchefa Biochemie	Rankem
Alfa Aesar	Genaxy	SRL
Borosil	Himedia	Sigma

The deionized water used for preparing media, buffers, HPLC solvents and aqueous solutions was obtained from Milli-Q water purification system (Millipore).

2.1.1. Special chemicals:

2.1.1.1. Chemicals used for Callus induction and maintenance of suspension culture:

Special chemicals used for callus induction and further in formation and maintenance of suspension culture are in [Table 2.1](#).

Table 2.1: Chemicals used for callus induction and suspension culture

Chemicals	Brand
6-Benzyl amino purine (6-BAP)	Himedia
2,4- Dichlorophenoxy acetic acid (2,4 D)	DuchefaBiochemie
Indole-3-acetic acid (IAA)	Himedia
α -Naphthalene acetic acid (NAA)	Himedia

2.1.1.2. Metabolite standards:

Various metabolite standards used as substrates and products in HPLC / GC-MS analyses are as follows (Table 2.2).

Table 2.2: Metabolite standards

Chemicals	Brand
Benzoic acid	Sigma
Benzaldehyde	Sigma
4-Hydroxybenzoic acid	Sigma
4-Hydroxybenzaldehyde	Sigma
3-Hydroxybenzoic acid	Sigma
3-Hydroxybenzaldehyde	Sigma
2-Hydroxybenzoic acid	Sigma
2-Hydroxybenzaldehyde	Sigma
Ferulic acid	Sigma
Vanillin	SRL
Vanillic acid	Sigma
<i>trans</i> -Cinnamic acid	Sigma
Cinnamaldehyde	Sigma
<i>p</i> -coumaric acid	Sigma
<i>o</i> -Coumaric acid	Sigma
Caffeic acid	Sigma
Protocatechuic acid	Sigma
Protocatechuic aldehyde	Sigma
Sinapic acid	Sigma
Syringaldehyde	Sigma
3,4,5-Trihydroxybenzaldehyde	Sigma
3,4,5-Trihydroxybenzoic acid	Sigma
L-Phenylalanine	Himedia
Benzoyl Co-A	Sigma
Malonyl-CoA lithium salt	Sigma-Aldrich
Aucuparin, and Noraucuparin	Synthesized in our research group

2.1.1.3. Enzyme assay / purification:

Co-factors, buffers and other chemicals used in enzyme assay and partial purification are listed in [Table 2.3](#).

Table 2.3: Chemicals used for enzyme assay / partial purification

Chemicals	Brand
DTT (dithiothreitol)	Sigma
HEPES Buffer	Sigma
Tris Buffer	SRL/Himedia
Ammonium acetate buffer	Himedia
NADP	Himedia
NAD	Himedia
FAD	Himedia
FMN	Himedia
ATP	Himedia
CoA (Coenzyme A)	Sigma
Polyvinylpyrrolidone	Himedia
Butylated hydroxyl toluene (BHT)	SRL
PD ₁₀ column	GE Health care

2.1.1.4. Elicitor used:

Yeast extract was used as elicitor to up-regulate biphenyl-dibenzofuran phytoalexins biosynthesis in cell cultures of *Pyrus pyrifolia* ([Table 2.4](#)).

Table 2.4: Elicitor used

Chemicals	Brand
Yeast extract	Himedia

2.2. Solvents & reagents:

Solvents and reagents were used for various experimental purposes are as follows (Table 2.5).

Table 2.5: Solvents and reagents

Solvents / reagents	Brand
Methanol (HPLC grade)	Merck
Ethanol (Rectified spirit)	Changshu Hyonsung chemicals
Ethyl acetate	Merck
Acetonitrile (HPLC grade)	Merck
Dichloromethane (HPLC grade)	Hi media
Sodium hypochlorite	Hi media
Folin-Ciocalteu reagent	Merck
Sodium carbonate	Hi media
DPPH	SRL
Aluminium chloride	Merck

2.3. Reagents for GC-MS analyses.

Chemicals used for GC- MS and reagents used for derivatization are as follows (Table 2.6).

Table 2.6: Solvents and reagents used for GC-MS analyses

Chemicals	Brand
Methanol (HPLC grade)	Merck
Ethyl acetate (HPLC grade)	Merck
Sodium sulphate	Himedia
Dichloromethane (HPLC grade)	Himedia
Phenyl phenol (internal standard)	Himedia
N-methyl-N-(trimethylsilyl)-trifluoroacetamide(MSTFA)	Sigma
Methoxy amine hydrochloride	Sigma
Pyridine (MB grade)	SRL

2.4. Equipments:

Equipment used for various analyses are listed in [Table 2.7](#).

Table 2.7: Equipment used.

Equipment	Model	Brand
Balance	ME 204 (mg range)	MettlerToledo
Centrifuge 1	1-14 K (cooling)	Sigma
Centrifuge 2	5810-R	Eppendorf
Rotary vacuum concentrator	Centrivap	Labconco
Incubator static	PT-420	Popular traders, Ambala, India
Incubator shaker	LSI 4018 R	Labtech
Vacuum pump	Millipore	Millipore
Vortex	3003-100	Rivotek
Hot plate	2MLH	Remi
Dry bath	MK-20 (pelltier controlled)	BiochemLifescience
Water bath	Rivotek	Polular Ltd
Digital pH meter	CL54	Toschon
Clean bench	Horizontal laminar flow	Clean air
Microwave oven	GMX20CA3	Godrej
Magnetic stirrer	MS 500	Remi
HPLC	LC- 20 AP HPLC pump SPD-M20A detector LC-Solution software	Shimadzu Shimadzu Shimadzu
GC-MS	Agilent 6890 gas chromatograph Agilent 5975C mass detector	Agilent Agilent
Spectrophotometer	Carry 400	Agilent
Thermocycler	Veriti	Applied Biosystem
Real time PCR system	Quant studio 3	Applied Biosystem

2.5. Nutrient media for plant tissue culture:

Readymade plant growth media (MS-media) was used for tissue culture (Table 2.8). 50 mL of media were poured into Erlenmeyer flask (250 mL capacity), then sealed with aluminum foil followed by autoclaving at 121⁰C for 20 min.

Table 2.8: Media composition for callus and suspension culture.

Medium	Brand name	Preparation & Storage
<p>A. For callus</p> <p>Murashige and Skoog (MS) medium (without sugar and hormone)</p> <p>For callus induction</p>	<p>Himedia, India</p>	<p>4.2 g media powder was dissolved in 800 mL of deionized water along with 30 g sucrose (3%), 2.2 μM BAP. pH was adjusted to 5.8 with 1 N NaOH, then adjust final volume to 1 L. Sterilize by autoclaving at 121⁰C for 20 min.</p> <p>For solid media, 0.7-0.8% agar was added prior to autoclaving.</p> <p>Stored at room temperature. Mostly used within 4-5 days.</p>
<p>B. For cell suspension culture</p> <p>Murashige and Skoog (MS) medium (without sugar and hormone)</p> <p>For Suspension culture</p>	<p>Himedia, India</p>	<p>4.2 g media powder was dissolved in 800 mL of deionized water along with 30 g sucrose (3%), 1 μM 2,4-D and 1 μM IAA. pH adjusted to 5.8 with 1 N NaOH, then adjust final volume to 1 L. Sterilize by autoclaving at 121⁰C for 20 min.</p> <p>Stored at room temperature. Mostly used within 4-5 days.</p>

2.6. Buffers and solutions for enzyme assay:

2.6.1. Buffer for enzyme extraction:

HEPES and potassium phosphate buffers were used for enzyme extraction of phenyl ammonia-lyase (PAL), benzaldehyde synthase (BS), benzaldehyde dehydrogenase (BD), benzoate-CoA ligase (BZL) and biphenyl synthase (BIS), respectively; as listed in (Table 2.9).

Table 2.9: Buffer used for enzyme extraction.

Name	Ingredient	Preparation & Storage
Extraction Buffers		
(A) For PAL, BS, BD (100 mM HEPES, pH 8.0 with 10 mM DTT).	HEPES buffer 2.4 g DTT 154 mg Water to 100 mL	Adjust pH 8.0 by 1 N NaOH, stored at 4 ^o C. DTT was added freshly. Polyclar AT was added before use.
(B) For BZL (100 mM potassium phosphate buffer, pH 7.5 with 2% Polyclar AT , 10mM DTT)	KH ₂ PO ₄ 1.36 g DTT 154 mg Water to 100 mL	Polyclar AT and DTT were freshly prepared and added during extraction. pH was adjusted by 1N KOH.
(C) For BIS (100 mM potassium phosphate buffer, pH 7.5 with 2% Polyclar AT , 1 mM DTT)	KH ₂ PO ₄ 1.36 g DTT 15.4 mg Water to 100 mL	Polyclar AT and DTT were freshly prepared and added during extraction. pH was adjusted by 1N KOH.

2.6.2. Buffer used for enzyme assay:

Following assay buffers were used (Table 2.10) to assay phenyl ammonia-lyase (PAL), benzaldehyde synthase (BS), benzaldehyde dehydrogenase (BD), benzoate-CoA ligase (BZL) and biphenyl synthase enzyme (BIS), respectively.

Table 2.10: Buffer used for enzyme assay

Enzymes to be assayed	Name of Buffer	Ingredient	Preparation & Storage
PAL	Assay buffer (100mM Tris-HCl, pH 8.6)	Tris buffer 1.21 g Water to 100 mL	Adjust pH by conc HCl, autoclaved and stored at 4 °C.
BS	Assay buffer (200mM Tris-HCl, pH 7.5; 10 mM DTT)	Tris buffer 2.42 g DTT 154 mg Water to 100 mL	Adjust pH by conc HCl, autoclaved and stored at 4 °C.
BD	Assay buffer (200mM Tris-HCl, pH 9.5)	Tris buffer 2.42 g Water to 100 mL	Adjust pH by conc HCl, autoclaved and stored at 4 °C.
BZL	Assay buffer (100 mM potassium phosphate -buffer, pH 7.5)	KH ₂ PO ₄ 1.36 g Water to 100 mL	Adjust pH by 1N KOH, autoclaved and stored at 4 °C.
BIS	Assay buffer (100 mM potassium phosphate -buffer, pH 7.5)	KH ₂ PO ₄ 1.36 g Water to 100 mL	Adjust pH by 1N KOH, autoclaved and stored at 4 °C.

2.6.3. Reagents used for protein estimation:

Bradford reagent was used for protein estimation ([Table 2.11](#)).

Table 2.11: Composition of Bradford reagent.

Name	Ingredient	Preparation & Storage
Bradford dye solution	Coomassie®-Brilliant Blue G 250 100 mg Ethanol (96%) 50 mL Orthophosphoric Acid(85%) 100 mL Water to 1000 mL	Dissolve well Coomassie®-Brilliant G 250 in ethanol, add Orthophosphoric acid and make up volume to 1 L with water. Filter the solution with filter paper (Whatman No. 1) and keep in refrigerator in dark bottle.

2.6.4. Solution for regeneration of PD₁₀ column:

Composition of washing solution used for regenerating PD₁₀ column was given in [Table 2.12](#).

Table 2.12: Composition of solution for washing and regenerating PD₁₀ column

Name	Ingredient	Washing procedure
NaOH Cleaning solution	NaOH 0.16 M	Wash PD10 column with five column volumes of NaOH cleaning solution followed by five volume of distilled water. After washing pH was checked pH (should be neutral) to confirm cleaning.

2.7. Reagents and enzymes used for molecular biology:

2.7.1. mRNA extraction, cDNA synthesis and real time PCR reagents:

Various reagents and enzymes used for mRNA extraction, cDNA synthesis and for real time PCR analyses are listed in [Table 2.13](#).

Table 2.13: Enzyme and reagents used in molecular biology.

Name	Brand
RNeasy plant mini kit (for mRNA extraction)	Qiagen
M-MuLV Reverse Transcriptase	NEB
M-MuLV Reverse Transcriptase Reaction Buffer (10x)	NEB
dNTPs	NEB
RibolockRnase inhibitor	Thermo scientific
Power Up™ SYBR™ Green Master Mix	Applied Biosystems

2.7.2. Buffer for DNA gel electrophoresis:

TAE buffer was used for DNA gel electrophoresis ([Table 2.14](#)).

Table 2.14: Composition of 50 X TAE buffer.

Name	Ingredient	Preparation & Storage
TAE Buffer	Tris HCL	2M
	EDTA	0.05M
	Water	upto 1000ml
		Store at room temp. Make 1x before use.

2.7.3. Primers for real time PCR analyses:

All primers used in various PCR amplifications were obtained from Eurofin genomics (Bangalore, India) details are given in [Table 2.15](#).

Table 2.15: Primers used in Real timePCR analyses

Gene name	Primer No.	Primer sequence (5' - 3')	GDR Accession No
<i>PAL</i>	1	TCCGGAGGCAGGAATCCTA	PCP008617.1
	2	GATGCCATGGCGATTTTCAG	
<i>C4H</i>	3	CCCACATGAACCTCCAGGAT	PCP002254.1
	4	TGCTCTCCGCCGGAATATC	
<i>F3H</i>	5	GGTTGTTGCAGCCTCTGCTT	PCP023049.1
	6	AATTGGCGTCATGGGTCTTC	
<i>AOX</i>	7	GGAGCGGCGACGGTTT	PCP016816.1
	8	GCGCGCTGCTCATCATC	
<i>Actin</i>	9	CTATGTTCCCTGGTATTGCAGACC	PCP017023.1
	10	GCCACAACCTTGATCTTCATGC	

2.8. Plant material:

Green house grown plants of *Pyrus pyrifolia* (Asian pear) and *Pyrus communis* (European pear) was used for metabolomics studies. Further, callus and cell suspension cultures were developed from *P. pyrifolia*. Pear plants were obtained from the **Central Institute of Temperate Horticulture** (ICAR-CITH), Srinagar, India. Pear plants were maintained in a green house at 25°C in Department of Biotechnology of Indian Institute of Technology Roorkee (Roorkee, India).

2.9. Comparative metabolomics of leaves of *P. pyrifolia* and *P. communis* by GC-MS based metabolomics approach:

2.9.1. Plant material and chemicals:

Two pear species, European pear (*Pyrus communis* L) ‘Bartlett’ and Asian pear (*Pyrus pyrifolia*) ‘Sand pear’ were selected for this study. Pear plants were maintained in a green house at 25 °C. Leaves from two year old pear plants were taken for the sample preparation. Before plugging, leaves were numbered from the top of the growing shoot toward the base, with leaf number one being the first youngest unfurled leaf. Leaf number 1 to 2 were pooled together before sample extraction and named as immature leaf (IL). Leaf number 10 and 11 from the top were pooled together and named as mature leaf (ML) to differentiate between the leaf age classes. Leaf samples were named as: *P. pyrifolia* immature leaf (PPIL); *P. pyrifolia* mature leaf (PPML); *P. communis* immature leaf (PCIL); and *P. communis* mature leaf (PCML). All extraction solvents used were of chromatography grade.

2.9.2. Extraction and sample preparation for GC-MS analyses of polar metabolites:

After plugging leaves were immediately rinsed in distilled water for 5 min with vigorous shaking followed by air drying. Dried leaf samples were crushed in liquid nitrogen. The extraction of polar metabolites for GC-MS analyses was performed following the protocol of (Kim et al., 2013) with suitable modifications. Extraction mixture was prepared by adding methanol/water/chloroform in 2.5:1:1 (v/v/v) ratio. One milliliter of pre-cooled (at -20 °C) extraction mixture was then added to 200 mg powdered leaf samples in a 1.5 ml micro centrifuge tube and vortexed vigorously at room temperature for 2 min. In order to identify extraction efficiency, 50 µL of 2-phenylphenol (2 mg/mL methanol stock) was spiked in the extraction mixture as the internal standard (IS) and re-vortexed for 1 min. The homogenized extracts were then centrifuged at 14000 g for 5 min. The resulting supernatant (0.8 mL) was transferred into a new 1.5 ml tube. Water (0.4 mL) was added to the supernatant, vortexed for 10 s and then centrifuged at 14000g for 5 min. The polar upper phase (methanol/water) was transferred to a new tube and used as Extract (1) for metabolite measurements by GC-MS. The second sample Extract (2) was prepared in the similar fashion (without addition of internal standard phenyl phenol) and used for the biochemical assays. The extract (2) was stored at -20 °C till analyses. The first extract was dried out in a vacuum concentrator (Labconco, Centrivap; USA) without heating for 2 h followed by freeze drying for 12 h in a lyophilizer. Finally dried

material was subjected to double derivatization for GC-MS analyses as described by (Lisec et al., 2006). For GC-MS derivatization, first derivatization was performed by dissolving the dried samples in 40 μ L of methoxyamine hydrochloride (stock solution: 20 mg/ml in pyridine) and incubating the solutions at 37 °C for 2h. Then second derivatization was performed by adding 80 μ L of N-methyl-N-(trimethylsilyl)-trifluoroacetamide (MSTFA) at 37 °C for 30 min. One derivatization reaction was also prepared using an empty reaction tube as a control.

2.9.3. GC-MS analyses:

GC- MS analysis was performed on Agilent GC-MS system comprising of Agilent 7890A gas chromatograph (Agilent technologies, CA, USA) coupled with an Agilent 5975C mass detector (Agilent technologies, CA, USA). Derivatized sample (1 μ L) was injected in GC-MS by automatic sampler (7683 B series, Agilent Technologies) with a split ratio of 1:10. Samples were separated on fused silica capillary column DB-5 MS (5 % phenyl methyl polysiloxane: 30m x 0.25mm i.d. x 0.25 μ m, Agilent technologies). The temperature program was as follows: Initial temperature of 80 °C for 1 min, followed by temperature increase to 220 °C at the ramp rate of 10 °C/min, followed by temperature increase to 310° at the ramp rate of 20 °C /min and finally a 15 min hold at 310° C. Total run time calculated was 34.5 min. Helium gas of ultra-high purity was used as carrier gas at a flow rate of 1ml/min. The inlet temperature and interface temp was set 280°C. The MS unit was tuned to its maximum sensitivity and the total ion current was recorded for mass range was m/z 80–700, and the detector voltage was set at 1700 V. Each sample was replicated three times. Scan was started after solvent delay of 7 min with scan frequency 4 S⁻¹ (2.0 HZ)

2.9.4. Metabolite identification:

Metabolites present in the leaf samples were identified by library matching of mass spectra of each compound (3:1 signal to noise ratio) using the NIST-11 mass spectral library (National Institute of Standards and Technology), and our in-house database that include several secondary metabolites, amino acids, organic acids, and sugar standards. Metabolite identity was obtained and reported only when the matching value of the mass spectra comparison was more than 75, and an increase in the area of the corresponding peak was observed when spiking the sample with the corresponding pure standard. In order to check for co-elution, the mass spectra

of all peaks were analyzed at three different points, beginning, middle, and end of each peak width. No coelution detected in any of the identified peaks.

2.9.5. Metabolite data pre-processing and statistical analyses:

Raw GC-MS data files obtained from Agilent ChemStation™ software were deconvoluted by Automated Mass Spectral Deconvolution and Identification System (AMDIS) using tools available with WsearchPro (www.wsearch.com.au). Metabolite data obtained were further converted into .csv (comma separated values) format before uploading. Finally the data obtained was normalized using internal standard. After that, the data were, log transformed with Pareto scaling (mean-centered and divided by the square root of standard deviation of each variable) followed by normalization before statistical analyses. Multivariate statistical analyses like ANOVA (using Fisher's LSD method; p value < 0.05), principal component analyses (PCA) were performed by using interactive online tool Metaboanalyst 3.0 (<http://www.metaboanalyst.ca>). The output for PCA data consisted of score plots for visualizing the contrast between different leaf samples and loading plots to explain the cluster separation. A heat map was created using interactive heat map tool of Metaboanalyst 3.0. A simplified metabolic pathway was manually constructed using information from the KEGG database via pathway analyses in Metaboanalyst 3.0.

2.9.6. Quantitative real time PCR:

Total RNA was isolated from the immature and mature leaf sample. An aliquot of total RNA (1 µg) was reverse transcribed at 42°C (Sircar et al., 2015). Quantitative RT-PCR was performed with the QuantStudio 3 Real-Time PCR System (Thermo Fisher Scientific) using Power Up™ SYBR™ Green Master Mix (Applied bio systems) following the manufacturer's instruction (Table 2.16 a). PCR program for each gene is given in Table 2.16 b. Melt-curve analyses was performed to evaluate gene-specific amplification. Amplification and correlation efficiencies of each PCR were determined using six serial dilutions of cDNA from all samples. The PCR efficiency was used to transform the cycle threshold values into raw data for relative quantification. Expression of the pear genes viz, *phenylalanine ammonia-lyase (PAL)*, *cinnamate-4-hydroxylase (C4H)*, *flavanone 3-hydroxylase (F3H)* and *alternative oxidase (AOX)* were evaluated using the gene-specific primers listed in (Table 2.15) [PAL: primers 1

forward and 2 reverse; *C4H*: primers 3 forward and 4 reverse; *F3H*: primers 5 forward and 6 reverse; *AOX*: primers 7 forward and 8 reverse]. Primers were designed based on the sequence of corresponding pear unigene present in GDR (Genome database of Rosaceae; www.rosaceae.org). All samples were normalized using mRNA of the reference gene, pear actin, as an internal control sample for each line (primers 9 forward and 10 reverse). Scaling of expression level was performed in relation to the respective mRNA expression levels in immature leaves of *P. pyrifolia*, which were set to 1. Three technical repeats were performed. Estimations of efficiency and expression level were based on the mathematical model of (Pfaffl, 2001). In Pfaffl method following algorithm was used calculate the Ct differences. The relative expressed level was calculated based on comparison with a reference gene.

$$\text{Ratio} = (E_{\text{target}})^{\Delta C_{\text{t}}_{\text{target}}(\text{control} - \text{sample})} / (E_{\text{ref}})^{\Delta C_{\text{t}}_{\text{ref}}(\text{control} - \text{sample})}$$

Table 2.16a: Composition of qPCR reaction.

Component	Volume	Remarks
Power Up™ SYBR™ Green Master Mix (2X)	5 µl	SYBR® Green I Dye, AmpliTaq Gold® DNA Polymerase, dNTPs with dUTP and buffer components.
Forward primer (10 pmole)	0.5 µl	Final concentration 0.125 µM
Reverse primer(10 pmole)	0.5 µl	Final concentration 0.125 µM
Template DNA	1 µl	Final concentration 1 ng
Water nuclease free	3 µl	Final volume to 10 µl

Table 2.16b: qPCR reaction program

Steps	Temperature °C	Time	Remarks
Initial denaturation	95	2 min	Denaturation and activation of the hot start Taq polymerase
Denaturation	95	15s	
Annealing	55 (<i>PAL; AOX</i>) 57 (<i>F3H</i>) 56 (<i>C4H</i>)	1 min	Veriflex step
Extension	72	1 min	Data acquisition
The last three steps are repeated for 40 cycles before the melt curve step			

2.9.7. Estimation of total phenolics content (TPC):

Total phenolic content was determined using Folin-Ciocalteu method (Singleton et al., 1999). Extract (2) obtained during extraction of leaf metabolites (in section 2.9.2) were dissolved in 500 µL of MeOH. Dissolved metabolites (100 µL) were used for the estimation of TPC. Briefly, 100 µL of extract was mixed with 500 µL Folin-Ciocalteu reagents (dilution 1:9 with water) and incubated at room temperature for 5 min to initiate the reaction. Thereafter, 400 µL of 5% sodium carbonate was added to the mixture followed by 20 min incubation in dark at room temperature. The absorbance was measured at 765 nm. Total phenolic content was expressed as micrograms of gallic acid equivalents per gram fresh mass.

2.9.8. Estimation of total flavonoids content (TFC):

Total flavonoids content was measured as essentially described by (Sarkate et al., 2017). Methanolic extract (100 µL of extract 2) was added to, 500 µL of 2% aluminium chloride

solution in ethanol and incubated at room temperature. After 1 h incubation, absorbance was measured at 420 nm. Total flavonoid content was expressed as micrograms of quercetin equivalent per gram fresh mass.

2.9.9. Free radical scavenging activity (FRSA):

FRSA or DPPH (1, 1-diphenyl-2-picrylhydrazyl) assay was performed as described by (Turkoglu et al., 2007). 200 μ L of methanolic extract was added to 800 μ L of 0.004% methanol solution of DPPH. After a 30 min incubation period at room temperature, the absorbance was measured at 517 nm using a blank. Blank reaction consisted of all reagents except the callus extract. Percent (%) inhibition of free radical by DPPH was calculated using following formula.

$$\text{Inhibition (\%)} = (A_{\text{blank}} - A_{\text{sample}} / A_{\text{blank}}) \times 100$$

The results were expressed as IC_{50} values. The EC_{50} value is the concentration of antioxidant required to lower the initial concentration of DPPH by 50%. Ascorbic acid was used as standard antioxidant. All experiments were performed in triplicates.

2.10. Chemical synthesis of aucuparin and noraucuparin:

Aucuparin and noraucuparin were synthesized from 3,4,5-trimethoxybiphenyl by following the protocols of Khalil. (2013) and Hüttner et al. (2010). First, 3,4,5-trimethoxybiphenyl was synthesized as described by Hüttner et al. (2010). Aucuparin was synthesized from 3,4,5-trimethoxybiphenyl by position selective single demethylation (removal of methoxy group at carbon no 4) using MgI_2 reagent (Bao et al., 2009). The second demethylation reaction was done by using BBr_3 to produce noraucuparin (Fig 2.1). Both aucuparin and noraucuparin was subjected to GC-MS analyses of their silylated-derivatives. In GC-MS, the temperature program was as follows: initial temperature of 70 $^{\circ}$ C for 3 min, followed by temperature increase to 300 $^{\circ}$ C at the ramp rate of 10 $^{\circ}$ C/min, followed by temperature increase to 310 $^{\circ}$ C at the ramp rate of 20 $^{\circ}$ C/min and finally a 3min hold at 300 $^{\circ}$ C. Total run time calculated was 29 min. Helium gas of ultra-high purity was used as carrier gas at a flow rate of 1ml/min. Split ration was 1/10. The MS scan range was set at m/z 80–600, and the detector voltage was set at 1700 V.



added in lieu of the YE. Three replicates were used for each treatment, and the experiment was repeated two times.

2.13. Extraction and HPLC analyses of phytoalexins:

Cell cultures were harvested at various post-elicitation time points [0, 12, 24, 48 and 72 hpe] by vacuum filtration. Phytoalexins were extracted in methanol from 1g cell mass as described previously (Hüttner et al., 2010). Briefly, 1g cell mass was homogenised in 2 mL of methanol, and the homogenate was centrifuged at 10,000 rpm for 20 min. The resulting supernatant was examined by HPLC for the presence of phytoalexins following the protocols of Teotia et al. (2016) with minor modifications. Separation was achieved on a PhenomenexTM (Torrance, USA) C₁₈ column (Synergi Hydro-RP: 250 × 4 mm, 4 μm) using a Shimadzu-HPLC system (Shimadzu Corporation, Kyoto, Japan) equipped with an SPD-M20A Photo Diode Array (PDA) detector. An isocratic solvent system comprising 1 mM TFA in water: methanol [60:40; (v/v)] with a flow rate of 1.0 mL/min for 60 min was used to elute the phytoalexins. The phytoalexins were identified by co-chromatography using authentic reference compounds at 269 nm.

2.14. Detection and characterization of benzaldehyde synthase (BS) activity from YE-treated cell suspension culture of *P. pyriformis*:

2.14.1. Cell culture condition and elicitation:

Pear (*P. pyriformis*) cell cultures were developed and maintained as described above. Cell cultures in the logarithmic growth phase (8th day old) were treated with yeast extract (YE) elicitor at a final concentration of 3 g/L. Elicitor-treated cells were harvested at defined post-elicitation time points: 0, 3, 6, 9, 12, 16, 18, 20 and 24 hours post elicitation (hpe) to prepare cell-free extracts for benzaldehyde synthase assay. Equal volume of sterile distilled water was added in the control treatments. All experiments were carried out at least in triplicates.

2.14.2. Precursor feeding experiments:

Precursor feeding experiments were performed to ensure whether *trans*-cinnamic acid to benzaldehyde conversion was really involved in benzoic acid biosynthesis and subsequent

formation of benzoate-derived biphenyl phytoalexins. *Trans*-cinnamic acid was dissolved in DMSO (50 % v/v with water), filter sterilized and subsequently fed to the cell culture (on 8th day of subculture) in a final concentration of 1mM simultaneously with the YE elicitor treatment. Control cultures were treated with an equal amount of only DMSO. After 24 h, the cells were harvested for phytoalexin analyses by HPLC.

2.14.3. Preparation of crude and partially purified enzyme extracts for benzaldehyde synthase (BS) assay:

Cell-free extracts were prepared according to (Sircar and Mitra, 2008) with minor modifications. All operations were carried out at 4 °C. Cell cultures were vacuum filtered and collected cell biomass (*ca.* 6 g) was slowly homogenized in 12 mL of 100 mM HEPES buffer, pH 8.0, supplemented with 10 mM dithiothreitol (DTT) and 1% (w/w) polyvinylpolypyrrolidone (PVPP). The resulting homogenate was centrifuged for 25 min at 14,000 x g and supernatant was used as a source of crude protein. To obtain partially purified cell-free extracts, ammonium-sulfate precipitation was performed by adding solid ammonium sulfate to the crude extract at 40% saturation, followed by 30 min incubation at 4°C. The precipitate was removed by centrifugation (20,000 g for 20 min) and the resulting supernatant was fractionated by hydrophobic interaction chromatography on Phenyl-Sepharose Cl-6B column. Column equilibration was done by Tris-HCl buffer (10 mM) at pH 7.0 containing 10 mM DTT (buffer X) with 2 M ammonium sulfate. The column was then washed with buffer X containing 2 M ammonium sulfate to elute all unbound proteins. BS activity was then eluted with ammonium sulfate gradient (1M). Fractions showing BS activity were pooled, concentrated using Amicon^R Ultra-4CFU membrane (Millipore, Bedford, USA) concentrator with 10 KDa cut off range followed by desalting using a PD₁₀ column (GE Healthcare) pre-equilibrated with 200 mM Tris-HCl buffer pH 7.5, containing 5 mM DTT. Soluble protein concentrations were estimated by Bradford method (Bradford., 1976) using bovine serum albumin (BSA) as standard protein for calibration.

2.14.4. Assay of benzaldehyde synthase (BS):

In vitro conversion of *trans*-cinnamic acid to benzaldehyde was monitored by HPLC to measure BS activity. The standard enzymatic reaction consisted of 50 µg partially purified enzyme extract, 10 mM *trans*-cinnamic acid and 10 mM DTT. Tris-HCl buffer (200 mM, pH

7.5) was used to adjust the final assay volume to 200 μ L. The assay was incubated at 35⁰C for 30 min; followed by termination of the reaction by adding 200 μ L of ice cold acetic acid/methanol (1:9, v/v). Stopped reaction product was centrifuged at 12, 000 x g for 15 min. The resulting supernatant was analyzed by HPLC for detection of BS activity. To check the effect of reducing agent in BS activity, separate reactions were performed with variable doses of dithiothreitol (2-20 mM); cysteine (2-20 mM), and β -mercaptoethanol (2-20 mM). Assay without any reducing agent and with boiled enzyme extract was set up to see if there was any non-enzymatic (spontaneous) conversion of *trans*-cinnamic acid to benzaldehyde. Three independent experiments were performed and mean values were calculated. For enzyme characterization, temperatures from 15⁰C to 65⁰C, pH values ranged from 5.5 to 11.5, incubation times from 1 to 90 min, and protein concentrations in the assay from 10 to 300 μ g, were tested. The stability of the enzyme was tested at room temperature, - 20⁰C and at 4 ⁰C for 24 h. In order to check the substrate specificity of BS, a set of potential substrates such as 4-coumaric acid, 2-coumaric acid, ferulic acid, caffeic acid and sinapic acid were tested at 10 mM concentration.

2.14.5. Analyses of BS catalyzed reaction by HPLC-DAD and GC-MS:

HPLC analyses was performed on a Shimadzu-HPLC system (Shimadzu Corporation, Kyoto, Japan), equipped with a CBM-20A controller, LC-20 AP pump, and a SPD-M20A Photo Diode Array detector. Data acquisition was done with Windows 7 based Lab Solutions Multi LC-PDA software (Shimadzu). Chromatographic separation was achieved on a SynergiTM Hydro RP (Phenomenex, USA) C₁₈ reverse phase column (250 x 4.6 mm, 4 μ m particle size) coupled with a Phenomenex Security GuardTM C₁₈ guard column 4 x 3 mm (Torrance, USA). BS reaction products were separated using an isocratic solvent system consisting of 1mM TFA in water and methanol [45:55; (v/v)] with a flow rate of 1.0 ml/min for 60 min. Detection wavelengths were 249 nm for benzaldehyde (product of *trans*-cinnamic acid), 280 nm for 4-hydroxybenzaldehyde (product of 4-coumaric acid), 256 nm for salicylaldehyde (product of 2-coumaric acid), 280 nm for 3,4-dihydroxybenzaldehyde (product of caffeic acid) and vanillin (product of ferulic acid) and 310 nm for syringaldehyde (product of sinapic acid) . The enzymatic products were identified in HPLC by comparing the retention time and DAD spectrum of the products with those of authentic standards.

For GC-MS analyses, the assay volume was increased to 1 mL. The reaction was stopped by adding 100 μ L of 3M trichloroacetic acid and extracted twice with equal volumes of

dichloromethane. Under the gentle stream of nitrogen, the organic phase in microvials were evaporated to dryness, In dried sample, 100 μ L of dichloromethane was added and then immediately analyzed by GC-MS without derivatization. GC-MS analyses was carried out using an 7890A gas chromatograph (Agilent technologies, CA, USA) coupled with an Agilent 5975C mass detector (Agilent technologies, CA, USA). Sample (1 μ L) was injected by automatic sampler (7683 B series, Agilent Technologies) with a split ratio of 1:5 and carrier (Helium) gas flow rate of 1mL/min. Samples were separated on fused silica capillary column DB-5MS (5 % phenyl methyl polysiloxane: 30m x 0.25mm i.d. x 0.25 μ m, Agilent technologies). The injector and transfer lines were set at 250⁰ C and 310⁰ C, respectively. The temperature program was set as: Initial temperature of 70⁰C for 3 min, followed by temperature increase to 310⁰ C and finally a 10 min hold at 310⁰ C. Linear interpolations of a set of hydrocarbons (even numbered C12 to C28) were used to calculate the retention index (RI).

2.14.6. Determination of kinetic parameters:

The kinetic properties of BS were determined using freely available software Hyper 32 (Sircar et al., 2011). For kinetic parameter determination, different concentration ranges of *trans*-cinnamic acid (0.05-20 mM) were used keeping DTT concentration fixed (10 mM). Three experiments were done for each value with independent enzyme preparations and mean the values were taken for the calculation of apparent K_m values using Hanes plot algorithm.

2.15. Detection and characterization of benzaldehyde dehydrogenase (BD) activity from YE-treated cell suspension culture of *P. pyrifolia*:

2.15.1 Cell culture condition and elicitation:

Elicitation was performed as exactly done for BS assay. Elicitor-treated cells were harvested at defined post-elicitation time points: 0, 3, 6, 9, 12, 16, 18, 20 and 24 hpe to prepare cell-free extracts for benzaldehyde dehydrogenase assay. Control treatment contained equal amount of water in lieu of YE. All experiments were carried out in triplicates.

2.15.2. Precursor feeding experiments:

To ascertain whether benzaldehyde-derived benzoic acid is the precursor for biphenyl phytoalexins, a feeding experiment was performed. Benzaldehyde was dissolved in DMSO (50

% v/v with water), filter sterilized and subsequently fed to the cell culture (on 8th day of subculture) in a final concentration of 1 mM at the same time as the YE elicitor. Culture treated with an equal amount of only DMSO served as control. After 24 h, the cells were harvested, extracted and analysed for phytoalexin content by HPLC.

2.15.3. Preparation of cell-free extracts for benzaldehyde dehydrogenase (BD) assay:

Cell-free extracts were prepared from elicitor-treated cell cultures at 0-4°C at defined post-elicitation time points (0, 3, 6, 9, 12, 16, 18, 20 and 24 hpe). Five grams of cells were collected by vacuum filtration, mixed with 10% (w/v) Polyclar AT (Lobachemie, India) and homogenized in 5 mL 100 mM HEPES buffer (pH 8.0) supplemented with 10 mM dithiothreitol (DTT). The homogenate was centrifuged at 12,000 x g for 25 min at 4°C. An of the supernatant (2.5 mL) was desalted through a PD₁₀ column (GE Healthcare) pre-equilibrated with 200 mM Tris-HCl buffer pH 7.5. Protein concentrations were determined according to [Bradford \(1976\)](#) using bovine serum albumin (BSA) as the standard.

2.15.4. Benzaldehyde dehydrogenase (BD) assay:

BD activity was determined by monitoring benzoic acid formation using HPLC as described previously ([Gaid et al., 2009](#)). The standard enzyme assay consisted of 0.5 mM benzaldehyde (substrate), 1 mM NAD⁺ and 100 µg protein. The final assay volume was adjusted to 200 µL with 200 mM Tris-HCl buffer pH 9.5. The reaction mixture was incubated at 40°C for 30 min. In separate reactions, NAD⁺ was replaced by 1 mM NADP⁺, 1 mM FAD and 1 mM FMN, respectively, to check the cofactor acceptability. Control assays contained boiled protein extract. The reaction was terminated by adding 200 µL of ice cold stopping mixture (methanol: acetic acid; 9:1 v/v) followed by centrifugation at 14000 x g for 15 min. Similar assay conditions were applied to other aromatic aldehyde substrates. The supernatant was directly analyzed by HPLC for product formation. Three independent experiments were performed, and mean values were calculated. For enzyme characterization, pH values ranged from 5.5 to 11.5, temperatures from 20°C to 60 °C, incubation times from 1 to 240 min, and protein concentrations in the assay from 1 to 320 µg. The stability of the enzyme was examined at room temperature, -20°C and at 4°C for 24 h. A spectrophotometric assay method was adopted for the aliphatic aldehyde substrates. The assay mixture contains 0.5 mM substrate, 1 mM NAD⁺ and 500 µg cell free extracts. The final reaction volume was adjusted to 1 mL with 200

mM Tris-HCl buffer pH 9.5. The activity was measured by monitoring the increase in the absorbance of NADH at 340 nm at 35 °C for 5 min. Assay without substrate used as blank. Molar absorption coefficient of NADH ($\epsilon_{340} = 6220 \text{ M}^{-1}\text{cm}^{-1}$) was used for the calculation of reaction rates.

2.15.5. Analyses of BD enzymatic products by HPLC-DAD:

The BD reaction product was analyzed on a Shimadzu-HPLC system (Shimadzu Corporation, Kyoto, Japan) equipped with an LC-20 AP pump, CBM-20A controller and an SPD-M20A Photo Diode Array [(PDA) 200 – 800 nm] detector. Chromatographic separation was achieved on a Phenomenex C₁₈Synergi™ Hydro RP reversed-phase column 250 × 4 mm, 4 μm particle size (Torrance, USA) coupled with a Phenomenex Security Guard™ C₁₈ guard column 4 × 3 mm (Torrance, USA). An isocratic linear solvent system of aqueous trifluoroacetic acid (70 %) and methanol (30 %) with a flow rate of 1 ml/min for 40 min was used to elute the BD reaction products. Detection wavelengths were 227 nm for benzoic acid and 2-hydroxybenzoic acid, 254 nm for 4-hydroxybenzoic acid and vanillic acid, 295 nm for 3-hydroxybenzoic acid, 280 nm for 3, 4-dihydroxybenzoic acid. The identity of the enzymatic products was confirmed by co-chromatography (HPLC) using authentic reference compounds. Data were acquired and processed with LC-Solution software (Shimadzu Corporation, Kyoto, Japan) on Windows 7™ platform.

2.15.6. Determination of kinetic parameters:

The kinetic properties of BD were determined using Hyper 32, a hyperbolic regression program for the analyses of enzyme kinetic data (Sircar et al., 2011). For kinetic parameter determination, different concentrations of benzaldehyde (0.005-1 mM) at a fixed concentration of NAD⁺ (2 mM) and different concentrations of NAD⁺(0.01-2 mM) at a fixed concentration of benzaldehyde (1 mM) were used. The experiments were repeated three times with independent enzyme preparation, and mean data values were taken for the calculation of *K_m* values using the HYPER 32 program. The apparent *K_m* values for the BD substrates were calculated from Hanes plots.

2.15.7. Identification of putative benzaldehyde dehydrogenase gene candidates in the pear genome:

The published aldehyde dehydrogenase superfamily 2 (*ALDH2*) gene sequences were used to search in the pear genome, which is available via the Rosaceae Genome Database (GDR: www.rosaceae.org). Pear sequences sharing a high degree of similarity (highest amino acid homology) with the published *ALDH2* gene sequences were filtered using the BLASTP search option in GDR. For each *ALDH2* query sequence, the two best pear candidates were selected based on highest homology matching ([Chagné et al., 2014](#)).

2.16. Identification and characterization of novel benzoate-CoA ligase (BZL) activity from YE-treated cell suspension culture of *P. pyrifolia*:

2.16.1 Cell culture condition and elicitation:

Elicitation was performed as exactly done for BS and BD assay. Elicitor-treated cells were harvested at 0, 3, 9, 12, 16, 18, 20 and 24 hpe to prepare cell-free extracts for BZL assay. Control treatment contained equal amount of water in lieu of YE. All experiments were carried out in triplicates.

2.16.2. Preparation of cell-free extracts for benzoate-CoA ligase (BZL) assay:

Cell-free extracts were prepared following the protocols of [Barillas and Beerhues. \(1997\)](#) with suitable modifications. Extraction was carried out at 4 °C. Vacuum filtered cell culture biomass (*ca.* 5 g) was slowly homogenized in 10 mL of 100 mM potassium phosphate buffer, pH 7.5, supplemented with 10 mM dithiothreitol (DTT), 2 % (w/w) polyvinylpyrrolidone, 1 mM PMSF and 2 mM ascorbic acid. The homogenate was centrifuged for 30 min at 14,000 x g and supernatant was used as a source of crude protein. To obtain partially purified cell-free extracts, ammonium-sulfate precipitation was performed by adding solid ammonium sulfate to the crude extract at 40% saturation, followed by 30 min incubation at 4°C. The precipitate was removed by centrifugation (20,000 g for 20 min) and the resulting supernatant was fractionated by ion-exchange chromatography. Supernatant was applied to the CM-Sepharose column (1.5 × 8 cm, Bio-Rad) pre-equilibrated with 100 mM potassium phosphate buffer pH 7.5. The flow through of CM column was collected and passed through DEAE-Sepharose column (1.5 × 10 cm, Bio-Rad), pre-equilibrated with 100 mM potassium phosphate buffer pH 7.5. The

bound proteins on DEAE column were eluted with a step gradient of NaCl in same buffer (50, 100, and 200, 500 and 1000 mM). Fractions showing BZL activity were pooled, concentrated using Amicon^R Ultra-4CFU membrane Millipore, Bedford, USA) concentrator with 10 KDa cut off range followed by desalting using a PD₁₀ column (GE Healthcare) pre-equilibrated with 100 mM potassium phosphate buffer pH 7.5. Protein concentrations were estimated by Bradford method (Bradford., 1976). This partially purified protein was used for BZL assay.

2.16.3. Assay of benzoate-CoA ligase (BZL):

BZL activity was measured by monitoring the in vitro conversion of benzoic acid to benzoyl-CoA using HPLC method. The standard enzymatic reaction consisted of 50 µg partially purified enzyme extract, 0.4 mM benzoic acid, 0.2 mM CoA, 2.5 mM ATP and 2.5 mM MgCl₂. The final assay volume was adjusted to 250 µL using potassium phosphate buffer (100 mM, pH 7.5). The assay was incubated at 30⁰ C for 2h; followed by reaction-termination by adding 10 µL of ice cold 3M tri-chloro acetic acid (TCA). Stopped reaction product was centrifuged at 12,000 x g for 15 min. The resulting supernatant was analyzed by HPLC for detection of BZL activity. For enzyme characterization, temperatures from 20°C to 60°C, pH values ranged from 5.5 to 11.5, incubation times from 5 to 120 min, and protein concentrations in the assay from 10 to 100 µg, were tested. The stability of the enzyme was tested at room temperature, - 20°C and at 4 °C for 24 h. For kinetic parameter determination, different concentrations of benzoic acid (1-1000µM) at a fixed concentration of CoA (0.5 mM), ATP(2.5 mM) and MgCl₂ (2.5 mM) were used.

2.16.4. Analyses of BZL catalyzed reaction by HPLC-DAD and ESI-MS:

HPLC analyses was performed on a Shimadzu-HPLC system (Shimadzu Corporation, Kyoto, Japan), equipped with a CBM-20A controller, LC-20 AP pump, and a SPD-M20A Photo Diode Array detector. Chromatographic separation was achieved on a LunaTM (Phenomenex, USA) C₁₈ reverse phase column (250 x 4.6 mm, 4µm particle size) coupled with a Phenomenex Security GuardTM C₁₈ guard column 4 × 3 mm (Torrance, USA). BZL reaction products were separated using an gradient solvent system consisting of 5mM ammonium acetate buffer pH= 5.7 as solvent A and acetonitrile as solvent B. Gradient was as 0% at 0 min for 2 min, 0 to 40% at 25 min, 40 to 100% at 28 min kept at 100% for 30 min then 0% B at 34 min and kept at 0% for 40 min with a flow rate of 1.0 ml/min. Detection wavelengths was 261 nm for benzoyl

CoA. The enzymatic products were identified in HPLC by comparing the retention time and DAD spectrum of the products with those of authentic benzoyl-CoA standard. The BZL reaction product was further confirmed by ESI-MS analyses. For ESI-LC-MS analyses of BZL products, the volume of enzyme assay was increased to 4 mL. CoA-ester was purified by solid-phase extraction using a Chromabond C (1000 mg) 18 ec cartridge (Macherey-Nagel) pre-equilibrated with consecutive washes of MeOH, H₂O, and ammonium acetate (4% solution; 5 column volume each time). The rest of the extraction procedure was exactly same as described by [Beuerle and Pichersky. \(2002a\)](#). Purified CoA-ester was dissolved in methanol and analyzed by a 3200 QTrap mass spectrometer (Applied Biosystem/MDS SCIEX) coupled with an ionization source (ESI, Turbo V). ESI was operated in the negative ion mode. Data acquisition and processing was done by the Analyst Software (Ver1.4.2) (Applied Biosystems). ESI conditions were exactly same as described by [Beuerle and Pichersky. \(2002a\)](#).

2.16.5. Substrate specificity test for BZL:

A luciferase-based assay system was used to evaluate substrate specificity of BZL ([Gaid et al., 2012](#)). An array of potential carboxylic acids was tested as substrate of BZL. The 200 μ L of final assay reaction contained carboxylic acid substrate (200 μ M), ATP (50 μ M), MgCl₂ (250 μ M), CoA (100 μ M), 10 μ g partially purified protein and 100 mM potassium phosphate buffer pH 7.5. The reaction mixture was incubated at room temperature for 2h, then 2 μ L sample was taken out and diluted to 100 μ L with 100 mM potassium phosphate pH 7.5) and put into a 96-microwell plate for analyses in a luminometer. Now 100 μ L of a second mixture containing 1 μ g luciferase (from firefly), 4.5 μ g luciferin (Sigma, India) and 100 mM potassium phosphate pH 7.5 was placed in the luminometer. Luminescence was measured after gentle shaking and 10 sec of time delay. The obtained raw data was transformed as relative luciferase activity, which inversely correlates with the ATP concentration. A reaction containing heat denatured protein was used to normalize the ATP quantification. Assay with denatured protein could not utilize ATP and thereby represents 100% ATP content.

2.17. Detection of biphenyl synthase (BIS) activity from YE-treated cell suspension culture of *P. pyrifolia*:

2.17.1 Cell culture condition and elicitation:

Elicitation was performed as exactly done for BS and BD assay. Elicitor-treated cells were harvested at defined post-elicitation time points: 0, 3, 6, 9, 12, 16, 18, 20 and 24 hpe to prepare cell-free extracts for biphenyl synthase (BIS) assay. All experiments were carried out in triplicates.

2.17.2. Preparation of cell-free extracts for biphenyl synthase (BIS) assay:

Cell-free extracts were prepared at 0-4°C. Freshly harvested cell culture (5 g) were mixed with 2 % (w/v) Polyclar AT (Lobachemie, India) and homogenized in 8 mL of 100 mM potassium phosphate buffer of pH 7.5 containing 1 mM freshly added DTT. The homogenate was centrifuged at 12,000 x g for 20 min at 4°C and supernatant was collected. Supernatant was subjected to ammonium sulphate precipitation. The protein fraction collected between 50 to 80% ammonium sulphate saturation was re-dissolved in 2.5 mL of 100 mM potassium phosphate buffer of pH 7.5, and immediately desalted by passing through a PD₁₀ column (GE Healthcare) pre-equilibrated with 100 mM potassium phosphate buffer pH 7.5. Protein concentrations were determined according to Bradford. (1976). This desalted protein was used as a source for BIS assay.

2.17.3. Biphenyl synthase (BIS) assay:

BIS activity was determined by monitoring the formation of 3, 5-dihydroxybiphenyl using HPLC. The standard enzyme assay mixture of 250 µL consisted of 6 µM benzoyl-CoA, 16µM of malonyl-CoA and 50 µg partially purified protein. The final assay volume was adjusted to 250 µL with 100 mM potassium phosphate buffer pH 7.5. The reaction mixture was incubated at 35 °C for 30 min. The reaction was stopped by adding 25 µL of ice cold acetic acid (50%), followed by centrifugation at 14000 x g for 15 min. Supernatant was extracted twice with 250 µL of ethyl acetate. Ethyl acetate phase was pooled together and evaporated to get dried sample. The dried sample was re-dissolved in 100 µL of methanol and analyzed by the HPLC for the detection of BIS product (3, 5-dihydroxybiphenyl).

2.17.4. Analyses of BIS reaction product by HPLC-DAD:

BIS reaction was separated on a PhenomenexTM (Torrance, USA) C₁₈ column (Synergi Hydro-RP: 250 × 4 mm, 4 μm) using a Shimadzu-HPLC system (Shimadzu Corporation, Kyoto, Japan) equipped with an SPD-M20A Photo Diode Array (PDA) detector. An isocratic solvent system comprising 1 mM TFA in water: methanol [60:40; (v/v)] with a flow rate of 1.0 mL/min for 60 min was used to elute the 3,5-dihydroxybiphenyl. BIS product (3,5-dihydroxybiphenyl) was identified based on co-chromatography with authentic 3,5-dihydroxybiphenyl reference. Detection wavelength was 261 nm.

2.18. Detection of phenylalanine ammonia-lyase (PAL) activity from YE-treated cell suspension culture of *P. pyriformis*:

2.18.1. Cell culture condition and elicitation:

Elicitation was performed as exactly done for BS and BD assay. Elicitor-treated cells were harvested at defined post-elicitation time points: 0, 3, 6, 9, 12, 16, 18, 20 and 24 hpe to prepare cell-free extracts for PAL assay. All experiments were carried out in triplicates.

2.18.2. Preparation of cell-free extract and assay of phenylalanine ammonia-lyase (PAL):

Cell-free extracts were prepared at 0-4°C as exactly mentioned for the preparation of cell-free extracts for BD assay (section 2.15.3). PAL activity was determined according to [Sircar and Mitra \(2008\)](#). The standard assay contained L-phenylalanine (20 mM) and 150 μg crude cell-free extract. The final assay volume was adjusted to 1 mL with 100 mM Tris-HCl buffer pH 8.6 and finally assay was terminated by adding 500 μL of 5 M HCl after 30 min incubation at 37 °C. The stopped assay mixture was centrifuged at 10,000 rpm for 10 min and supernatant was used for the detection of cinnamic acid by HPLC. Heat-denatured protein was used in control assay. Experiments were done in triplicates and average values were calculated. Cinnamic acid was separated and detected by HPLC using Waters SymmetryTM (Waters, Milford, MA, USA) C₁₈ reversed-phase column (3.5 μm, 75 x 4.6 mm). An isocratic solvent combination of 1mM trifluoroacetic acid in water (55%) and methanol (45%) with a 1 mL/min flow rate for 10 min was used to eluate the cinnamic acid. Cinnamic acid was monitored at 280 nm and quantified by co-chromatography using cinnamic acid standard. PAL activity was expressed as pkat/mg protein.



Chapter 3

Results

3.1. Comparative leaf metabolomics of two pear species at young and mature stage:

Pyrus pyrifolia (PP) and *Pyrus communis* (PC) differs in their susceptibility towards scab disease. *Pyrus pyrifolia* are very susceptible to *V. nashicola* infection but *Pyrus communis* are less susceptible. Similarly, *Pyrus pyrifolia* are resistant to infection by *V. pirina* due to non-host resistance; whereas *Pyrus communis* are highly susceptible to the *V. pirina* infections. The reason for these differences in basal metabolism and ontogenic resistance is not well understood. In order to gain insight into the status of basal constitutive metabolite level in *Pyrus pyrifolia* and *Pyrus communis* leaf grown under similar green house conditions, leaf metabolomic profiling was performed. Leaves of PP and PC were picked up at immature and mature stage (Fig 3.1) and their extracted metabolites were analyzed by GC-MS. In total, 93 metabolites were detected by the GC-MS analyses, out of which 30 metabolites were accurately identified based on library search on standard database [National Institute of Standards and Technology (NIST)], and in-house database at IIT Roorkee and then by confirming the metabolite identity with available standard spiking. The representative GC-MS (total ion current: TIC) chromatograms were shown in (Fig 3.2). Complete information on 30 metabolites identified by GC-MS was given in (Table 3.1). Metabolites were characterized based on their retention time and specific fragmentation pattern (Fig 3.3). Metabolites were further grouped into specific classes based on their chemical nature (Fig 3.4). The most represented classified metabolite groups were **amino acids** (04), **sugar alcohols** (4), **sugars** (4), **organic acids** (6), **phenolics** (10), and **vitamin** (2). The dominance of carbohydrates and phenolics detected in leaves of both PP and PC signifies their important role in plant metabolism and defense. In order to find out the metabolic differences between the leaves ages, the metabolic profile of *Pyrus pyrifolia* immature leaf (PPIL), *Pyrus pyrifolia* mature leaf (PPML), *Pyrus communis* immature leaf (PCIL) and *Pyrus communis* mature leaf (PCML) were compared with focus on following major metabolite classes:





Table 3.1: List of 30 identified metabolites from pear leaves. The peak area of the quantification ion was used for comparative quantification.

S. No	Metabolite	Derivate	KEGG ID	Retention Time	Qualification Ions [m/z]
1	Aspartic acid	3 TMS	C00049	13.52	349,334
2	Arbutin	6 TMS	C06186	24.22	450, 361
3	Ascorbic acid	4 TMS	C00072	18.26	449, 374
4	Benzoic acid	1 TMS	C00180	10.66	194, 179
5	p-OH Benzoic acid	2 TMS	C00156	15.65	282, 267
6	Caffeic acid	3TMS	C01481	19.4	396, 381
7	Catechin	5 TMS	C06562	25.27	649, 461
8	Chlorogenic acid	6TMS	C00852	29.97	419, 345
9	o- Coumaric acid	2 TMS	C01772	14.18	308, 293
10	p-Coumaric acid	2TMS	C00811	18.35	308, 293
11	t-Cinnamic acid	1 TMS	C00423	14.82	220, 205
12	Fructose	5 TMS	C02336	17.33	437, 347
13	Fumaric acid	2 TMS	C00122	11.32	245, 230
14	D- Glucose	5 TMS	C00031	18.17	358, 319
15	Glycolic acid	2 TMS	C00160	13.53	205, 177
16	Glycerol	3 TMS	C00116	16.69	293, 218
17	Glycine	2 TMS	C00037	9.33	204, 176
18	Malic acid	3 TMS	C00149	14.41	335, 319
19	Mannose	5 TMS	C00159	18.81	435, 393
20	Mannitol	6 TMS	C00392	24.85	421, 319
21	Myo-inositol	6 TMS	C00137	19.18	432, 318
22	Proline	2 TMS	C00148	11.85	259, 216
23	Protocatechuic acid	3TMS	C00230	17.36	370, 355
24	Pyruvic acid	2 TMS	C00022	7.58	232, 217
25	3- Phosphoglyceric acid	4 TMS	C00197	14.58	292, 133
26	Serine	3 TMS	C00065	12.75	306, 218
27	D-Sorbitol	6 TMS	C00794	24.89	497, 421
28	Succinic acid	2 TMS	C00042	12.03	247, 218
29	Sucrose	8 TMS	C00089	21.63	451, 437
30	α -Tocopherol	1 TMS	C02477	30.67	502, 487







3.1.3. Sugars (04):

Sucrose, glucose, fructose and mannose sugars were detected from leaves of PP and PC (Fig 3.5 I-L). These sugar molecules generally stem from photosynthesis and storage reserves (Kunz et al., 2014). Glucose and fructose is derived from sucrose after hydrolyses. Moreover, fructose transforms into mannose. Sucrose and mannose levels were higher in PC. Our results showed that, in PC leaves as compared to PP leaves. This indicates that sucrose catabolism was higher in PP. Likewise, glucose and fructose levels were also higher in PC leaves, which is probably due to increase turnover number of glycolyses and subsequent TCA cycle in PP. This hypothesis was further supported by enhanced accumulation of intermediates of glycolyses and TCA cycle in PP leaves. Conversion of fructose to mannose was down regulated in PP, resulting into lower mannose accumulation in PP leaves.

3.1.4. Organic acids (06):

The levels of all identified organic acids (3-phosphoglyceric acid, pyruvic acid, succinic acid, fumaric acid, malic acid and glycolic acid) were higher in the PP leaves with highest accumulation in mature leaves (PPML > PPIL) (Fig 3.5 M-R). We hypothesized that, high organic acid accumulation was due to higher turnover number of glycolysis and TCA cycle.

3.1.5. Vitamins (02):

Among vitamins, ascorbic acid (vitamin C) and α -tocopherol (vitamin E) were identified in the leaves of both the *Pyrus* species (Fig 3.5 S-T). Ascorbic acid level was higher in the PP with more accumulation in mature leaves. In both the species, mature leaves had higher ascorbic acid content than that of immature leaves. Ascorbic acid is known to fortify defense responses in many plant species (Pastori et al., 2003). The amount of α -tocopherol remained almost unaltered in both the species with higher accumulation pattern observed in the mature leaves (Fig 3.5 T). In plants, tocopherols (vitamin E) comprise of four types (α , β , γ , and δ form) of lipid-soluble antioxidants which has prominent role in plant defense (Atanasova-Penichon et al., 2016).

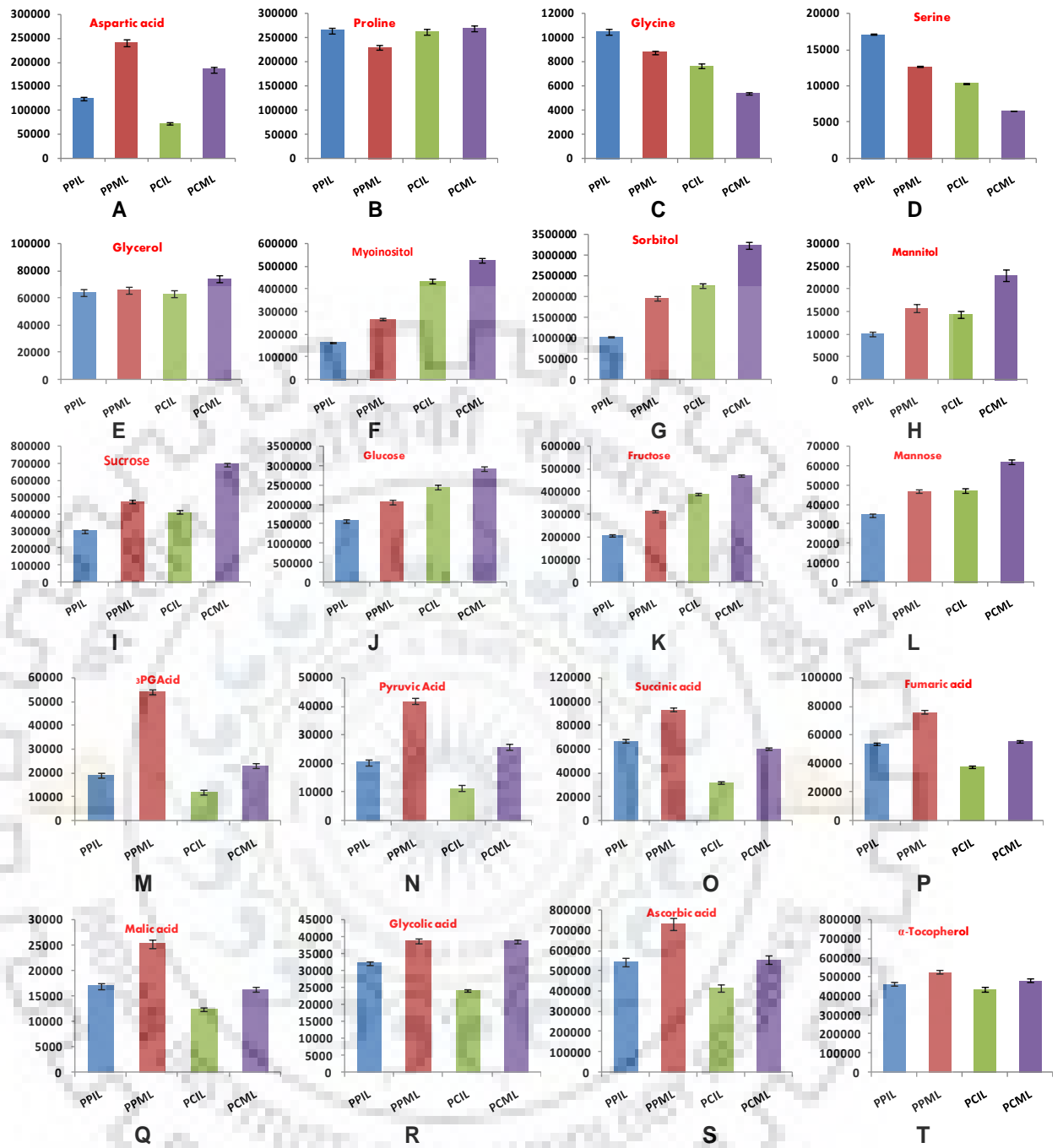


Figure 3.5: Leaf metabolites showing significant differences among *P. pyrifolia* and *P. communis*. Amino acids (A-D); Sugar alcohols (E-H); Sugars (I-L); Organic acids (M-R); Vitamins (S-T). Error bars represent standard deviations. PPIL: *P. pyrifolia* immature leaf; PPML: *P. pyrifolia* mature leaf; PCIL: *P. communis* immature leaf; PCML: *P. communis* mature leaf.



A similar accumulation pattern was observed for chlorogenic acid, caffeic acid, protocatechuic acid, and *trans*-cinnamic acid with higher accumulation in the PPML. However, the contents of catechin, *o*-coumaric acid and *p*-coumaric acid were higher in PC leaves, with more accumulation in mature leaves than that of immature leaves. *p*-Hydroxy benzoic acid was only detected in immature leaves of both the pear species with higher accumulation in PP (Fig 3.6 F). No significant difference was observed in arbutin content among both the species.

3.2. Principal component analyses (PCA) reveals changes in leaf metabolite profile between two pear species:

In order to detect changes in metabolite profile between immature and mature leaves of PP and PC, GC-MS analyses were performed. The systemic variations between the samples were analyzed by PCA. The dimensionality of complex data sets is reduced by PCA, which helps to better visualize the inherent patterns in the data. PCA analyses uses, orthogonal linear transformation of the original data variables to generate a new set of uncorrelated variables known as principal components (PCs) (Park et al., 2015). As shown in (Fig 3.7), the first and second PCs of the analyzed PCA score plot represented 56.3% (PC1) and 38.3 % (PC 2) of the total variance of the samples. The variance of the differences in metabolites among leaf sample was successfully recorded in the two PCs. The PC 1 determined the metabolomics profiles of PP and PC leaves. The Metabolomics profile between immature and mature leaves was separated by PC 2. Furthermore, a PCA loading plot (Fig 3.7 B) was constructed to show the abundant variable (metabolites) contributing the PCA results. Metabolites included in loading plot were differentially accumulating 30 metabolites as shown in Table 3.1.



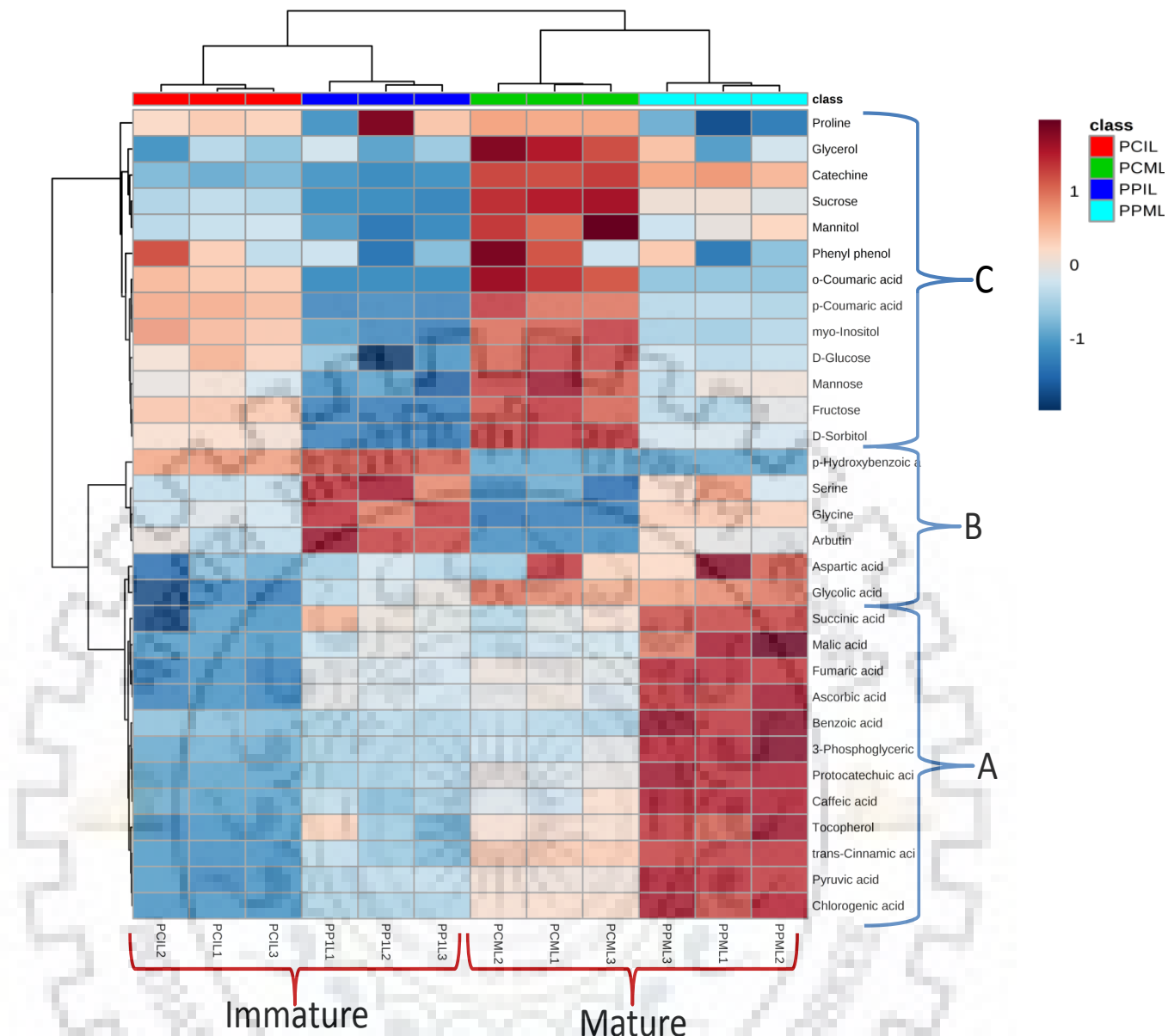


Figure 3.8: Hierarchical clustering analyses of 30 detected metabolites from *P. pyrifolia* and *P. communis* leaves at immature and mature stage. Similarity assessment for clustering was done on the basis of Elucidean distance coefficient and the average linkage method (metaboanalysts 3.0). Rows and columns represent individual metabolites and different samples, respectively. The change in metabolite levels was organized in three clusters named as A, B and C. [**Cluster A:** metabolites with higher concentration in *P. pyrifolia* were grouped; **cluster B:** metabolites that had same changing patterns in both *Pyrus* species; **cluster C:** metabolites which has more abundance in *P. communis* than that of *P. pyrifolia*].

3.4. Changes in metabolic pathways: metabolic pathway network:

A simplified metabolic pathway was reconstructed using key metabolic pathways, such as the glycolytic pathway, the pentose phosphate pathway, the shikimic acid pathway, the phenylpropanoid pathway, the biphenyl phytoalexin biosynthetic pathway, the flavonoids biosynthesis pathway, the amino acid biosynthetic pathway and the TCA cycle to show the regulated pattern diversity of each detected metabolites with respect to their proportional incorporation into key metabolic pathways. As shown in Fig 3.9, sucrose, as the precursor for glucose and fructose was higher in PC than PP. Nevertheless, glucose and fructose derived from the hydrolysis of sucrose were in higher amount in the mature leaves of PP than those of PC, suggesting that more active sucrose metabolism occurring in the mature leaves of PP. The level of mannose, sorbitol and manitol were higher in PC leaves suggesting that fructose is metabolized more towards these metabolites rather than re-entering into glycolytic pathway through fructose-6-phosphate. Metabolites of glycolyses pathway, especially pyruvic acid and 3-phosphoglyceric acid level were up accumulated in the *P. pyrifolia* leaves whereas amino acid levels remained mostly unaltered among PP and PC leaves. Aspartic acid level, however, were higher in the PP leaves. The level of identified TCA cycle metabolites such as succinic acid, malic acid and fumaric acid, were up-accumulated in leaves of PP. The metabolites derived from shikimate pathway showed an absolutely distinct accumulation pattern. Except for *o*-coumaric acid and *p*-coumaric acid, the level of rest of the identified shikimate pathway derived metabolites such as benzoic acid, catechin, chlorogenic acid, caffeic acid, protocatechuic acid and *trans*-cinnamic acid were higher in the leaves of PP with more accumulation in mature leaves as compared to the immature leaves. In contrary, 2-coumaric acid and *p*-coumaric acid level were higher in the PC leaves. No significant variation in the level of *p*-hydroxybenzoic acid was detected among the two species. Tocophenol and ascorbic acid levels were identical in both the species. Arbutin, a glycosylated hydroquinone, level remained almost same in both the species.



3.5. Expression analyses of phenylpropanoid biosynthetic genes in the leaves of both *Pyrus* species:

Since the level of phenolics were significantly higher in the leaves of PP than that of PC, we have examined the expression levels of four genes (*PAL*, *C4H*, *F3H* and *AOX*) related to phenylpropanoid and flavonoids biosynthesis in the immature and mature leaves of both the pear species using qRT-PCR. For qPCR analyses, efficiency of qPCR reaction with the designed primer was checked. Efficiency was calculated with the formula $E = 10^{(-1/\text{slope})}$. Efficiency was obtained by plotting the cDNA concentrations against Ct values. Ideally efficiency should be within 90-100% but sometime low efficiency (80%) also works (Pfaffl., 2001). Specificity of the PCR product was checked by agarose gel electrophoresis and by melt curve analyses using a built PCR program of Quantstudio 3. Efficiency test results are mentioned in Table 3.2.

Table 3.2: Efficiency test for qPCR reactions. PCR efficiencies are the average of three independent reaction \pm SD

Gene name	qPCR efficiency (%) ^a
<i>PAL</i>	92.4 \pm 2.2
<i>C4H</i>	94.1 \pm 2.6
<i>F3H</i>	89.8 \pm 1.6
<i>AOX</i>	95.2 \pm 2.4
<i>Actin</i>	93.0 \pm 2.5

^a = average of 3 replications \pm SD

The expression levels of *PAL*, *C4H*, *F3H* and *AOX* are shown in (Fig 3.10). The expression levels of the above mentioned genes, with the exception of *C4H* and *F3H*, were highest in the PPML, demonstrating that phenylpropanoid biosynthesis was highest in the mature leaves of PP. This was well correlated with the enhanced accumulation of phenyl propanoids such as cinnamic acid in the mature leaves of PP. Enhanced expression of *PAL* gene is known to be associated with increase in the phenylpropanoid biosynthesis (Mukherjee et al., 2016; Sil et al.,



3.6. Total phenolics (TPC), total flavonoid (TFC) and free radical scavenging activity (FRSA):

TPC, TFC and FRSA of immature and mature leaves of both the *Pyrus* species were listed in Table 3.3. PPML showed the highest value of TPC followed by PPIL. The TPC values of PC leaves (PCML and PCIL) were significantly lesser than that of PP leaves. TFC content was, however higher in the PC as compared to PP. Highest accumulation was observed in PCML. A significantly higher TPC value in the leaves of PP indicated that TPC contents were directly correlated with the high amount of phenolics in PP as compared to PC leaves. Similar to TPC, FRSA activity were of highest in the PPML ($IC_{50} = 74 \pm 5.0 \mu\text{g/mL}$) followed by PPIL ($IC_{50} = 102 \pm 9.0 \mu\text{g/mL}$). These significant correlations could be due to the use of methanol (2 in the extraction process) which was known to be an efficient extraction solvent for phenolics (Belkheir et al., 2016; Visweswari et al., 2013).

Table 3.3: Total phenolics (TPC), total flavonoid (TFC) and DPPH free radical scavenging activity (FRSA) of pear leaves. Data are the mean \pm SD of three independent experiments. PPIL: *P. pyrifolia* immature leaf; PPML: *P. pyrifolia* mature leaf; PCIL: *P. communis* immature leaf; PCML: *P. communis* mature leaf

Test	PPIL	PPML	PCIL	PCML
TPC ($\mu\text{g GAE/g FW}$)	265 ± 11.7	326 ± 16.3	218.3 ± 8.5	276 ± 11.7
TFC ($\mu\text{g QE/g FW}$)	32 ± 4.0	40 ± 2.6	38 ± 6.0	49 ± 6.5
FRSA ($IC_{50} \mu\text{g/mL}$)	102 ± 9.0	74 ± 5.0	128 ± 7.0	96 ± 7.5

3.7. Chemical synthesis of aucuparin and noraucuparin:

Since aucuparin and noraucuparin are not available commercially, they were synthesized following the published protocols. The starter substrate for the synthesis of both aucuparin and noraucuparin was 3,4,5-trimethoxybiphenyl, which was synthesized as described by Hüttner et al. (2010). Newly synthesized aucuparin and noraucuparin were derivative with MSTFA and subjected to GC-MS analyses. Chemical identity of newly synthesized aucuparin and noraucuparin was confirmed by comparing the mass spectrum with authentic aucuparin and

noraucuparin (obtained from Prof. L. Beerhues, TU-BS, Germany as gift). Silylated-derivative of aucuparin showed molecular ion peak of 302.10 (Fig 3.11A) and noraucuparin showed molecular ion peak of 360.20 (Fig 3.11B), which is the characteristic identity as per published record (Hüttner et al., 2010; Khalil, 2013). Since mass-spectrum were in complete agreement with the standard aucuparin and noraucuparin, no further structural confirmation was performed. Both these aucuparin and noraucuparin were dissolved in methanol (100%) at 50 mM final concentration and stored at -20°C till further use.

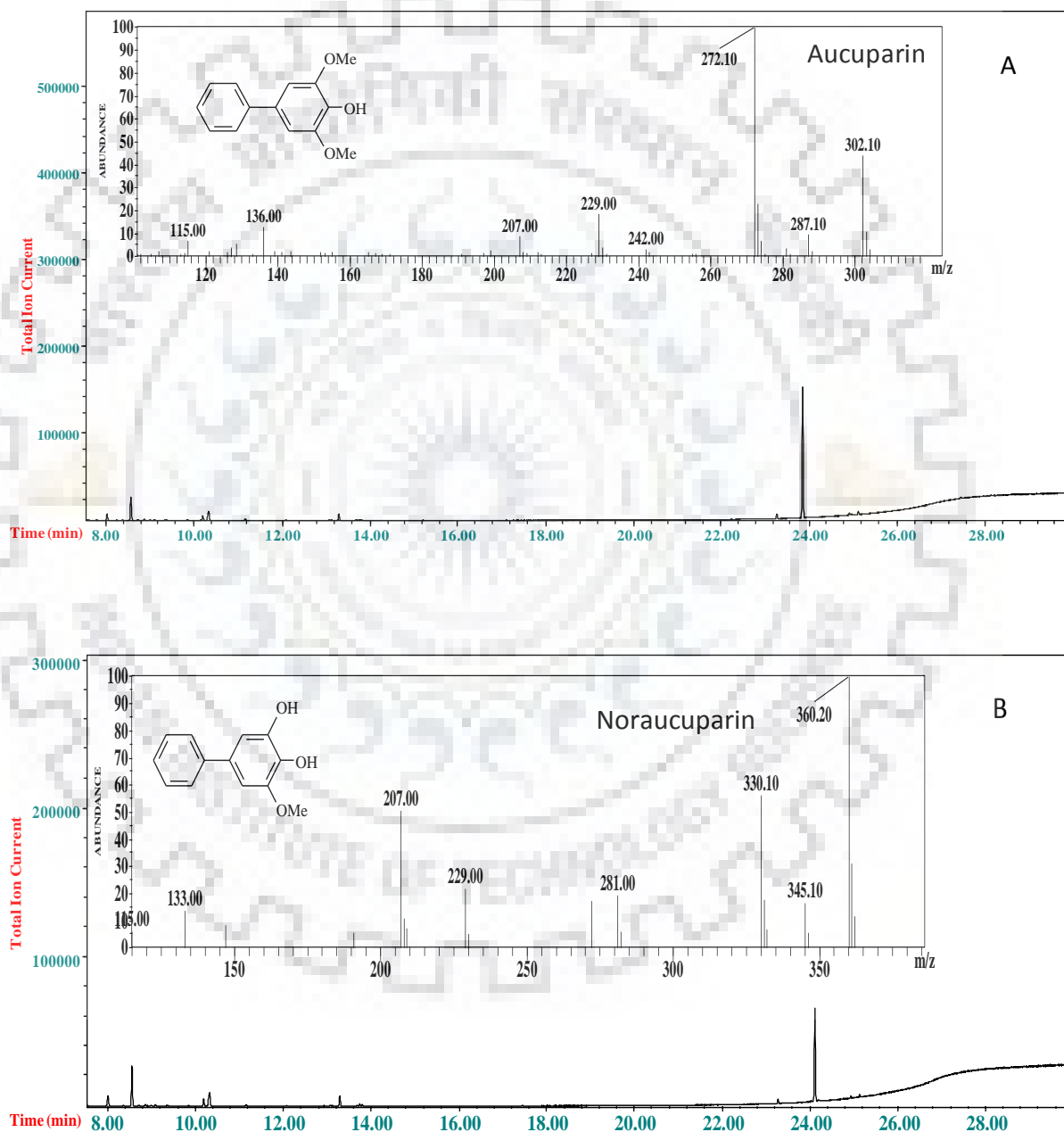


Figure 3.11: TIC and mass-spectrum (GC-MS) of chemically synthesized aucuparin (A) and nor-aucuparin (B).









ended with 3,5-dihydroxybiphenyl (Fig. 3.16). The chemical structures of natural compounds provided the clue to re-construct the metabolic pathway the selection of its precursor(s) and the reaction product. This process was applied to elucidate and characterize the sequence of predicted biosynthetic steps leading to formation of 3,5-dihydroxybiphenyl, the precursor of noraucuparin and aucuparin.

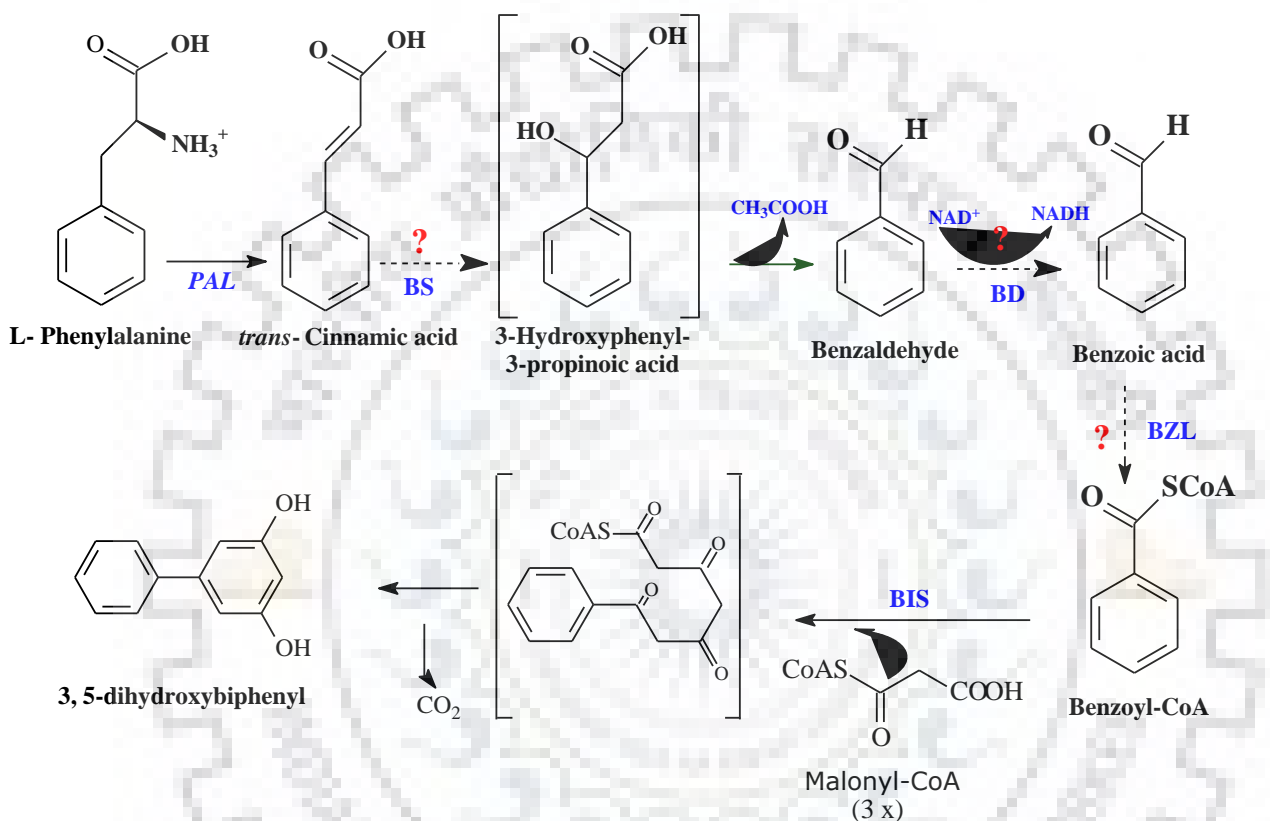


Figure 3.16: Predicted biosynthetic pathway of benzoic acid and benzoyl-CoA in pear. [*PAL* = Phenylalanine ammonia-lyase; *BS* = biphenyl synthase; *BD* = benzaldehyde dehydrogenase; *BZL* = benzoate-CoA ligase; *BIS* = biphenyl synthase]. Question marked reaction steps drawn with dashed arrow has not been yet identified for benzoic acid biosynthesis in pear or any other Malinae. Solid arrow showed established reactions.

3.10.1. Detection and characterization of benzaldehyde synthase (BS) activity from yeast-extract (YE)-treated cell suspension culture of *Pyrus pyrifolia*:

Benzaldehyde synthase (BS) activity catalyzing the *in vitro* conversion of *trans*-cinnamic acid to benzaldehyde was detected from the elicited cell cultures of *P. pyrifolia*.

3.10.1.1. Effects of precursor feeding (*trans*-cinnamic acid) on biphenyl phytoalexin accumulation

In *trans*-cinnamic acid fed YE-treated cell cultures, higher accumulation biphenyl phytoalexins (noraucuparin and aucuparin) were observed (Fig. 3.17). Compared to cultures treated with elicitor alone, values of noraucuparin and aucuparin in *trans*-cinnamic acid-fed cultures were higher by 1.4-fold and 1.2-fold, respectively. Further, in *trans*-cinnamic acid fed cultures, detectable accumulation of *trans*-cinnamic acid (0.4 $\mu\text{g/g}$ FW), benzaldehyde (1.8 $\mu\text{g/g}$ FW) and minor amount of benzoic acid (0.6 $\mu\text{g/g}$ FW) was also observed. Any detrimental effect was not observed in only DMSO (50 % v/v with water) fed cultures.

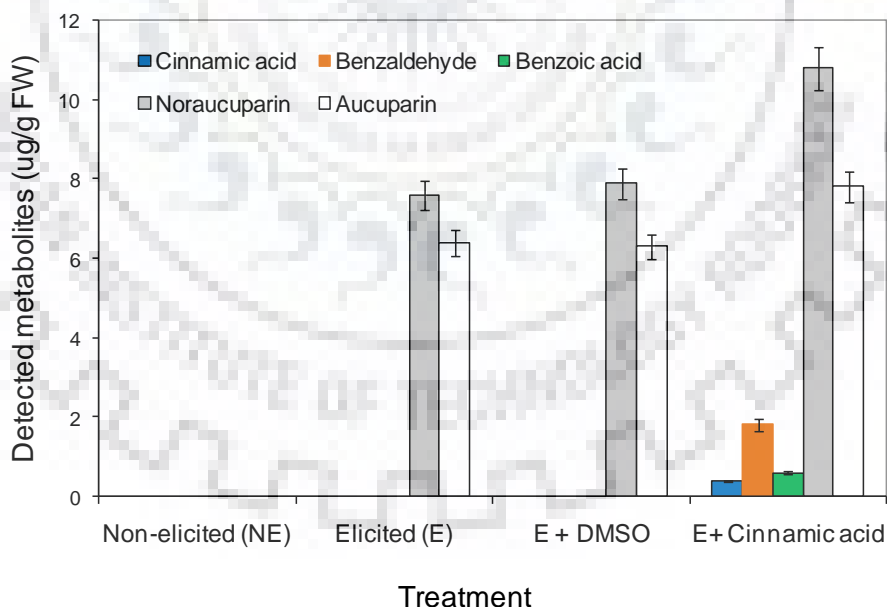


Figure 3.17: Effect of feeding *trans*-cinnamic acid on aucuparin and noraucuparin accumulation in yeast extract-treated cell cultures of *P. pyrifolia*. Results are the mean \pm SD of triplicate analyses.

3.10.1.2. *In vitro* conversion of *trans*-cinnamic acid to benzaldehyde:

In order to access the presence of benzaldehyde synthase (BS) activity, partially purified enzyme extracts (see section “2.14.3” under materials and method) were prepared from YE-treated cell cultures and incubated with *trans*-cinnamic acid and dithiothreitol (DTT). Subsequent HPLC analyses revealed the formation of benzaldehyde (Fig. 3.18) suggesting *in vitro* conversion of *trans*-cinnamic acid to benzaldehyde by the cell-free extract. The enzymatic product formation was identified by co-chromatography with authentic benzaldehyde standard (by matching the retention time and DAD spectrum). The product identity was further confirmed by mass-spectrum matching in GC-MS analyses (Fig 3.19). In control reaction containing heat-denatured protein, a slow but spontaneous conversion of *trans*-cinnamic acid to benzaldehyde (6-10 % of actual product formation in 30 min) was observed in the presence of DTT or other reducing agents (Table 3.4).

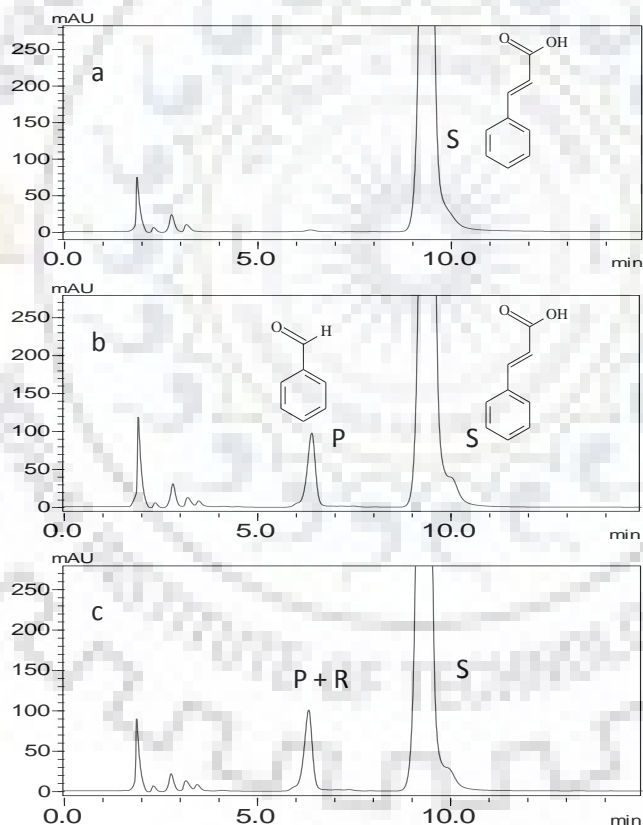


Figure 3.18: HPLC chromatograms showing benzaldehyde synthase activity from yeast extract-treated cell cultures of pear: (a) control assay with boiled protein extract, (b) standard assay, (c) co-chromatography of standard assay and reference compound. Peak identity keys: S, substrate (*trans*-cinnamic acid); P, product (benzaldehyde); R, authentic reference benzaldehyde. The chromatograms were monitored at 249 nm.



Table 3.4: Changes in the benzaldehyde synthase (BS) activity in presence of various reducing agents. The standard assay contained *trans*-cinnamic acid (10 mM), reducing agent (2-20 mM) and 50 µg partially purified cell-free extract. The results are the means ± SD of three independent experiments.

Reducing agent	BS relative activity (%)	Specific activity (pkat/mg protein)
No reducing agent	4.9	2.5 ± 0.18
DTT (1 mM)	22.1	11.3 ± 1.3
DTT (5 mM)	58.8	30.1 ± 2.0
DTT (10 mM)	100	51 ± 4.2
DTT (20 mM)	86.2	44 ± 3.7
Cysteine (10 mM)	78.4	40 ± 3.3
Coenzyme A (10 mM)	10.3	5.3 ± 0.8
Coenzyme A (10 mM) + ATP (10 mM)	12.1	6.2 ± 0.8
Coenzyme A (10 mM) + ATP (10 mM) + MgCl ₂	59.0	30.1 ± 2.7
DTT (10mM), with boiled protein	10.0	5.1 ± 0.5
Cyeteine (10mM), with boiled protein	9.4	4.8 ± 0.4

3.10.1.3. Elicitor induced changes in BS activity:

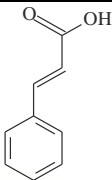
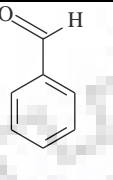
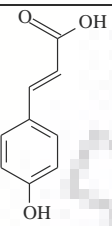
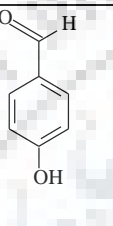
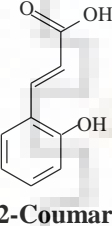
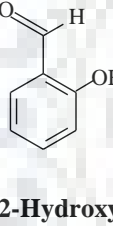
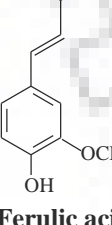
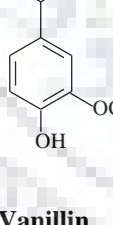
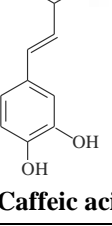
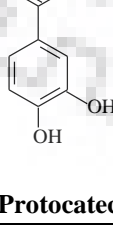
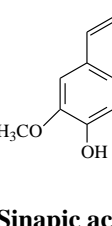
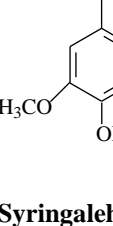
Time course analyses of BS activities were performed using YE-treated pear cell cultures extracted at defined time points (0-24 h) (Fig. 3.20). There was a basal level of BS activity at 0h (3.8 ± 0.3 pkat/mg protein). BS activity attained peak at 12 h (51 ± 3.2pkat/mg protein) after elicitor treatment and thereafter activity started to decrease. At 24 h post-elicitation, BS activity had nearly reached to the basal level. During the similar time-course study, non-elicited control







Table 3.5: Substrate specificity studies of benzaldehyde synthase (BS) from yeast extract-treated cell cultures of *P. pyriformis*. Results are expressed as relative activity (%). The activity with *trans*-cinnamic acid (50.8 ± 4.6 pkat/mg protein) was set to 100%. The results are the means of three independent experiments \pm SD.

S.No	Substrate	Product	Relative activity (%)	Specific activity (pkat/mg protein)
1	 Trans-cinnamic acid	 Benzaldehyde	100	50.8 ± 4.6
2	 4-Coumaric acid	 4-Hydroxybenzaldehyde	24	12.2 ± 1.2
3	 2-Coumaric acid	 2-Hydroxybenzaldehyde	2.6	1.3 ± 0.2
4	 Ferulic acid	 Vanillin	1.5	0.8 ± 0.06
5	 Caffeic acid	 Protocatechuic aldehyde	0	0
6	 Sinapic acid	 Syringaldehyde	0	0



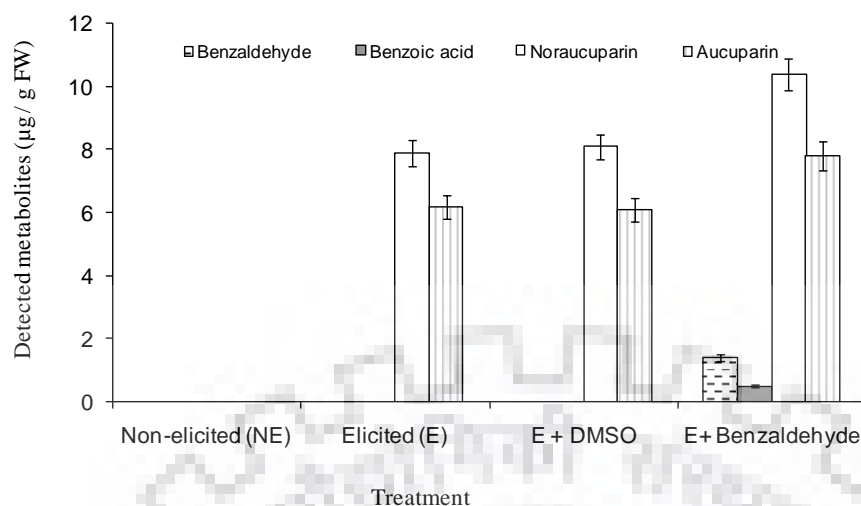


Figure 3.24: Effect of feeding benzaldehyde on phytoalexin accumulation in YE-treated cell cultures of *P. pyriformis*. Data represent the average of triplicate measurements \pm SD.

3.10.2.2. Detection of benzaldehyde dehydrogenase (BD) activity from elicitor-treated cell suspension cultures of *P. pyriformis*:

Upon YE-treatment *P. pyriformis* cell cultures accumulated two biphenyl phytoalexins, noraucuparin and aucuparin. YE is a well-known elicitor to trigger phytoalexin biosynthesis in plant cell cultures (Gaid et al., 2012). YE-treated cell cultures were used to prepare cell-free extracts for the incubation with benzaldehyde and NAD^+ to detect BD activity. Subsequent HPLC analysis revealed the formation of benzoic acid (Fig. 3.25 a-b). The identity of this enzymatic product was confirmed by co-chromatography with authentic benzoic acid (Fig. 3.25 c) and UV spectroscopy. In control assays containing heat-denatured cell-free extract, no enzymatic product was observed.

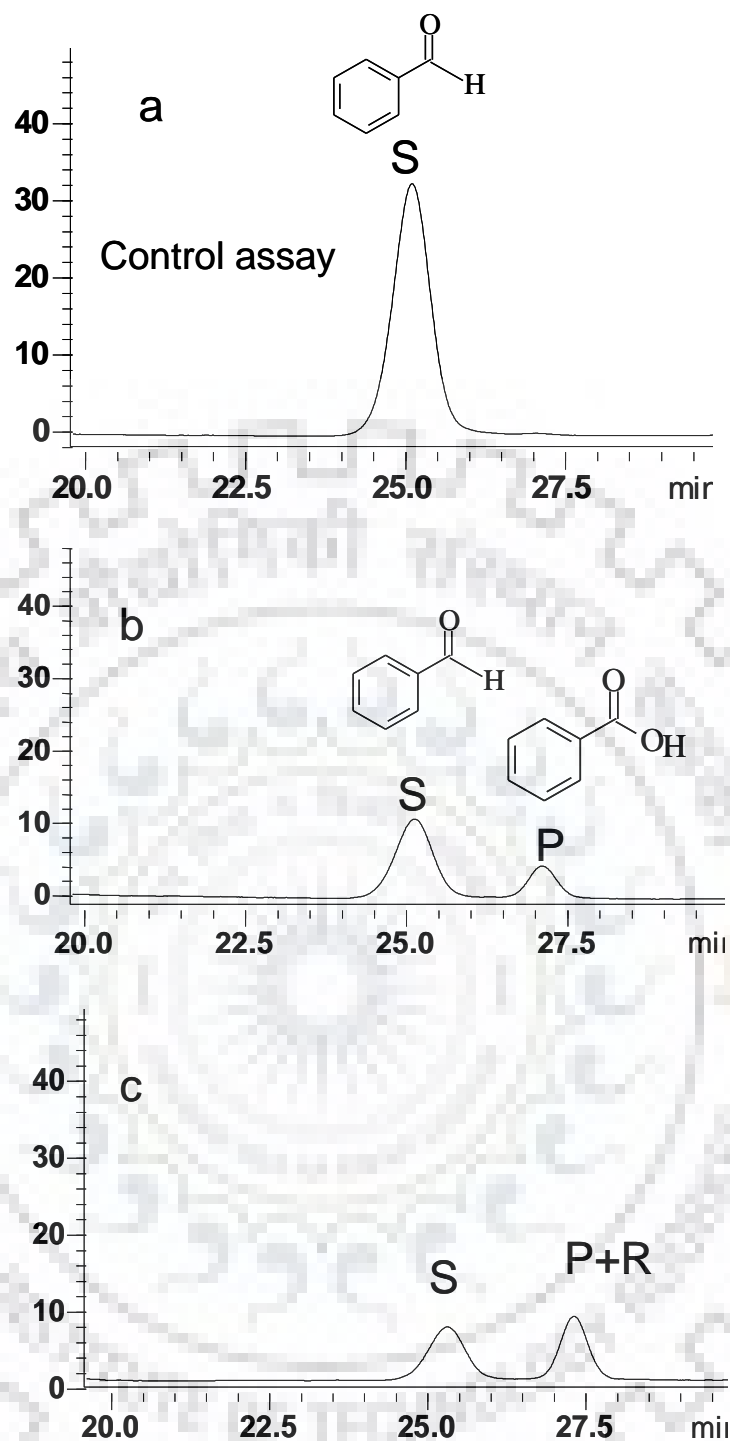


Figure 3.25: HPLC chromatograms showing benzaldehyde dehydrogenase activity: (a) control assay with boiled protein extract, (b) standard assay, (c) co-chromatography of standard assay and reference compound. Peak identity keys: S, substrate (benzaldehyde); P, BD-catalyzed product (benzoic acid); R, authentic reference benzoic acid. The chromatograms were monitored at 227 nm.







Table 3.6: Substrate specificity studies of benzaldehyde dehydrogenase (BD) from yeast-extract-treated cell cultures of *P. pyriformis*. The results are expressed as relative activity (%). The activity with benzaldehyde (42 ± 3.7 pkat/mg protein) was set to 100 %. Aldehyde substrates were used at a concentration of 0.5 mM. The results are the means of three independent experiments \pm SD.

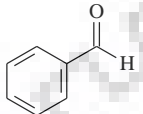
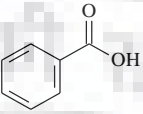
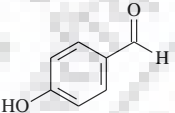
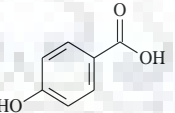
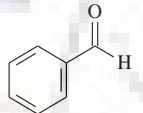
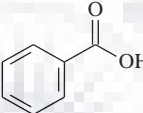
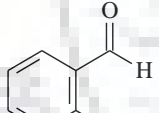
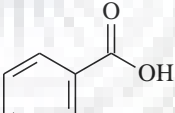
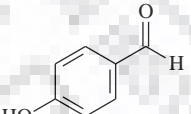
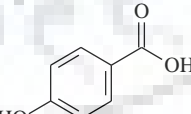
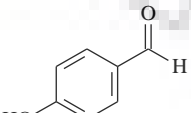
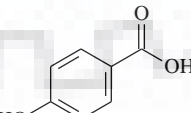
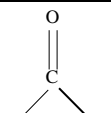
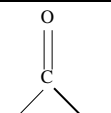
S.No	Substrate	Product	Relative activity (%)	Specific activity (pkat/mg protein)
1	 Benzaldehyde	 Benzoic Acid	100	42.7 ± 3.7
2	 4-Hydroxy Benzaldehyde	 4-Hydroxy Benzoic Acid	14.7 ± 2.1	6.2 ± 0.9
3	 3-Hydroxy Benzaldehyde	 3-Hydroxy Benzoic Acid	1.5 ± 0.4	0.6 ± 0.1
4	 2-Hydroxy Benzaldehyde	 2-Hydroxy Benzoic acid	2.0 ± 2.7	0.8 ± 0.1
5	 Protocatechuic aldehyde	 Protocatechuic acid	0	0
6	 Vanillin	 Vanillic Acid	0	0
7	 Formaldehyde	 Formic acid	6.3 ± 0.5	2.6 ± 0.2



Table 3.7: Putative benzaldehyde dehydrogenase unigenes detected in the pear genome via *in silico* analyses.

Gene Name	Plant Name	NCBI Gene ID	NCBI Protein ID	Pear gene homologue sharing highest homology (blastp)	Sequence identity
ALDH2B4	<i>Arabidopsis thaliana</i>	823955	NP_190383.1 (Brocker et al., 2013)	PCP000501.1	83%
				PCP006670.1	83%
ALDH2B7	<i>Arabidopsis thaliana</i>	838991	NP_564204.1 (Brocker et al., 2013)	PCP020461.1	81%
				PCP000501.1	79%
ALDH2C4	<i>Arabidopsis thaliana</i>	822042	NP_566749.1 (Nair et al., 2004)	PCP029125.1	70%
				PCP036892.1	68%
AmBALDH	<i>Antirrhinum majus</i>	FJ151199.1	ACM89738.1 (Long et al., 2009)	PCP000501.1	80%
				PCP020461.1	78%
ALDH2B2	<i>Zea mays</i>	KJ004510	AHM26656.1 (Koncitikova et al., 2015)	PCP020461.1	82%
				PCP000501.1	77%
ALDH2B5	<i>Zea mays</i>	KJ004511	AHM26657.1 (Koncitikova et al., 2015)	PCP000501.1	76%
				PCP006670.1	70%
ALDH2C1	<i>Zea mays</i>	KJ004512	AHM26658.1 (Koncitikova et al., 2015)	PCP029125.1	70%
				PCP036892.1	71%
ALDH2C2	<i>Zea mays</i>	KM225857	AIV00510.1 (Koncitikova et al., 2015)	PCP029125.1	67%
				PCP036892.1	66%
ALDH2C4	<i>Zea mays</i>	KM225858	AIV00511.1 (Koncitikova et al., 2015)	PCP029125.1	67%
				PCP036892.1	65%
ALDH2C5	<i>Zea mays</i>	KJ004513	AHM26659.1 (Koncitikova et al., 2015)	PCP029125.1	62%
				PCP036892.1	61%
ALDH2B4	<i>Vitis vinifera</i>	100262043	XP_002283132.1 (Zhang et al., 2012)	PCP000501.1	85%
				PCP006670.1	85%
ALDH2B9	<i>Vitis vinifera</i>	100259296	XP_002274863.1 (Zhang et al., 2012)	PCP000501.1	81%
				PCP006670.1	80%
ALDH2	<i>Hordeum vulgare</i>	AB055519.1	BAB62757.1 (Brocker et al., 2013)	PCP006670.1	74%
				PCP000501.1	79%



















Chapter 4

Discussion

Among plant natural products, benzoic acid and its derivatives are of special interest because it acts as biosynthetic precursor for wide-range of natural products of physiological and economical importance, such as, methyl benzoates, methylsalicylate (Verberne et al., 2003) late, taxol, xanthenes and biphenyls (Abd El-Mawla and Beerhues, 2002; Abd El-Mawla et al., 2001; Wildermuth, 2006). Benzoic acid serves as the precursors for biosynthesis of biphenyl and dibenzofuran class of phytoalexins through intermediate formation of benzoyl-CoA. These phytoalexins are produced only by the members of sub-tribe Malinae of Rosaceae family, which bears a number of economically important fruit plants such as apple and pear (Chizzali and Beerhues, 2012). Despite its simple structure, biosynthesis of benzoic acid and subsequent formation of benzoyl-CoA in Malinae is only partially understood (Gaid et al., 2009). In plants benzoic acid is known to be mostly derived from cinnamic acid (Widhalm and Dudareva, 2015), but the details of enzymatic route of its formation is not clearly demonstrated so far in Malinae.

The first aim of this doctoral thesis work was to delineate the difference in the basal metabolite levels in two most economically important pear species, the European pear (*Pyrus communis*) and the Asian pear (*Pyrus pyrifolia*). The second aim of my thesis work was to elucidate enzymatic steps of benzoic acid and benzoyl-CoA formation in the cell suspension culture of *Pyrus pyrifolia*, where benzoic acid biosynthesis remains incompletely understood till date. The enzymes that catalyze C₂-side chain cleavage of cinnamic acid, the intermediate dehydrogenation step and the final CoA-ligase activity leading to the formation of benzoyl-CoA were the main focus of this investigation.

In order to delineate the basal metabolite differences between *P. communis* and *P. pyrifolia*, non-targeted GC-MS analyses were performed taking the immature and mature leaves. Since basal level of benzoic acid (precursor for biphenyl biosynthesis) content was higher in the leaves of *P. pyrifolia*, cell suspension culture was developed from *P. pyrifolia*. In those cell cultures, then biphenyl phytoalexin biosynthesis was enhanced by elicitor-treatment. It was anticipated that perhaps it would be easier to trace the preceding enzyme activities responsible for the synthesis of the benzoic acid and benzoyl-coA in such condition, when the product formation could be uplifted by suitable empirical means. Feeding experiments with

different putative precursors of benzoic acid pathway were performed to probe the enzymatic route of benzoic acid formation. Finally, enzymes involved in conversion of *trans*-cinnamic acid to benzoyl-CoA were identified and biochemically characterized from cell-free extracts.

GC-MS based metabolomics analyses identified 30 differentially accumulating metabolites in both the pear species under study. Results revealed that, among detected metabolites there was dominance of carbohydrates and phenolics. In case of proline, no significant differences were observed between two pear species. Proline is known to act as osmoprotectant (Delauney and Verma, 1993) as well as helps in preventing membrane damage from reactive oxygen species (Saradhi et al., 1995). In case of sugar alcohols, high myo-inositol accumulation was observed in the leaves of *P. communis*. Myo-inositol accumulation is generally linked with salinity stress tolerance in plants (Senthil et al., 2015). Under especial conditions, myo-inositol could serve as a precursor for the synthesis of D-ononitol and D-pinitol, which protects plants against drought stress (Vernon and Bohnert, 1992). The enhanced level of myo-inositol in *P. communis* leaves might be attributed towards higher water-stress or salinity stress tolerance. For all the organic acids detected, higher accumulation was observed in the *P. pyrifolia* leaves with highest accumulation in mature leaves (PPML > PPIL). It is worthy to hypothesize that, high organic acid accumulation was due to higher turnover number of glycolysis and TCA cycle which generated more abundant intermediate. High organic acid concentration is known to be associated with higher disease resistance due to its effect on facilitating better ion absorption (Hudina and Štampar, 2000). Similar to leaves, organic acids were detected in higher concentration in the fruits of many pear cultivars (Sha et al., 2011). Similarly, for vitamins, ascorbic acid level was higher in the *P. pyrifolia* with more accumulation in mature leaves. Ascorbic acid is known to fortify defense responses in many plant species (Pastori et al., 2003). High ascorbic acid might attribute greater tolerance to scab infection in *P. pyrifolia*. The amount of α -tocopherol remained almost unaltered in both the plant species. In plants, tocopherols (vitamin E) comprise of four types (α , β , γ , and δ form) of lipid-soluble antioxidants which has prominent role in plant defense (Atanasova-Penichon et al., 2016).

Phenolics were the most abundant metabolites in pear leaves among the studied metabolites. In this study, no qualitative differences in phenolics were observed between *P. pyrifolia* and *P. communis* leaves, however, quantitative differences were detected. Interestingly, leaves of *P. pyrifolia* showed very high content of benzoic acid. Benzoic acid serves as the precursor for biphenyl and dibenzofuran class of phytoalexins of pear and other species of Malinae (Chizzali et al., 2012, 2016; Saini et al., 2017). It is speculated that upon pathogen attack, benzoic acid is

first converted into benzoyl-CoA, which combines with malonyl-CoA to produce biphenyl phytoalexin scaffold (Gaid et al., 2009). Biphenyl and dibenzofuran phytoalexin are known to inhibit the growth of *Venturia* species and *E. amylovora* (Chizzali et al., 2012). High benzoic acid content in *P. pyrifolia* leaves might attribute its higher resistance against *V. pirina* (Abe et al., 2008) and *E. amylovora* (Chizzali et al., 2012) via forming biphenyl phytoalexins upon pathogen attack. Similarly, high catechin content known to confers resistance towards fungal infection (Amil-Ruiz et al., 2011). It was reported that strawberry plant with higher level of catechin exhibit strong resistance against *Alternaria alternata* and *Botrytis cinerea* (Hébert et al., 2002). Likewise, high content of chlorogenic acid, caffeic acid and protocatechuic acid is also associated with higher level of resistance towards fungal infection (Mandal, 2010; Morrissey and Osbourn, 1999). Upon fungal infection, enhancement of caffeic acid and protocatechuic acid were observed in many plant species as part of phytoalexin defense system (Bostock et al., 1999). Higher level of scab resistance was previously detected in apple cultivar Golden delicious which was rich in phenolic acids such as caffeic acid, protocatechuic acid and benzoic acid (Singh et al., 2015). Fire-blight resistant pear cultivar also showed enhanced level of phenolic acids (Gunen et al., 2005). In our study, high level of chlorogenic acid, caffeic acid and protocatechuic acid in the *P. pyrifolia* leaves probably attribute strong resistance against scab infection, especially to the mature leaves which has higher ontogenic resistance. *Trans*-cinnamic acid is the starting point of phenylpropanoid pathway and serves as the rich source of many defense metabolites, such as phenylpropanoids, lignans, flavonoids, benzoic acid and coumarins (Gaid et al., 2012; Widhalm and Dudareva, 2015). Recently, (Saini et al., 2017) has shown that pear phytoalexin, aucuparin and nor-aucuparin is derived from benzoic acid. Benzoic acid in turn derived from benzaldehyde, and benzaldehyde is likely to be derived from *trans*-cinnamic acid through C₂-chain shortening, as demonstrated before in hairy roots of *Daucus carota* (Sircar and Mitra, 2008). High level of *trans*-cinnamic acid in *P. pyrifolia* leaves thereby explains the reason underlying enhanced benzoic acid accumulation. Upon pathogen infection, benzoic acid is converted into biphenyl phytoalexins, which probably confers further resistance against fungal infection. In contrary to the level of cinnamic acid, our results demonstrated that the content of *o*-coumaric acid and *p*-coumaric acid were higher in *P. communis* leaves. This is quite logical because *trans*-cinnamic acid acts as precursors for both *p*-coumaric acid benzoic acids. Since the level of benzoic acid is lower in *P. communis*, probably the flux of *trans*-cinnamic acid is more directed towards synthesis of *p*-coumaric acid in *P. communis* leaves, which in turn synthesize flavonoids. High level of *o*-coumaric acid is linked with synthesis of salicylic acid through intermediate formation of salicylaldehyde

synthase (Malinowski et al., 2007), however, in this experiment, no salicylic acid was detected. Perhaps, salicylic acid biosynthetic pathway triggers only after pathogen infection (Hendrawati et al., 2006). *p*-Hydroxybenzoic acid is an important cell wall bound phenolics, which helps plant in protecting from fungal infection (Sircar et al., 2007). It was previously demonstrated that 4-hydroxy benzoic acid is synthesized in the cytoplasm and then transported and accumulated in the cell-wall (Sircar et al., 2007). This could be the probable reason of not getting *p*-hydroxybenzoic acid accumulation in mature leaves of both the *Pyrus* species. Arbutin (4-hydroxyphenyl- β -D-glucopyranoside), a hydroquinone derivative was detected in the leaves of both the pear species with no significant difference in their content. Occurrence of arbutin in pear and many other plant species has been reported before (Cui et al., 2005) with known antimicrobial activity (Zbigniew et al., 2014). Based on metabolic pathway network (Fig 3.9; Result section), when the differences between PP and PC leaves were considered, the significant different components were, aspartic acid, pyruvic acid, fumaric acid, succinic acid, benzoic acid, chlorogenic acid, protocatechuic acid, caffeic acid, *o*-coumaric acid, *p*-coumaric acid, *trans*-cinnamic acid, catechin, glucose, mannose, sorbitol, myo-inositol, 3-phosphoglyceric acid, pyruvic acid, succinic acid, malic acid and fumaric acid.

The high expression level of *PAL* and *AOX* genes in the mature leaves of *P. pyrifolia* demonstrates that phenylpropanoid biosynthesis was highest in the mature leaves of *P. pyrifolia*. This was well correlated with the enhanced accumulation of phenylpropanoids such as cinnamic acid in the mature leaves of *P. pyrifolia*. Enhanced expression of *PAL* gene is known to be associated with increase in the phenylpropanoid biosynthesis (Mukherjee et al., 2016; Sil et al., 2015; Sircar and Mitra, 2008). However, the expression level of *C4H* gene was higher in the mature leaves of *P. communis*, which is indicative of higher accumulation of *p*-coumaric acid; the product of *C4H* catalyzed reaction. A direct correlation between *C4H* expression level and *p*-coumaric acid level has been reported in many plant species (Kundu et al., 2012). Metabolite analyses revealed that *p*-coumaric acid level was higher in the mature leaves of *P. communis*. Likewise, high *F3H* expression is associated with higher accumulation of catechin. High *AOX* expression level in the leaves of *P. pyrifolia* is probably associated with the enhanced biosynthesis of phenylpropanoids. Previously, it was demonstrated that *AOX* expression is linked with high phenylpropanoid biosynthesis in many plant species (Campos et al., 2015, 2016; Sircar et al., 2012). High *AOX* expression level is known to be associated with the plant's ability to facilitate metabolic re-programming to cope up with the stressed conditions (Arnholdt-Schmitt et al., 2006). The TPC, TFC and FRSA values obtained agrees with the previous finding of Fotirić Akšić et al. (2015) in the leaves of several *Pyrus* species.

As revealed from the result of this comparative metabolomics, the metabolite profile of both the *Pyrus* species were dominated by 30 identified metabolites, including amino acids, sugars, sugar alcohols, organic acids, vitamins and phenolics. Among phenolics, especially the level of benzoic acid, chlorogenic acid, caffeic acid, protocatechuic acid, *trans*-cinamic acid and 4-hydroxybenzoic acid were significantly higher in the leaves of *P. pyrifolia* than those of *P. communis*, grown under similar green house conditions. This is possibly the main reason why *P. pyrifolia* leaves showed higher ontogenic resistance towards pathogen infection, particularly for the pear scab fungus, *V. pirina*. Notably, benzoic acid is the precursor of biphenyl (aucuparin and noraucuparin) class of metabolites, which are the marker defense metabolite for pears and other members of sub-tribe Malinae. High benzoic acid level might provide metabolic flexibility to *P. pyrifolia* cells to rapidly synthesize these biphenyl phytoalexins upon pathogen infection, and consequently the higher degree of resistance against pathogen infections. Moreover, high TPC and FRSA in *P. pyrifolia* might indicate that these values are positively correlated with the high phenolics content of *P. pyrifolia* leaves. **Based on our results, it is postulated that the ability of *P. pyrifolia* leaves to exhibit higher ontogenic resistance towards pathogen attack is based on its ability to synthesize an array of defense metabolites, especially phenolics, in significantly higher level.** These results demonstrated that GC-MS based metabolomics technology possibly provides a powerful approach to quickly discriminate the scab disease-resistance characteristics of *Pyrus* species.

Since, *P. pyrifolia* leaves contained higher amount of benzoic acid, it was further selected for the development of callus and cell suspension culture. Cell cultures of *P. pyrifolia* showed excellent growth characteristics. Yeast-extract (YE) was used to elicit the biphenyl phytoalexin formation in those *P. pyrifolia* cell cultures, because previously YE known to elicit a number of natural products, including biphenyls (Liu et al., 2004; Sarkate et al., 2017). The *P. pyrifolia* cell cultures accumulated biphenyl phytoalexin aucuparin and noraucuparin upon YE-elicitor treatment. A similar induction of biphenyl phytoalexins was previously reported in elicitor-treated cell cultures of *Malus domestica* and *S. aucuparia* (Hrazdina et al., 1997; Hüttner et al., 2010). However, in contrast to the previous studies, no dibenzofurans were detected in *P. pyrifolia* cell cultures. Upon elicitor treatment of *P. pyrifolia* cell cultures, the accumulation of biphenyl phytoalexins (aucuparin and nor-aucuparin) was preceded by increases in the activities of phenylalanine ammonia-lyase (PAL), benzaldehyde synthase (BS), benzaldehyde dehydrogenase (BD), benzoate-CoAligase (BZL) and biphenyl synthase (BIS), which strongly suggests that all of these enzymes are involved in the biphenyl phytoalexin biosynthesis pathway. Sequential steps of involvement of these enzymes have been postulated in Fig 4.1.

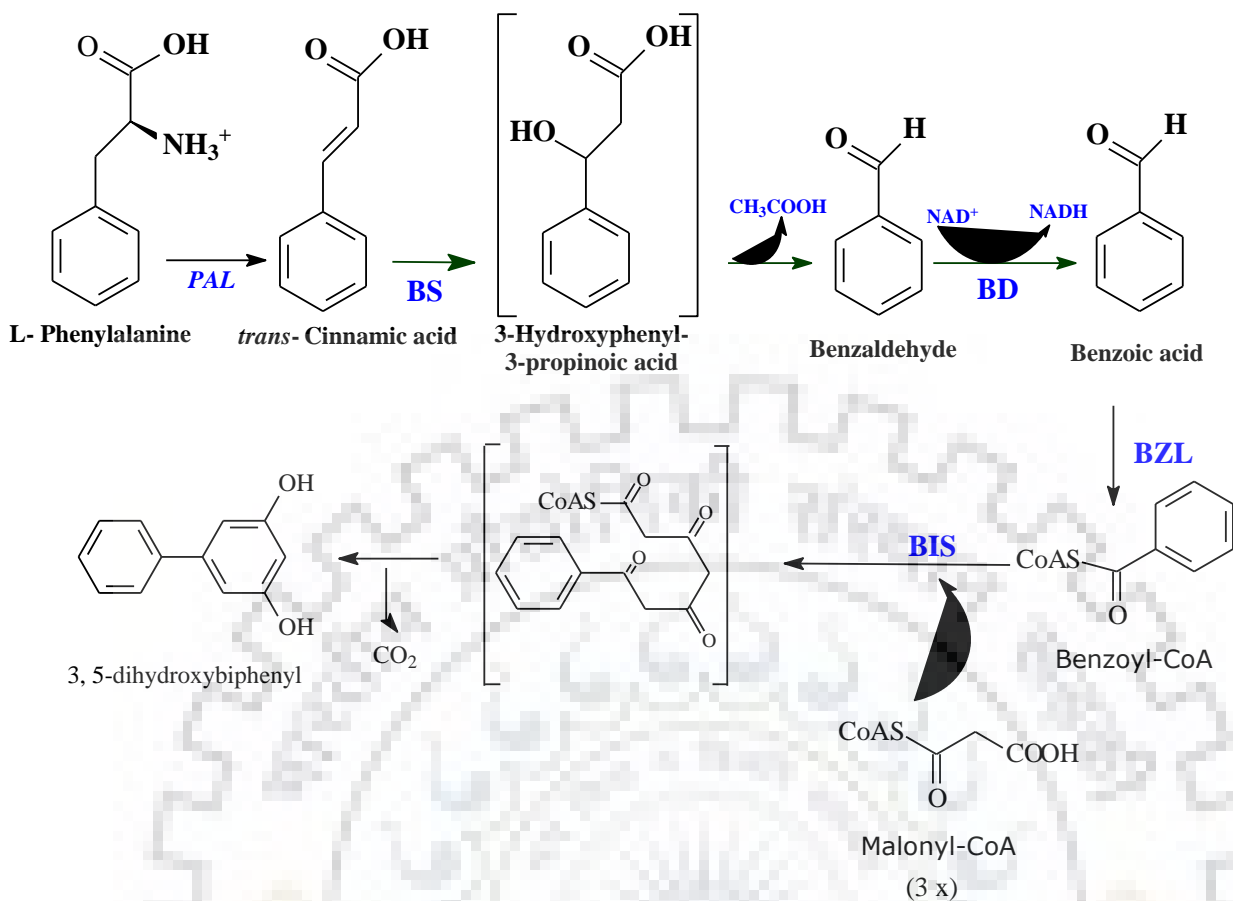


Fig 4.1 Enzymatic route of benzoate derive phytoalexins in pear. Solid arrow indicates elucidated enzymes. [BS = benzaldehyde synthase; BD = benzaldehyde dehydrogenase; BZL = benzoate - CoA ligase].

PAL catalyzes the first committed step in phenylpropanoid pathway. In response to yeast-extract (YE) elicitor treatment PAL activity increased strongly and over a longer time period, which is attributed to the involvement of this enzyme in general phenylpropanoid pathway along with benzoic acid biosynthesis. A huge increase in PAL activity together with general phenylpropanoid pathway metabolites has previously been observed in plant cell-cultures (Abd El-Mawla and Beerhues, 2002; Gaid et al., 2012; Sarkate et al., 2017; Sircar et al., 2015). From time-course data it was evident that aucuparin and noraucuparin (benzoate-derived biphenyl phytoalexin) acid accumulation was preceded by increase in PAL activity in YE-treated pear cell cultures, which further demonstrate that PAL activity was required for benzoic acid and subsequent biosynthesis of aucuparin and noraucuparin.

The second step in benzoic acid biosynthesis was catalyzed by benzaldehyde synthase (BS) enzyme. In this work, first time I have reported a new catalytic activity from the YE-treated cell culture of *P. pyrifolia* which efficiently converts *trans*-cinnamic acid into benzaldehyde suggesting benzaldehyde synthase (BS) activity. The mechanism of C₂ side chain cleavage was non- β -oxidative, which proceeds without the requirement of ATP and coenzyme A. The mechanism of C₂-chain shortening of *trans*-cinnamic acid probably involves a hydrolase activity which removes C₂-side chain from *trans*-cinnamic acid backbone to yield benzaldehyde and acetic acid, as suggested by Podstolski et al. (2002) for 4-hydroxybenzaldehyde synthase activity. So far, such non- β oxidative C₂ chain cleavage activity has been poorly characterized in plants. Earlier, a similar chain shortening mechanism was reported in the Tobacco Mosaic Virus (TMV) infected *N. tabacum*, where salicylaldehyde synthase (SAS) enzyme catalyzed the in vitro conversion of 2-coumaric acid into salicylaldehyde (Malinowski et al., 2007). An analogous C₂-chain shortening reaction was previously shown by the 4-hydroxybenzaldehyde synthase (HBS), detected from few plant species. HBS-catalyzed conversion of 4-coumaric acid to 4-hydroxybenzaldehyde was detected in the tubers of *Solanum tuberosum* (French et al., 1976), in the cell cultures of *Lithospermum erythrorhizon* (Yazaki et al., 1991), in *Daucus carota* (Schnitzler et al., 1992; Sircar and Mitra, 2008) and in the *Vanilla planifolia* cell culture (Podstolski et al., 2002). BS activity detected from *P. pyrifolia* cell cultures showed similar characteristics like HBS activity detected from the hairy roots of *D. carota* (Sircar and Mitra, 2008) and pods of *V. planifolia* (Podstolski et al., 2002). In all these cases, chain cleavage activity was found to be strictly dependent on the presence of reducing agent. BS showed highest activity with 10 mM DTT. HBS from *V. planifolia* and *D. carota* also showed maximum activity with 10 mM DTT. In contrary, SAS from *N. tabacum* showed maximum activity with 10 mM of cysteine. Interestingly, the DTT

concentration required for *in vitro* BS activity is unusually very high. HBS enzyme from *V. planifolia* was purified and HBS peptide sequence showed strong homology with plant cysteine proteases, particularly senescence induced cysteine proteases (Havkin-Frenkel et al., 2003). Active site of *V. planifolia* cysteine protease is characterized by a catalytic diad of cysteine and histidine residue (Havkin-Frenkel et al., 2003). Disulfide bond between cysteine residues are known to stabilize protein. DTT is known to prevent the activity loss of enzyme under *in vitro* condition. It was observed that supplementation of DTT activated cysteine protease activity (Havkin-Frenkel et al., 2003; Sircar and Mitra, 2008). This could be a possible reason for getting higher BS activity with increasing concentration of DTT. However, the actual role of DTT in promoting BS activity could be better understood in future with recombinant BS protein. The preferred substrate for pear BS was *trans*-cinnamic acid, followed by 4-coumaric acid. BS activity with 2-coumaric acid and ferulic acid showed very minor product. This is in agreement with the HBS activity from *V. planifolia*, which showed distinct substrate specificity with 4-coumaric acid as preferred substrate (Podstolski et al., 2002). In contrary, tobacco SAS showed no distinct substrate specificity. Alike vanilla HBS and tobacco SAS, pear BS did not show any activity with caffeic and sinapic acid.

Feeding experiments with *trans*-cinnamic acid enhanced the accumulation of biphenyl phytoalexins aucuparin and noraucuparin, which is further suggestive of involvement of BS in the biphenyl biosynthesis.

Recently, vanillin synthase gene (*VpVAN*) has been cloned and functionally characterized from *V. planifolia* which catalyzes the similar non- β -oxidative C₂-chain cleavage in vanillin biosynthetic pathway (Gallage et al., 2014). *VpVAN* catalyzes ferulic acid to vanillin conversion without requirement of ATP and NAD. For *VpVAN*, the preferred substrate was ferulic acid; no activity was detected with 4-coumaric acid and caffeic acid. The apparent *K_m* value for pear BS was 0.50 ± 0.04 mM. In case of Vanilla and carrot HBS, *K_m* values could not be determined because lack of substrate saturations (Podstolski et al., 2002; Sircar and Mitra, 2008). Although, detected *K_m* value for pear BS was relatively high, it suggests better affinity towards *trans*-cinnamic acid as compared to vanillin and carrot HBS. In comparison to the catalytic activity exhibited by benzaldehyde dehydrogenase, the another benzoic acid biosynthetic enzyme from *P. pyriformis* [benzaldehyde *K_m* = 52.0 ± 1.1 μ M] (Saini et al., 2017), the apparent catalytic activity of *P. pyriformis* BS is notably high [*trans*-cinnamic acid *K_m* = 0.45 ± 0.04 mM]. A similar high *K_m* value was reported in the case of tobacco SAS [2-coumaric

acid $K_m = 0.625$ mM] (Malinowski et al., 2007). This issue of getting relatively high K_m could be better addressed in future through attempts to clone and purify recombinant pear BS.

The activity peak of BS was recorded at 12 hpe (hours post elicitation) which preceded the peak of third enzyme [benzaldehyde dehydrogenase (BD); peak at 16 hpe] from the similar *P. pyrifolia* cell cultures (Saini et al. 2017). This suggests the involvement of BS upstream of BD in the similar CoA-independent and non- β -oxidative pathway. In conclusion, benzaldehyde synthase (BS), a new catalytic activity converting *trans*-cinnamic acid into benzaldehyde, in presence of reducing agent, was detected first time from the elicitor-treated cell cultures of *P. pyrifolia*. *P. pyrifolia* cell cultures could be used as a model system to characterize crucial enzymes and their underlying genes involved in the CoA-independent and non- β -oxidative route of plant benzoic acid biosynthesis.

The third step in benzoic acid biosynthesis was catalyzed by benzaldehyde dehydrogenase (BD), which catalyzes the *in vitro* conversion of benzaldehyde to benzoic acid in presence of NAD^+ . Using cell-free extracts from YE-treated cell cultures of *P. pyrifolia*, BD activity was biochemically characterized, which can efficiently convert benzaldehyde into benzoic acid. Benzoic acid is later incorporated into the backbone of biphenyl phytoalexins. Plant benzaldehyde dehydrogenases belong to the aldehyde dehydrogenase superfamily 2 (*ALDH2*) (Long et al., 2009). Plant ALDHs constitute a superfamily of $NAD(P)^+$ -dependent homotetrameric enzymes known for their ability to irreversibly convert various aliphatic and aromatic aldehydes into their corresponding carboxylic acids (Končítíková et al., 2015). To date, 13 superfamilies of plant ALDHs exist, of which the *ALDH2* superfamily comprises mitochondrial and cytosolic isoforms, further divided into *ALDH2B*, *C*, *D* and *E* subfamilies (Brocker et al., 2013). One of the important characteristic features of the *ALDH2* superfamily is wide substrate specificity and homotetrameric structure. *ALDH2* superfamily genes have been well-characterized in many plant species, such as the *ALDH2* superfamily in *A. thaliana*, which contains three genes (Sophos and Vasiliou, 2003; Brocker et al., 2013), *Oryza sativa* with five genes (Gao and Han, 2009), *Zea mays* contains six genes (Liu, 2002; Končítíková et al., 2015) *Vitis vinifera* contains five genes (Zhang et al., 2012), and *Sorghum bicolor* contains five genes (Brocker et al., 2013). Recently, benzaldehyde dehydrogenase (BALDH) cDNA was cloned and functionally characterized from snapdragon, a member of the ALDH superfamily 2. Snapdragon BALDH converts benzaldehyde into benzoic acid (Long et al., 2009). Another *ALDH2* gene converting ferulic acid to sinapic acid during cell wall biosynthesis was reported in *A. thaliana* (Nair et al., 2004). Bioinformatic processing of pear genome revealed the

presence of at least five putative pear unigenes belonging to the *ALDH2* superfamily. The pear unigene *PCP000501.1* showed 80 % similarity at the amino acid level with *A. majus* benzaldehyde dehydrogenase (Table 3.7 in Result section). These five putative pear unigenes could be excellent targets for the cloning and functional characterization of pear BD cDNA involved in biphenyl phytoalexin biosynthesis.

In comparison to the catalytic activity exhibited by *A. majus* BALDH [benzaldehyde $K_m = 1.37 \pm 0.04 \mu\text{M}$] (Long et al., 2009), the apparent catalytic activity of *P. pyrifolia* BD is notably high [benzaldehyde $K_m = 52.0 \pm 1.1 \mu\text{M}$]. A similar high K_m value was reported in the case of *S. aucuparia* BD [benzaldehyde $K_m = 49 \mu\text{M}$] (Gaid et al., 2009).

Detection of BD activity with FAD and FMN as co-factor was slightly unusual, since ALDH2 superfamily dehydrogenases have a high affinity and specificity for only NAD^+ or NADP^+ as cofactors. Because cell-free extract was used in the activity measurement, the activity shown by FAD and FMN may come from unspecific dehydrogenases of primary metabolism. A similar BD activity in the presence of FAD and FMN was also observed with cell free extract of *S. aucuparia* (Gaid et al., 2009).

The preferred substrate of *P. pyrifolia* BD was benzaldehyde. Among the tested substrates, the second-best substrate was aliphatic aldehyde acetaldehyde. In contrast, for *A. majus* BALDH, the maximum relative activity was observed with acetaldehyde and benzaldehyde was the third best substrate. Affinity towards acetaldehyde (acetaldehyde dehydrogenase activity) was indicative of mitochondrial *ALDH2*. However, the catalytic efficiency of BALDH was 4.8 times higher than that of acetaldehyde (Long et al., 2009). In maize *ALDH2* family members, the K_m value for acetaldehyde was quite high, indicative of poor substrate (Končítiková et al., 2015).

P. pyrifolia cell cultures showed significant BD activity upon elicitation, which indicates that benzoic acid biosynthesis proceeds via intermediate formation of benzaldehyde. Benzoic acid is then converted into its CoA thioester (benzoyl-CoA) and serves as the starter substrate for the synthesis of biphenyls. Benzoyl-CoA combines with three molecules of malonyl-CoA to form 3,5-dihydroxybipenyl in a reaction catalyzed by BIS (Liu et al., 2007). Later, 3,5-dihydroxybipenyl undergoes a series of hydroxylation and methylation reaction to produce further substituted biphenyls. Upon YE treatment, PAL, BS and BD activities were coordinately induced. However, the span of PAL activity was longer than that of BD activity. The peak of PAL activity preceded the maximum BD activity due to the involvement of PAL in the general phenylpropanoid pathway. The basal dehydrogenase activity detected at early time

points after elicitation might be due to the presence of non-specific dehydrogenases from primary metabolism present in the cell-free extract. A similar pattern of BD induction was previously reported for the chitosan-treated cell culture of *S. aucuparia*, which also accumulated biphenyl phytoalexin.

In 4-hydroxybenzoic acid biosynthesis, aldehyde dehydrogenase activity was reported in the cell cultures of *Lithospermum erythrorhizon* (Yazaki et al., 1991b) as well as elicitor-treated cell cultures and hairy root cultures of *D. carota* (Schnitzler et al., 1992; Sircar and Mitra, 2008). However, the product of this reaction was 4-hydroxybenzoic acid with 4-hydroxybenzaldehyde as the preferred substrate. Benzaldehyde was a poor substrate for those enzymes.

The fourth enzymatic step leading to the formation of benzoyl-CoA from benzoic acid was detected. Using partially purified cell-free extracts from YE-treated cell cultures of *P. pyrifolia*, BZL activity was biochemically characterized, which can efficiently convert benzoic acid into benzoyl-CoA which is later incorporated into the backbone of biphenyl phytoalexins. Till date BZL activity has been very poorly reported from plants. So far the only BZL activity reported from plants at biochemical level was from *Clarkia breweri* (Beuerle and Pichersky, 2002a). In comparison to the catalytic activity exhibited by *C. breweri* BZL [benzoic acid $K_m = 45 \mu\text{M}$] (Beuerle and Pichersky, 2002a), the apparent catalytic activity of *P. pyrifolia* BZL is comparatively better [benzoic acid $K_m = 42.0 \mu\text{M}$].

The preferred substrate of *P. pyrifolia* BZL was benzoic acid. Among the tested substrates, the second-best substrate was 4-hydroxybenzoic acid. Strict substrate specificity was also observed for *C. breweri* BZL. A similar to BZL activity, 3-hydroxybenzoateCoA-ligase (HBZL) activity has been detected from the *Centaureum erythraea* (Barillas and Beerhues, 1997). *Clarkia* BZL showed a molecular mass of 59-65 KDa (monomeric) whereas *C. erythraea* HBZL showed a molecular mass of 50-60 KDa. In this study, only partially purified BZL activity was assayed, so no molecular mass information is available. However, attempt will be made in future to detect actual molecular mass using recombinant BZL protein from *P. pyrifolia*.

P. pyrifolia cell cultures showed significant BZL activity upon elicitation, which indicates that biphenyl biosynthesis proceeds via intermediate formation of benzoyl-CoA. The peak of BZL activity (18 hpe) follows the peak of previous enzyme BD (16 hpe), suggesting that BZL activity comes after BD activity. BZL activity was found to be completely inducible with no basal activity. This agrees with detection of no phytoalexins at the non-elicited cell cultures of

P. pyrifolia. After *C. breweri*, this is the only example of BZL activity reported from any plant system.

Finally the fifth enzyme of the the biosynthetic pathway leading to the formation of first biphenyl skeleton, 3,5-dihydroxybiphenyl has also been detected from the elicited cell cultures of *P. pyrifolia*. Using partially purified cell-free extracts from YE treated cell cultures of *P. pyrifolia*, biphenyl synthase (BIS) activity has been detected. BIS catalyzes condensation of one molecule of benzoyl-CoA with three molecules of malonyl-CoA to form 3,5-dihydroxybiphenyl. Later 3,5-dihydroxybiphenyl undergoes series of substitution reaction to form noraucuparin, aucuparin and other biphenyls. BIS activity has been well characterized from many members of Malinae such as *S. aucuparia*, *M. domestica*, *P. communis* etc (Chizzali et al., 2016; Chizzali and Beerhues, 2012; Liu et al., 2004, 2007).

Interestingly, upon YE treatment, PAL, BS, BD, BZL and BIS activities were coordinately induced. However, the span of PAL activity was longer than that of all other enzymes of the pathway. The peak of PAL activity (9 hpe) preceded the peak of BS activity (12 hpe). Similarly the peak of BS activity (12 hpe) preceded the peak of BD activity (16 hpe). BZL and BIS attained maximum activity after peak of BD activity. BZL and BIS showed peak at 18 hpe. Phytoalexin accumulation attained peak at 24 hpe. These suggest the involvement of all of these enzymes in the benzoic acid and subsequent biphenyl biosynthetic pathway.

These results demonstrated that biosynthesis of benzoic acid in elicited cell cultures of *P. pyrifolia* is found to proceed via CoA-independent and non- β -oxidative route. The C₂-side-chain shortening reaction was catalyzed by BS enzyme leading to the formation of 4-benzaldehyde, which is subsequently converted into benzoic acid by a NAD⁺-dependent dehydrogenase (BD) enzyme. Benzoic acid is then converted into benzoyl-CoA in a reaction catalyzed by BZL. Benzoyl-CoA enters into biphenyl biosynthetic pathway through condensation with three molecules of malonyl-CoA to give 3,5-dihydroxybiphneyl.

Chapter 5

Summary, Conclusion and Future scopes

5.1. Summary:

- In order to understand the biochemical basis of ontogenic resistance in *Pyrus pyrifolia* (Asian pear) and *Pyrus communis* (European pear), comparative non-targeted GC-MS-based metabolomics were performed using immature and mature leaves.
- GC-MS metabolomics identified 30 differentially accumulating metabolites among both the pear species. Out of these thirty metabolites, phenolics were dominated. *P. pyrifolia* leaves contained significantly higher amount of phenolics such as benzoic acid, chlorogenic acid, protocatechuic acid, caffeic acid and *trans*-cinnamic acid. High phenolic acid content might provide higher ontogenic resistance to the *P. pyrifolia* leaves compared to *P. communis* leaves.
- *P. pyrifolia* leaves showed higher total phenolics (TPC) and free radical scavenging activity (FRSA) as compared to *P. communis* leaves. In contrary, total flavonoid contents (TFC) were higher in the *P. communis* leaves. Moreover, high TPC and FRSA in *P. pyrifolia*, might indicate that these values are positively correlated with the high phenolics content of *P. pyrifolia* leaves.
- Biosynthesis of benzoic acid is poorly understood in plants. Since *P. pyrifolia* leaves contained high basal level of benzoic acid (precursor of biphenyls), therefore, *P. pyrifolia* leaves were used to develop cell cultures. Those cell cultures were used as an experimental system to elucidate the enzymatic route of benzoic acid biosynthesis.
- Callus and cell suspension culture of *P. pyrifolia* were developed in Murashige and Skoog (MS)-medium supplemented with suitable growth regulators [2.2 μ M 6-benzylaminopurine (BAP) for callus induction; 1.0 μ M 2,4-D and 1.0 μ M IAA for cell suspension cultures].
- Optimum concentrations of yeast-extract (YE) elicitor was used to trigger biphenyl phytoalexin biosynthesis in the *P. pyrifolia* cell cultures. Cell cultures responded to YE-

treatment by producing two biphenyls, the aucuparin and the noraucuparin. No dibenzofuran phytoalexin was detected.

- Cell-free extract was prepared from YE-treated cell cultures to perform *in vitro* enzyme assay to decipher biosynthetic route of benzoic acid formation.
- Phenylalanine ammonia-lyase (PAL) activity was detected from the YE-treated cell cultures of pear, which catalyzes conversion of phenylalanine into *trans*-cinnamic acid.
- A novel chain-shortening enzyme, benzaldehyde synthase (BS) was first time reported from elicited cell cultures of *P. pyrifolia*. BS catalyzed *in vitro* formation of *trans*-cinnamic acid to benzaldehyde by a C₂-side chain cleavage. BS activity was cofactor independent and massively uplifted by supplementation of a thiol-reagent, such as DTT. BS was biochemically characterized using partially purified cell-free extract.
- The next step in the benzoic acid biosynthetic pathway was catalyzed by a NAD⁺-dependent benzaldehyde dehydrogenase (BD) which converts benzaldehyde into benzoic acid. BD activity was biochemically characterized and putative BD genes has been identified from pear genome.
- The next enzymatic step was catalyzed by benzoate-CoA-ligase (BZL), which converts benzoic acid into benzoyl-CoA. Later, benzoyl-CoA enters into biphenyl-phytoalexin biosynthetic pathway. BZL activity was biochemically characterized. Detection of BZL activity in pear is unique, till date, BZL activity is only reported from *Clarkia breweri* among plants.
- Finally, biphenyl synthase (BIS) activity, catalyzing condensation of benzoyl-CoA with malonyl-CoA has been detected from the YE-treated cell cultures of pear. Time-course of BIS activities were correlated with PAL, BS, BD and BZL activities.
- The activities of benzoic acid biosynthetic enzymes increased co-coordinately in response to yeast-extract elicitor treatment. In elicited cell cultures, biphenyl phytoalexin (aucuparin and noraucuparin) accumulation was preceded by increase in the activities of PAL, BS, BD, BZL an BIS suggesting the involvement of these enzymes in benzoic acid and subsequently biphenyl biosynthesis.

5.2. Conclusion:

The metabolomics profile of immature and mature leaves of *P. pyrifolia* and *P. communis* were analyzed by non-targeted GC-MS metabolomics analyses. As a result of this comparative analyses, it was observed that the metabolite profile of both the *Pyrus* species were dominated by 30 identified metabolites, including amino acids, sugars, sugar alcohols, organic acids, vitamins and phenolics. Among phenolics, especially the level of benzoic acid, chlorogenic acid, caffeic acid, protocatechuic acid, *trans*-cinnamic acid and 4-hydroxybenzoic acid were significantly higher in the leaves of *P. pyrifolia* than those of *P. communis*, grown under similar green house conditions. This is possibly the main reason explaining why *P. pyrifolia* leaves showed higher ontogenic resistance towards pathogen infection, particularly for the pear scab fungus, *V. pirina*. Notably, benzoic acid is the precursor of biphenyl (aucuparin and noraucuparin) class of metabolites, which are the marker defense metabolite for pears and other members of sub-tribe Malinae. High benzoic acid level might provide metabolic flexibility to *P. pyrifolia* cells to rapidly synthesize these biphenyl phytoalexins upon pathogen infection, and consequently the higher degree of resistance against pathogen infections. Moreover, high TPC and FRSA in *P. pyrifolia* might indicate that these values are positively correlated with the high phenolics content of *P. pyrifolia* leaves. Accordingly, high expression level of phenylalanine ammonia-lyase (*PAL*) was suggestive of high turnover of phenylpropanoid pathway. Higher availability of glycolyses and TCA cycle intermediate in *P. pyrifolia* leaves were possibly due to faster turn-over of these two pathways along with shikimic acid pathway which stems from phosphoenolpyruvate, one intermediate of glycolysis. Based on these results, it is conclude that the ability of *P. pyrifolia* leaves to exhibit higher ontogenic resistance towards pathogen attack is based on its ability to synthesize an array of defense metabolites, especially phenolics, in significantly higher level. This GC-MS-based metabolomics technology possibly provides a powerful approach to quickly discriminate the scab disease-resistance characteristics of *Pyrus* species.

Biosynthesis of benzoic acid and benzoate-derived biphenyl phytoalexin formation from *trans*-cinnamic acid has been studied in the yeast-extract (YE)-treated cell cultures of *P. pyrifolia* (Asian pear). Upon YE-treatment, *P. pyrifolia* cell cultures accumulated two biphenyl phytoalexins, the aucuparin and the noraucuparin. Enzymatic route for the formation of benzoic acid in *P. pyrifolia* cell cultures was found to be **CoA-independent and non β -oxidative**. Starting from phenylalanine, five enzymatic steps were required for the biosynthesis of the starter biphenyl scaffold, 3, 5-dihydroxybiphenyl. First, phenylalanine undergoes deamination

to give cinnamic by a PAL catalyzed reaction. Cinnamic acid is subsequently converted non-oxidatively into benzaldehyde by the action of a novel C₂-chain shortening enzyme, benzaldehyde synthase (BS). Benzaldehyde was subsequently converted into benzoic acid by a NAD⁺-dependent benzaldehyde dehydrogenase (BD) enzyme. Benzoic acid is then converted into benzoyl-CoA by the action of enzyme benzoate-CoA ligase (BZL). Finally benzoyl-CoA combines with three molecules of malonyl-CoA in a reaction catalyzed by the biphenyl synthase (BIS) enzyme.

Time course analyses revealed that activities of all these five biosynthetic enzymes are increased in a coordinated fashion in response to yeast-extract treatment. BS, BD and BZL enzymes were biochemically characterized using cell-free extract or partially purified proteins. Further precursor feeding experiments were performed to establish BS and BD enzymatic functions. **In conclusion, biosynthesis of benzoic acid in elicited cell cultures of *P. pyrifolia* was found to proceed via CoA-independent and non β -oxidative route. Benzaldehyde synthase (BS) activity was reported first time from any plant system. Detection of BZL activity is also unique, so far in plant system, only one report of BZL activity is available (from *Clarkia breweri*).**

The outcome of this thesis work gives details of some crucial enzymes involved in the biosynthesis of benzoic acid and benzoyl-CoA, which ultimately lead to the formation of biphenyl phytoalexins in pear. The findings will substantially contribute to peoples understanding of the organization of this biosynthetic pathway and the underlying regulatory processes. Taken together, this knowledge will provide the basis for successful metabolic engineering approaches for fortifying defense potential of pears.

5.3. Future scopes

- In this work, basal metabolite level in the leaves of Asian and European pear has been investigated. Future research warrants detailed metabolomics of *Pyrus* species infected with pear scab fungus *V. pirina* or *V. nashicola* to elucidate the exact role of these phenolics in plant defense mechanism upon pathogen infection.
- Till date, there is no report available on molecular details of benzaldehyde synthase-type of enzyme from plant system. The *VpVAN* from *Vanilla planifolia* (Gallage et al., 2014) is the only gene known so far, encoding a C₂-chain shortening enzyme involved in vanillin

biosynthesis. **In this context BS from *P. pyrifolia* is a promising candidate for future cDNA cloning and functional expression.** Since pear genome database is available (GDR: Genome Database of Rosaceae) a sequence homology based cloning could be a quicker approach to clone BS cDNA from elicited *P. pyrifolia* cell cultures using sequence information from *VpVAN* or from *HBS* from *V. planifolia* (Havkin-Frenkel et al., 2003). Future cloning and functional analyses of BS cDNA from *P. pyrifolia* will provide new insight on regulation of BS upon pathogen infection.

- Likewise BS, molecular details of aromatic cytosolic plant aldehyde dehydrogenase (ALDH) is poorly understood; particularly any ALDH related to benzoic acid biosynthesis in phytoalexin pathway is yet to discover. **Thereby, taking the advantage of pear genome database, cloning and functional analyses of benzaldehyde dehydrogenase (BD) from *P. pyrifolia* is an area of research with considerable interest.** A set of putative genes has already been identified in this work (Table 3.7; under Result section), which need to be functionally validated using cloning and functional analyses.
- Similarly, cloning and functional analyses of benzoate-CoA ligase (BZL) would be an excellent future target. Availability of pear genome database will provide the opportunity of functional genomics.
- Information on *BS*, *BD* and *BZL* gene sequence will be a pre-requisite for rational manipulation of benzoate-derived phytoalexin biosynthesis. This knowledge will provide the basis for successful metabolic engineering approaches for enhanced phytoalexin biosynthesis in pear and other members of Malinae. Manipulation of biphenyl biosynthesis may result in enhanced resistance of pear cultivars against the most devastating pathogens.

6. References

1. Abd El-Mawla, A.M., Beerhues, L., 2002. Benzoic acid biosynthesis in cell cultures *Hypericum androsaemum*. *Planta* 214, 727–733. doi:10.1007/s004250100657.
2. Abd El-Mawla, A. M. A. A., Schmidt, W., Beerhues, L., 2001. Cinnamic acid is a precursor of benzoic acids in cell cultures of *Hypericum androsaemum* L. but not in cell cultures of *Centaurium erythraea* RAFN. *Planta*, 212(2), 288–293. <https://doi.org/10.1007/s004250000394>
3. Abe, K., Saito, T., Terai, O., Sato, Y., Kotobuki, K., 2008. Genotypic difference for the susceptibility of Japanese, Chinese and European pears to *Venturia nashicola*, the cause of scab on Asian pears. *Plant Breed.* 127, 407–412. doi:10.1111/j.1439-0523.2007.01482.x.
4. Agrios, G.N., 2005. *Plant Pathology*, 5th edn (San Diego, California, USA: Academic Press Ltd).
5. Allen, J., Davey, H.M., Broadhurst, D., Heald, J.K., Rowland, J.J., Oliver, S.G., Kell, D.B., 2003. High-throughput classification of yeast mutants for functional genomics using metabolic foot printing. *Nat. Biotechnol.* 21, 692–6. doi:10.1038/nbt823.
6. Amil-Ruiz, F., Blanco-Portales, R., Muñoz-Blanco, J., Caballero, J.L., 2011. The strawberry plant defense mechanism: a molecular review. *Plant Cell Physiol.* 52, 1873–1903. doi:10.1093/pcp/pcr136.
7. Arnholdt-Schmitt, B., Costa, J.H., de Melo, D.F., 2006. AOX-a functional marker for efficient cell reprogramming under stress? *Trends Plant Sci.* 11, 281–7. doi:10.1016/j.tplants.2006.05.001.
8. APEDA ., 2014. Agri exchange data. National horticulture board. India
9. Atanasova-Penichon, V., Barreau, C., Richard-Forget, F., 2016. Antioxidant secondary metabolites in cereals: potential involvement in resistance to *Fusarium* and mycotoxin accumulation. *Front. Microbiol.* 7. doi:10.3389/fmicb.2016.00566.
10. Ateyyat, M., Abu-Romman, S., Abu-Darwish, M., Ghabeish, I., 2012. Impact of flavonoids against woolly apple Aphid, *Eriosoma lanigerum* (Hausmann) and its sole parasitoid, *Aphelinus mali* (Hald.). *J. Agric. Sci.* 4. doi:10.5539/jas.v4n2p227.

11. Baldwin, I.T., Halitschke, R., Paschold, A., von Dahl, C.C., Preston, C.A., 2006. Volatile signaling in plant-plant interactions: “talking trees” in the genomics era. *Science* 311, 812–5. doi:10.1126/science.1118446.
12. Bao, K., Fan, A., Dai, Y., Zhang, L., Zhang, W., Cheng, M., Yao, X., 2009. Selective demethylation and debenzoylation of aryl ethers by magnesium iodide under solvent-free conditions and its application to the total synthesis of natural products. *Org. Biomol. Chem.* 7, 5084. doi:10.1039/b916969e.
13. Baohua, L., Meiqi, Z., 2001. Relationship between leaf age of pear and its resistance to *Venturia nashicola*. *Acta Phytopylacica Sin.* 28, 309—312.
14. Barbosa, A.C.L., Sarkar, D., Pinto, M.D.S., Ankolekar, C., Greene, D., Shetty, K., 2013. Type 2 diabetes relevant bioactive potential of freshly harvested and long-term stored pears using in vitro assay models. *J. Food Biochem.* 37, 677–686. doi:10.1111/j.1745-4514.2012.00665.x.
15. Barillas, W., Beerhues, L., 2000. 3-Hydroxybenzoate:coenzyme A ligase from cell cultures of *Centaureum erythraea*: isolation and characterization. *Biol. Chem.* 381, 155–60. doi:10.1515/BC.2000.021.
16. Barillas, W., Beerhues, L., 1997. 3-Hydroxybenzoate:coenzyme A ligase and 4-coumarate: coenzyme A ligase from cultured cells of *Centaureum erythraea*. *Planta* 202, 112–116.
17. Belkheir, A.K., Gaid, M., Liu, B., Hänsch, R., Beerhues, L., 2016. Benzophenone synthase and chalcone synthase accumulate in the mesophyll of *Hypericum perforatum* leaves at different developmental stages. *Front. Plant Sci.* 7, 921. doi:10.3389/fpls.2016.00921.
18. Bera, P., Mukherjee, C., Mitra, A., 2017. Enzymatic production and emission of floral scent volatiles in *Jasminum sambac*. *Plant Sci.* 256, 25–38. doi:10.1016/j.plantsci.2016.11.013.
19. Beuerle, T., Pichersky, E., 2002a. Purification and characterization of benzoate: coenzyme A ligase from *Clarkia breweri*. *Arch. Biochem. Biophys.* 400, 258–264. doi:10.1016/S0003-9861(02)00026-7.
20. Beuerle, T., Pichersky, E., 2002b. Enzymatic synthesis and purification of aromatic coenzyme A esters. *Anal. Biochem.* 302, 305–312. doi:10.1006/abio.2001.5574.

21. Bisht, S., Kant, R., Kumar, V., 2013. α -d-Glucosidase inhibitory activity of polysaccharide isolated from *Acacia tortilis* gum exudate. *Int. J. Biol. Macromol.* 59, 214–220. doi:10.1016/j.ijbiomac.2013.04.057.
22. Bonn, W.G., Zwet, T. van der, 2000. Distribution and economic importance of fire blight. In: *Fire blight. The disease and its causative agent, Erwinia amylovora*. CABI, Wallingford, Chapter 3: 37–53. doi:10.1079/9780851992945.0037.
23. Borejsza-Wysocki, W., Lester, C., Attygalle, A., Hrazdina, G., 1999. Elicited cell suspension cultures of apple (*Malus domestica*) cv. Liberty produce biphenyl phytoalexins. *Phytochemistry* 50, 231–235. doi:10.1016/S0031-9422(98)00509-3.
24. Bostock, R.M., Wilcox, S.M., Wang, G., Adaskaveg, J.E., 1999. Suppression of *Monilinia fructicola* cutinase production by peach fruit surface phenolic acids. *Physiol. Mol. Plant Pathol.* 54, 37–50. doi:10.1006/pmpp.1998.0189.
25. Bradford, M., 1976. A rapid and sensitive method for the quantitation of microgram quantities of protein utilizing the principle of protein– dye binding. *Anal. Biochem.* 72, 248–254. doi:10.1016/0003-2697(76)90527-3.
26. Brewer, L., Alspach, P., Bus, V., 2005. Fruit and leaf incidence of pear scab (*Venturia pirina* Aderh.) in mixed European and Asian pear progenies. *Acta Hort.* 595–600. doi:10.17660/ActaHortic.2005.671.83.
27. Brewer, L.R., Alspach, P.A., Morgan, C., Bus, V.G.M., 2009. Resistance to scab caused by *Venturia pirina* in interspecific pear (*Pyrus* spp.) hybrids. *New Zeal. J. Crop Hortic. Sci.* 37, 211–218. doi:10.1080/01140670909510266.
28. Brocker, C., Vasiliou, M., Carpenter, S., Carpenter, C., Zhang, Y., Wang, X., Kotchoni, S.O., Wood, A.J., Kirch, H.-H., Kopečný, D., Nebert, D.W., Vasiliou, V., 2013. Aldehyde dehydrogenase (ALDH) superfamily in plants: gene nomenclature and comparative genomics. *Planta* 237, 189–210. doi:10.1007/s00425-012-1749-0.
29. Bunzel, M., Ralph, J., 2006. NMR characterization of lignins isolated from fruit and vegetable insoluble dietary fiber. *J. Agric. Food Chem.* 54, 8352–8361. doi:10.1021/jf061525z.
30. Bussell, J.D., Reichelt, M., Wiszniewski, A.A.G., Gershenzon, J., Smith, S.M., 2014. Peroxisomal ATP-binding cassette transporter COMATOSE and the multifunctional protein abnormal inflorescence meristem are required for the production of benzoylated

metabolites in *Arabidopsis* seeds. *Plant Physiol.* 164, 48–54. doi:10.1104/pp.113.229807.

31. Campbell, C.S., Evans, R.C., Morgan, D.R., Dickinson, T.A., Arsenault, M.P., 2007. Phylogeny of subtribe Pyrinae (formerly the Maloideae, Rosaceae): limited resolution of a complex evolutionary history. *Plant Syst. Evol.* 266, 119–145. doi:10.1007/s00606-007-0545-y.
32. Campos, C., Cardoso, H., Nogales, A., Svensson, J., Lopez-Ráez, J.A., Pozo, M.J., Nobre, T., Schneider, C., Arnholdt-Schmitt, B., 2015. Intra and inter-spore variability in *Rhizophagus irregularis* AOX gene. *PLoS One* 10, e0142339. doi: 10.1371 /journal.pone.0142339.
33. Campos, M.D., Nogales, A., Cardoso, H.G., Kumar, S.R., Nobre, T., Sathishkumar, R., Arnholdt-Schmitt, B., 2016. Stress-induced accumulation of DcAOX1 and DcAOX2a transcripts coincides with critical time point for structural biomass prediction in carrot primary cultures (*Daucus carota* L.). *Front. Genet.* 7, 1. doi:10.3389/fgene.2016.00001.
34. Chagné, D., Crowhurst, R.N., Pindo, M., Thrimawithana, A., Deng, C., Ireland, H., Fiers, M., Dzierzon, H., Cestaro, A., Fontana, P., Bianco, L., Lu, A., Storey, R., Knäbel, M., Saeed, M., Montanari, S., Kim, Y.K., Nicolini, D., Larger, S., Stefani, E., Allan, A.C., Bowen, J., Harvey, I., Johnston, J., Malnoy, M., Troggio, M., Percepied, L., Sawyer, G., Wiedow, C., Won, K., Viola, R., Hellens, R.P., Brewer, L., Bus, V.G.M., Schaffer, R.J., Gardiner, S.E., Velasco, R., 2014. The draft genome sequence of European pear (*Pyrus communis* L. “Bartlett”). *PLoS One* 9, e92644.
35. Chakraborty, M., Karun, A., Mitra, A., 2009. Accumulation of phenylpropanoid derivatives in chitosan-induced cell suspension culture of *Cocos nucifera*. *J. Plant Physiol.* 166, 63–71. doi:10.1016/j.jplph.2008.02.004.
36. Chizzali, C., Beerhues, L., 2012a. Phytoalexins of the Pyrinae: Biphenyls and dibenzofurans. *Beilstein J. Org. Chem.* 8, 613–620. doi:10.3762/bjoc.8.68.
37. Chizzali, C., Khalil, M.N.A., Beuerle, T., Schuehly, W., Richter, K., Flachowsky, H., Peil, A., Hanke, M.V., Liu, B., Beerhues, L., 2012b. Formation of biphenyl and dibenzofuran phytoalexins in the transition zones of fire blight-infected stems of *Malus domestica* cv. “Holsteiner Cox” and *Pyrus communis* cv. “Conference.” *Phytochemistry* 77, 179–185. doi:10.1016/j.phytochem.2012.01.023.

38. Chizzali, C., Swiddan, A.K., Abdelaziz, S., Gaid, M., Richter, K., Fischer, T.C., Liu, B., Beerhues, L., 2016. Expression of biphenyl synthase genes and formation of phytoalexin compounds in three fire blight-infected *Pyrus communis* cultivars. PLoS One 11, e0158713. doi:10.1371/journal.pone.0158713.
39. Christenhusz, M.J.M., Byng, J.W., 2016. The number of known plant species in the world and its annual increase. Phytotaxa 261, 201–217. doi:10.11646/phytotaxa.261.3.1.
40. Colquhoun, T.A., Marciniak, D.M., Wedde, A.E., Kim, J.Y., Schwieterman, M.L., Levin, L.A., Van Moerkerke, A., Schuurink, R.C., Clark, D.G., 2012. A peroxisomally localized acyl-activating enzyme is required for volatile benzenoid formation in a *Petunia*×*hybrida* cv. “Mitchell Diploid” flower. J. Exp. Bot. 63, 4821–4833. doi:10.1093/jxb/ers153.
41. Costa, J. H., Cardoso, H. G., Campos, M. D., Zavattieri, A., Frederico, A. M., Fernandes de Melo, D., Arnholdt-Schmitt, B., 2009. *Daucus carota* L.--an old model for cell reprogramming gains new importance through a novel expansion pattern of alternative oxidase (AOX) genes. Plant Physiology and Biochemistry : PPB, 47(8), 753–9. <https://doi.org/10.1016/j.plaphy.2009.03.011>
42. Costa, J. H., Santos, C. P. dos, de Sousa e Lima, B., Moreira Netto, A. N., Saraiva, K. D. da C., and Arnholdt-Schmitt, B., 2017. In silico identification of alternative oxidase 2 (AOX2) in monocots: A new evolutionary scenario. Journal of Plant Physiology, 210, 58–63.
43. Coyne, S., Litomska, A., Chizzali, C., Khalil, M.N.A., Richter, K., Beerhues, L., Hertweck, C., 2014. Control of plant defense mechanisms and fire blight pathogenesis through the regulation of 6-thioguanine biosynthesis in *Erwinia amylovora*. ChemBiochem 15, 373–6. doi:10.1002/cbic.201300684.
44. Cui, T., Nakamura, K., Ma, L., Li, J.-Z., Kayahara, H., 2005. Analyses of arbutin and chlorogenic acid, the major phenolic constituents in Oriental pear. J. Agric. Food Chem. 53, 3882–7. doi:10.1021/jf047878k.
45. Dai, H., Xiao, C., Liu, H., Tang, H., 2010. Combined NMR and LC-MS analysis reveals the metabonomic changes in *Salvia miltiorrhiza* bunge induced by water depletion. J. Proteome Res. 9, 1460–1475. doi:10.1021/pr900995m.
46. Deckers, T., Schoofs, H., 2008. Status of the pear production in Europe. Acta Hort. 95–106. doi:10.17660/ActaHortic.2008.800.8.

47. Delausaradhiney, A.J., Verma, D.P.S., 1993. Proline biosynthesis and osmoregulation in plants. *Plant J.* 4, 215–223. doi:10.1046/j.1365-313X.1993.04020215.x.
48. FAOSTAT., 2017. <http://www.fao.org/faostat/en/#data/QC>
49. Ferreira, D., Guyot, S., Marnet, N., Delgadillo, I., Renard, C.M.G.C., Coimbra, M.A., 2002. Composition of phenolic compounds in a Portuguese pear (*Pyrus communis* L. Var. S. Bartolomeu) and changes after sun-drying. *J. Agric. Food Chem.* 50, 4537–4544. doi:10.1021/jf020251m.
50. Fiehn, O., 2002. Metabolomics - the link between genotypes and phenotypes. *Plant Mol. Biol.* 48, 155–171. doi:10.1023/A:1013713905833.
51. Fotirić Akšić, M.M., Dabić, D.Č., Gašić, U.M., Zec, G.N., Vulić, T.B., Tešić, Ž.L., Natić, M.M., 2015. Polyphenolic profile of pear leaves with different resistance to pear Psylla (*Cacopsylla pyri*). *J. Agric. Food Chem.* 63, 7476–7486. doi:10.1021/acs.jafc.5b03394.
52. Fourie, P.C., Hansmann, C.F., Oberholzer, H.M., 1991. Sugar content of fresh apples and pears in South Africa. *J. Agric. Food Chem.* 39, 1938–1939. doi:10.1021/jf00011a008.
53. French, C.J., Vance, C.P., Neil Towers, G.H., 1976. Conversion of p-coumaric acid to p-hydroxybenzoic acid by cell free extracts of potato tubers and *Polyporus hispidus*, *Phytochemistry*. doi:10.1016/S0031-9422(00)88979-7.
54. Gaid, M.M., Sircar, D., Beuerle, T., Mitra, A., Beerhues, L., 2009. Benzaldehyde dehydrogenase from chitosan-treated *Sorbus aucuparia* cell cultures. *J. Plant Physiol.* 166, 1343–1349. doi:10.1016/j.jplph.2009.03.003.
55. Gaid, M.M., Sircar, D., Muller, A., Beuerle, T., Liu, B., Ernst, L., Hansch, R., Beerhues, L., 2012. Cinnamate:CoA ligase initiates the biosynthesis of a benzoate-derived xanthone phytoalexin in *Hypericum calycinum* cell cultures. *Plant Physiol.* 160, 1267–1280. doi:10.1104/pp.112.204180.
56. Gallage, N.J., Hansen, E.H., Kannangara, R., Olsen, C.E., Motawia, M.S., Jørgensen, K., Holme, I., Hebelstrup, K., Grisoni, M., Møller, B.L., 2014. Vanillin formation from ferulic acid in *Vanilla planifolia* is catalysed by a single enzyme. *Nat. Commun.* 5, 4037. doi:10.1038/ncomms5037.

57. Gao, C., Han, B., 2009. Evolutionary and expression study of the aldehyde dehydrogenase (ALDH) gene superfamily in rice (*Oryza sativa*). *Gene* 431, 86–94. doi:10.1016/j.gene.2008.11.010.
58. Gerardy, R., Zenk, M.H., 1992. Formation of salutaridine from (R)-reticuline by a membrane-bound cytochrome P-450 enzyme from *Papaver somniferum*. *Phytochemistry* 32, 79–86. doi:10.1016/0031-9422(92)80111-Q.
59. Gosch, C., Halbwirth, H., Stich, K., 2010. Phloridzin: biosynthesis, distribution and physiological relevance in plants. *Phytochemistry* 71, 838–43. doi:10.1016/j.phytochem.2010.03.003.
60. Gunen, Y., Misirli, A., Gulcan, R., 2005. Leaf phenolic content of pear cultivars resistant or susceptible to fire blight. *Sci. Hortic. (Amsterdam)* 105, 213–221. doi:10.1016/j.scienta.2005.01.014.
61. Güven, K., Yücel, E., Cetintaş, F., 2006. Antimicrobial activities of fruits of *Crataegus* and *Pyrus* species. *Pharm. Biol.* 44, 79–83. doi:10.1080/13880200600591253.
62. Hamauzu, Y., Forest, F., Hiramatsu, K., Sugimoto, M., 2007. Effect of pear (*Pyrus communis* L.) procyanidins on gastric lesions induced by HCl/ethanol in rats. *Food Chem.* 100, 255–263. doi:10.1016/j.foodchem.2005.09.050.
63. Hancock, J.F., 2008. In: Temperate fruit crop breeding: Germplasm to genomics, temperate fruit crop breeding: Germplasm to Genomics. Springer Netherlands, Chapter doi:10.1007/978-1-4020-6907-9.
64. Harish, M.C., Dachinamoorthy, P., Balamurugan, S., Bala Murugan, S., Sathishkumar, R., 2013. Enhancement of α -tocopherol content through transgenic and cell suspension culture systems in tobacco. *Acta Physiol. Plant.* 35, 1121–1130. doi:10.1007/s11738-012-1149-x.
65. Hébert, C., Charles, M.T., Gauthier, L., Willemot, C., Khanizadeh, S., Cousineau, J., 2002. Strawberry proanthocyanidins: Biochemical markers for *Botrytis cinerea* resistance and shelf-life predictability. *Acta Hortic.* 659–662. doi:10.17660/ActaHortic.2002.567.143.
66. Hendrawati, O., Yao, Q., Kim, H. K., Linthorst, H. J. M., Erkelens, C., Lefeber, A. W. M., Verpoorte, R., 2006. Metabolic differentiation of Arabidopsis treated with methyl jasmonate using nuclear magnetic resonance spectroscopy. *Plant Science*, 170(6), 1118–

1124. <https://doi.org/10.1016/j.plantsci.2006.01.017>

67. Hrazdina, G., 2003. Response of scab-susceptible (McIntosh) and scab-resistant (Liberty) apple tissues to treatment with yeast extract and *Venturia inaequalis*. *Phytochemistry* 64, 485–492. doi:10.1016/S0031-9422(03)00150-X.
68. Hrazdina, G., Borejsza-Wysocki, W., Lester, C., 1997. Phytoalexin production in an apple cultivar resistant to *Venturia inaequalis*. *Phytopathology* 87, 868–876. doi:10.1094/PHYTO.1997.87.8.868.
69. Hudina, M., Štampar, F., 2000. Sugars and organic acids contents of European *Pyrus comminus* L. and Asian *Pyrus serotina* Rehd. pear cultivars. *Acta Aliment.* 29, 217–230. doi:10.1556/AAlim.29.2000.3.2.
70. Hüttner, C., Beuerle, T., Scharnhop, H., Ernst, L., Beerhues, L., 2010. Differential effect of elicitors on biphenyl and dibenzofuran formation in *Sorbus aucuparia*. *Cell Cultures. J. Agric. Food Chem.* 58, 11977–11984. doi:10.1021/jf1026857.
71. Ibdah, M., Pichersky, E., 2009. Arabidopsis Chy1 null mutants are deficient in benzoic acid-containing glucosinolates in the seeds. *Plant Biol.* 11, 574–581. doi:10.1111/j.1438-8677.2008.00160.x.
72. Jarvis, A.P., Schaaf, O., Oldham, N.J., 2000. 3-Hydroxy-3-phenylpropanoic acid is an intermediate in the biosynthesis of benzoic acid and salicylic acid but benzaldehyde is not. *Planta* 212, 119–126. doi:10.1007/s004250000377.
73. Jovanovic-Malinovska, R., Kuzmanova, S., Winkelhausen, E., 2014. Oligosaccharide profile in fruits and vegetables as sources of prebiotics and functional foods. *Int. J. Food Prop.* 17, 949–965. doi:10.1080/10942912.2012.680221.
74. Kanwal, Q., Hussain, I., Latif Siddiqui, H., Javaid, A., 2010. Antifungal activity of flavonoids isolated from mango (*Mangifera indica* L.) leaves. *Nat. Prod. Res.* 24, 1907–14. doi:10.1080/14786419.2010.488628.
75. Kaufholdt, D., Baillie, C. K., Bikker, R., Burkart, V., Dudek, C.-A., von Pein, L., Hänsch, R. 2016. The molybdenum cofactor biosynthesis complex interacts with actin filaments via molybdenum insertase Cnx1 as anchor protein in *Arabidopsis thaliana*. *Plant Science: An International Journal of Experimental Plant Biology*, 244, 8–18. <https://doi.org/10.1016/j.plantsci.2015.12.011>

76. Kaufholdt, D., Baillie, C.-K., Wille, T., Lang, C., Hallier, S., Herschbach, C., Hänsch, R., 2015. Prospective Post-translational Regulation of Plant Sulfite Oxidase BT - Molecular Physiology and Eco physiology of Sulfur. In L. J. De Kok, M. J. Hawkesford, H. Rennenberg, K. Saito, & E. Schnug (Eds.) (pp. 179–187). Cham: Springer International Publishing. https://doi.org/10.1007/978-3-319-20137-5_18
77. Katayama, H., Amo, H., Wuyun, T., Uematsu, C., Iketani, H., 2016. Genetic structure and diversity of the wild ussurian pear in East Asia. *Breed. Sci.* 66, 90–99. doi:10.1270/jsbbs.66.90.
78. Khalil, M.N.A., Beuerle, T., Müller, A., Ernst, L., Bhavanam, V.B.R., Liu, B., Beerhues, L., 2013. Biosynthesis of the biphenyl phytoalexin aucuparin in *Sorbus aucuparia* cell cultures treated with *Venturia inaequalis*. *Phytochemistry* 96, 101–9. doi:10.1016/j.phytochem.2013.09.003.
79. Khalil, M.N.A., Brandt, W., Beuerle, T., Reckwell, D., Groeneveld, J., Hänsch, R., Gaid, M.M., Liu, B., Beerhues, L., 2015. O-Methyl transferases involved in biphenyl and dibenzofuran biosynthesis. *Plant J.* 83, 263–76. doi:10.1111/tpj.12885.
80. Kim, J.K., Choi, S.R., Lee, J., Park, S.-Y., Song, S.Y., Na, J., Kim, S.W., Kim, S.-J., Nou, I.-S., Lee, Y.H., Park, S.U., Kim, H., 2013. Metabolic Differentiation of Diamondback Moth (*Plutella xylostella* (L.)) Resistance in Cabbage (*Brassica oleracea* L. ssp. capitata). *J. Agric. Food Chem.* 61, 11222–11230. doi:10.1021/jf403441t.
81. Klempien, A., Kaminaga, Y., Qualley, A., Nagegowda, D.A., Widhalm, J.R., Orlova, I., Shasany, A.K., Taguchi, G., Kish, C.M., Cooper, B.R., D’Auria, J.C., Rhodes, D., Pichersky, E., Dudareva, N., 2012. Contribution of CoA ligases to benzenoid biosynthesis in *Petunia* flowers. *Plant Cell* 24, 2015–2030. doi:10.1105/tpc.112.097519.
82. Kliebenstein, D.J., D’Auria, J.C., Behere, A.S., Kim, J.H., Gunderson, K.L., Breen, J.N., Lee, G., Gershenzon, J., Last, R.L., Jander, G., 2007. Characterization of seed-specific benzoyloxy glucosinolate mutations in *Arabidopsis thaliana*. *Plant J.* 51, 1062–76. doi:10.1111/j.1365-313X.2007.03205.x.
83. Kokubun, T., Harborne, J.B., 1995. Phytoalexin induction in the sapwood of plants of the Maloideae (Rosaceae): Biphenyls or dibenzofurans. *Phytochemistry* 40, 1649–1654. doi:10.1016/0031-9422(95)00443-B.

84. Kokubun, T., Harborne, J.B., 1994. A survey of phytoalexin induction in leaves of the Rosaceae by copper ions. *Zeitschrift fur Naturforsch. - Sect. C J. Biosci.* 49, 628–634. doi:10.1515/znc-1994-9-1014.
85. Končítíková, R., Vigouroux, A., Kopečná, M., Andree, T., Bartoš, J., Šebela, M., Moréra, S., Kopečný, D., 2015. Role and structural characterization of plant aldehyde dehydrogenases from family 2 and family 7. *Biochem. J.* 468, 109 LP-123.
86. Kraus, P.F., Kutchan, T.M., 1995. Molecular cloning and heterologous expression of a cDNA encoding berbamunine synthase, a C-O phenol-coupling cytochrome P450 from the higher plant *Berberis stolonifera*. *Proc. Natl. Acad. Sci. U. S. A* 92, 2071–5.
87. Kuc, J., 1982. Phytoalexins from the Solanaceae. *Phytoalexins / Gen. Ed. J.A. Bailey J.W. Mansf.*
88. Kumar, V., Nagar, S., 2014. Studies on *Tinospora cordifolia* monosugars and correlation analysis of uronic acids by spectrophotometric methods and GLC. *Carbohydr. Polym.* 99, 291–296. doi:10.1016/j.carbpol.2013.07.083.
89. Kundu, A., Jawali, N., Mitra, A., 2012. Shikimate pathway modulates the elicitor-stimulated accumulation of fragrant 2-hydroxy-4-methoxybenzaldehyde in *Hemidesmus indicus* roots. *Plant Physiol. Biochem.* 56, 104–108. doi:10.1016/j.plaphy.2012.04.005.
90. Kunz, S., Pesquet, E., Kleczkowski, L.A., 2014. Functional dissection of sugar signals affecting gene expression in *Arabidopsis thaliana*. *PLoS One* 9, e100312. doi:10.1371/journal.pone.0100312.
91. Lattanzio, V., Lattanzio, V.M.T., Cardinali, A., Amendola, V., 2006. Role of phenolics in the resistance mechanisms of plants against fungal pathogens and insects, *Phytochemistry*.
92. Lakhera, A. K., Kumar, V., 2017. Monosaccharide composition of acidic gum exudates from Indian *Acacia tortilis* ssp. *raddiana* (Savi) Brenan. *International Journal of Biological Macromolecules*, 94(Pt A), 45–50. <https://doi.org/10.1016/j.ijbiomac.2016.09.097>
93. Lee, S., Kaminaga, Y., Cooper, B., Pichersky, E., Dudareva, N., Chapple, C., 2012. Benzoylation and sinapoylation of glucosinolate R-groups in *Arabidopsis*. *Plant J.* 72, 411–22. doi:10.1111/j.1365-313X.2012.05096.x.

94. Lee, Y.G., Cho, J.-Y., Park, J., Lee, S.-H., Kim, W.-S., Park, K.-H., Moon, J.-H., 2013. Large-scale isolation of highly pure malaxinic acid from immature pear (*Pyrus pyrifolia* Nakai) fruit. *Food Sci. Biotechnol.* 22, 1539–1545. doi:10.1007/s10068-013-0249-8.
95. Leontowicz, H., Gorinstein, S., Lojek, A., Leontowicz, M., Ciz, M., Soliva-Fortuny, R., Park, Y.S., Jung, S.T., Trakhtenberg, S., Martin-Belloso, O., 2002. Comparative content of some bioactive compounds in apples, peaches and pears and their influence on lipids and antioxidant capacity in rats. *J. Nutr. Biochem.* 13, 603–610.
96. Li, X., Wang, T., Zhou, B., Gao, W., Cao, J., Huang, L., 2014. Chemical composition and antioxidant and anti-inflammatory potential of peels and flesh from 10 different pear varieties (*Pyrus* spp.). *Food Chem.* 152, 531–538. doi:10.1016/j.foodchem.2013.12.010.
97. Lisec, J., Schauer, N., Kopka, J., Willmitzer, L., Fernie, A.R., 2006. Gas chromatography mass spectrometry-based metabolite profiling in plants. *Nat. Protoc.* 1, 387–96. doi:10.1038/nprot.2006.59.
98. Liu, B., Beuerle, T., Klundt, T., Beerhues, L., 2004. Biphenyl synthase from yeast-extract-treated cell cultures of *Sorbus aucuparia*. *Planta* 218, 492–496. doi:10.1007/s00425-003-1144-y.
99. Liu, B., Raeth, T., Beuerle, T., Beerhues, L., 2007. Biphenyl synthase, a novel type III polyketide synthase. *Planta* 225, 1495–1503. doi:10.1007/s00425-006-0435-5.
100. Liu, F., 2002. Functional specialization of maize mitochondrial aldehyde dehydrogenases. *Plant Physiol.* 130, 1657–1674. doi:10.1104/pp.012336.
101. Long, M.C., Nagegowda, D.A., Kaminaga, Y., Ho, K.K., Kish, C.M., Schnepf, J., Sherman, D., Weiner, H., Rhodes, D., Dudareva, N., 2009. Involvement of snapdragon benzaldehyde dehydrogenase in benzoic acid biosynthesis. *Plant J.* 59, 256–65. doi:10.1111/j.1365-313X.2009.03864.x.
102. Malinowski, J., Krzymowska, M., Godoń, K., Hennig, J., Podstolski, A., 2007. A new catalytic activity from tobacco converting 2-coumaric acid to salicylic aldehyde. *Physiol. Plant.* 129, 461–471. doi:10.1111/j.1399-3054.2006.00837.x.
103. Mandal, S., 2010. Induction of phenolics, lignin and key defense enzymes in eggplant (*Solanum melongena* L.) roots in response to elicitors. *African J. Biotechnol.* 9, 8038–8047. doi:10.5897/AJB10.984.

104. Mandal, S., Das, R.K., Mishra, S., 2011. Differential occurrence of oxidative burst and antioxidative mechanism in compatible and incompatible interactions of *Solanum lycopersicum* and *Ralstonia solanacearum*. *Plant Physiol. Biochem.* PPB 49, 117–23. doi:10.1016/j.plaphy.2010.10.006.
105. Mir, J.I., Ahmed, N., Singh, D.B., Rashid, R., Shafi, W., Zaffer, S., Sheikh, M.A., Noor, U., Khan, M.H., Rather, I., 2013. Fast and efficient in-vitro multiplication of apple clonal root stock MM-106. *Vegetos* 26, 198–202. doi:10.5958/j.2229-4473.26.2.075.
106. Mir, J.I., Ahmed, N., Wani, S.H., Rashid, R., Mir, H., Sheikh, M.A., 2010. In vitro development of micro corms and stigma like structures in saffron (*Crocus sativus* L.). *Physiol. Mol. Biol. Plants* 16, 369–73. doi:10.1007/s12298-010-0044-4.
107. Mitra, A., Mayer, M.J., Mellon, F.A., Michael, A.J., Narbad, A., Parr, A.J., Waldron, K.W., Walton, N.J., 2002. 4-Hydroxycinnamoyl-CoA hydratase/lyase, an enzyme of phenylpropanoid cleavage from *Pseudomonas*, causes formation of C6-C1 acid and alcohol glucose conjugates when expressed in hairy roots of *Datura stramonium* L. *Planta* 215, 79–89. doi:10.1007/s00425-001-0712-2.
108. Morgan, D.R., Soltis, D.E., Robertson, K.R., 1994. Systematic and evolutionary implications of rbcL sequence variation in Rosaceae. *Am. J. Bot.* 81, 890–903. doi:10.2307/2445770.
109. Morrissey, J.P., Osbourn, A.E., 1999. Fungal resistance to plant antibiotics as a mechanism of pathogenesis. *Microbiol. Mol. Biol. Rev.* 63, 708–24.
110. Mukherjee, C., Samanta, T., Mitra, A., 2016. Redirection of metabolite biosynthesis from hydroxybenzoates to volatile terpenoids in green hairy roots of *Daucus carota*. *Planta* 243, 305–320. doi:10.1007/s00425-015-2403-4.
111. Murashige, T., Skoog, F., 1962. A revised medium for rapid growth and bio assays with Tobacco tissue cultures. *Physiol. Plant.* 15, 473–497. doi:10.1111/j.1399-3054.1962.tb08052.x.
112. Nair, R.B., Bastress, K.L., Ruegger, M.O., Denault, J.W., Chapple, C., 2004. The *Arabidopsis thaliana* reduced epidermal FLUORESCENCE1 gene encodes an aldehyde dehydrogenase involved in ferulic acid and sinapic acid biosynthesis. *Plant Cell* 16, 544–554. doi:10.1105/tpc.017509.

113. Obata, T., Fernie, A.R., 2012. The use of metabolomics to dissect plant responses to abiotic stresses. *Cell. Mol. Life Sci.* 69, 3225–3243. doi:10.1007/s00018-012-1091-5.
114. Oikawa, A., Otsuka, T., Nakabayashi, R., Jikumaru, Y., Isuzugawa, K., Murayama, H., Saito, K., Shiratake, K., 2015. Metabolic profiling of developing pear fruits reveals dynamic variation in primary and secondary metabolites, including plant hormones. *PLoS One* 10, e0131408. doi:10.1371/journal.pone.0131408.
115. Park, S.-W., Kaimoyo, E., Kumar, D., Mosher, S., Klessig, D.F., 2007. Methyl salicylate is a critical mobile signal for plant systemic acquired resistance. *Science* 318, 113–6. doi:10.1126/science.1147113.
116. Park, Y.J., Thwe, A.A., Li, X., Kim, Y.J., Kim, J.K., Arasu, M.V., Al-Dhabi, N.A., Park, S.U., 2015. Triterpene and flavonoid biosynthesis and metabolic profiling of hairy roots, adventitious roots and seedling roots of *Astragalus membranaceus*. *J. Agric. Food Chem.* 63, 8862–9. doi:10.1021/acs.jafc.5b02525.
117. Pastori, G.M., Kiddle, G., Antoniw, J., Bernard, S., Veljovic-Jovanovic, S., Verrier, P.J., Noctor, G., Foyer, C.H., 2003. Leaf vitamin C contents modulate plant defense transcripts and regulate genes that control development through hormone signaling. *Plant Cell* 15, 939–51.
118. Peters, S., Schmidt, W., Beerhues, L., 1997. Regioselective oxidative phenol couplings of 2,3,4,6-tetrahydroxybenzophenone in cell cultures of *Centaureum erythraea* RAFN and *Hypericum androsaemum* L. *Planta* 204, 64–69. doi:10.1007/s004250050230.
119. Petersen, M., 2007. Current status of metabolic phytochemistry. *Phytochemistry* 68, 2847–2860. doi:10.1016/j.phytochem.2007.07.029.
120. Pfaffl, M.W., 2001. A new mathematical model for relative quantification in real-time RT-PCR. *Nucleic Acids Res.* 29, e45.
121. Podstolski, A., Havkin-Frenkel, D., Malinowski, J., Blounta, J.W., Kourteva, G., Dixon, R.A., 2002. Unusual 4-hydroxybenzaldehyde synthase activity from tissue cultures of the vanilla orchid *Vanilla planifolia*. *Phytochemistry* 61, 611–620. doi:10.1016/S0031-9422(02)00285-6.
122. Potter, D., Eriksson, T., Evans, R.C., Oh, S., Smedmark, J.E.E., Morgan, D.R., Kerr, M., Robertson, K.R., Arsenault, M., Dickinson, T.A., Campbell, C.S., 2007. Phylogeny

- and classification of Rosaceae. *Plant Syst. Evol.* 266, 5–43. doi:10.1007/s00606-007-0539-9.
123. Qualley, A. V., Widhalm, J.R., Adebesein, F., Kish, C.M., Dudareva, N., 2012. Completion of the core-oxidative pathway of benzoic acid biosynthesis in plants. *Proc. Natl. Acad. Sci.* 109, 16383–16388. doi:10.1073/pnas.1211001109.
124. Rajeev Kumar, S., Kiruba, R., Balamurugan, S., Cardoso, H.G., Birgit, A.-S., Zakwan, A., Sathishkumar, R., 2014. Carrot antifreeze protein enhances chilling tolerance in transgenic tomato. *Acta Physiol. Plant.* 36, 21–27. doi:10.1007/s11738-013-1383-x.
125. Ranjeet Kaur, L., Arya, V., 2012. Ethnomedicinal and phytochemical perspectives of *Pyrus*. *J. Pharmacogn. Phytochem.* 1, 14–19.
126. Reiland, H., Slavin, J., 2015. Systematic review of pears and health. *Nutr. Today* 50, 301–305. doi:10.1097/NT.0000000000000112.
127. Reveal, J., 2012. Newly required infrafamilial names mandated by changes in the code of nomenclature for algae, fungi and plants. *Phytoneuron* 33, 1–32.
128. Ribnicky, D.M., Shulaev, V., Raskin, I., 1998. Intermediates of salicylic acid biosynthesis in Tobacco. *Plant Physiol.* 118, 565–572. doi:10.1104/pp.118.2.565.
129. Roberts, S.C., 2007. Production and engineering of terpenoids in plant cell culture. *Nat. Chem. Biol.* 3, 387–95. doi:10.1038/nchembio.2007.8.
130. Russell, W.R., Labat, A., Scobbie, L., Duncan, G.J., Duthie, G.G., 2009. Phenolic acid content of fruits commonly consumed and locally produced in Scotland. *Food Chem.* 115, 100–104. doi:10.1016/j.foodchem.2008.11.086.
131. Saini, S.S., Teotia, D., Gaid, M., Thakur, A., Beerhues, L., Sircar, D., 2017. Benzaldehyde dehydrogenase-driven phytoalexin biosynthesis in elicitor-treated *Pyrus pyrifolia* cell cultures. *J. Plant Physiol.* doi:10.1016/j.jplph.2017.06.004.
132. Saradhi, P.P., Alia, Arora, S., Prasad, K. V, 1995. Proline accumulates in plants exposed to UV radiation and protects them against UV induced peroxidation. *Biochem. Biophys. Res. Commun.* 209, 1–5.
133. Sarkate, A., Banerjee, S., Mir, J.I., Roy, P., Sircar, D., 2017. Antioxidant and cytotoxic activity of bioactive phenolic metabolites isolated from the yeast-extract treated cell culture of apple. *Plant Cell, Tissue Organ Cult.* doi:10.1007/s11240-017-1253-0.

134. Sax, K., 1931. The origin and relationships of the Pomoideae. *J. Arnold Arbor.* 12, 3–22.
135. Schnitzler, J.-P., Madlung, J., Rose, A., Ulrich Seitz, H., 1992. Biosynthesis of p-hydroxybenzoic acid in elicitor-treated carrot cell cultures. *Planta* 188. doi:10.1007/BF00197054.
136. Senthil, K., Thirugnanasambantham, P., Oh, T.J., Kim, S.H., Choi, H.K., 2015. Free radical scavenging activity and comparative metabolic profiling of in vitro cultured and field grown *Withania somnifera* roots. *PLoS One* 10, e0123360. doi:10.1371/journal.pone.0123360.
137. Sha, S., Li, J., Wu, J., Zhang, S., 2011. Characteristics of organic acids in the fruit of different pear species. *Afr. J. Agric. Res* 6, 2403–2410. doi:10.5897/AJAR11.316.
138. Shen, J., Wang, Y., Chen, C., Ding, Z., Hu, J., Zheng, C., Li, Y., 2015. Metabolite profiling of tea (*Camellia sinensis* L.) leaves in winter. *Sci. Hortic. (Amsterdam)*. 192, 1–9. doi:10.1016/j.scienta.2015.05.022.
139. Shulaev, V., Silverman, P., Raskin, I., 1997. Airborne signalling by methyl salicylate in plant pathogen resistance. *Nature* 385, 718–721. doi:10.1038/385718a0.
140. Sil, B., Mukherjee, C., Jha, S., Mitra, A., 2015. Metabolic shift from withasteroid formation to phenylpropanoid accumulation in cryptogein-cotransformed hairy roots of *Withania somnifera* (L.) Dunal. *Protoplasma* 252, 1097–1110. doi:10.1007/s00709-014-0743-8.
141. Silva, G.J., Medeiros Souza, T., Barbieri, R.L., Costa de Oliveira, A., 2014. Origin, domestication, and dispersing of Pear (*Pyrus* spp.). *Adv. Agric.* 2014, ID article 541097. doi:10.1155/2014/541097..
142. Singh, K.P., Singh, A., Singh, U.P., 2015. Phenolic acid content of some apple cultivars with varying degrees of resistance to apple scab. *Int. J. Fruit Sci.* 15, 267–280. doi:10.1080/15538362.2015.1022113.
143. Singleton, V.L., Orthofer, R., Lamuela-Raventós, R.M., 1999. [14] Analysis of total phenols and other oxidation substrates and antioxidants by means of folin-ciocalteu reagent. pp. 152–178. doi:10.1016/S0076-6879(99)99017-1.
144. Sircar, D., Gaid, M., Chizzali, C., Reckwell, D., Kaufholdt, D., Beuerle, T., Broggin, G. a. L., Flachowsky, H., Liu, B., Hänsch, R., Beerhues, L., 2015. Biphenyl 4-

- hydroxylases involved in aucuparin biosynthesis in Rowan and Apple are CYP736A proteins. *Plant Physiol.* 168, 428–442. doi:10.1104/pp.15.00074.
145. Sircar, D., Mitra, A., 2008. Evidence for p-hydroxybenzoate formation involving enzymatic phenylpropanoid side-chain cleavage in hairy roots of *Daucus carota*. *J. Plant Physiol.* 165, 407–414. doi:10.1016/j.jplph.2007.05.005..
146. Sircar, D., Mukherjee, C., Beuerle, T., Beerhues, L., Mitra, A., 2011. Characterization of p-hydroxybenzaldehyde dehydrogenase, the final enzyme of p-hydroxybenzoic acid biosynthesis in hairy roots of *Daucus carota*. *Acta Physiol. Plant.* 33, 2019–2024. doi:10.1007/s11738-011-0723-y.
147. Sircar, D., Roychowdhury, A., Mitra, A., 2007. Accumulation of p-hydroxybenzoic acid in hairy roots of *Daucus carota*. *J. Plant Physiol.* 164, 1358–1366. doi:10.1016/j.jplph.2006.08.002.
148. Smith-Becker, J., Marois, E., Huguet, E.J., Midland, S.L., Sims, J.J., Keen, N.T., 1998. Accumulation of salicylic acid and 4-hydroxybenzoic acid in phloem fluids of cucumber during systemic acquired resistance is preceded by a transient increase in phenylalanine ammonia-lyase activity in petioles and stems. *Plant Physiol.* 116, 231–8.
149. Sophos, N.A., Vasiliou, V., 2003. Aldehyde dehydrogenase gene superfamily: the 2002 update. *Chem. Biol. Interact.* 143–144, 5–22.
150. Stadler, R., Zenk, M.H., 1993. The purification and characterization of a unique cytochrome P-450 enzyme from *Berberis stolonifera* plant cell cultures. *J. Biol. Chem.* 268, 823–31.
151. Teotia, D., Saini, S.S., Gaid, M., Beuerle, T., Beerhues, L., Sircar, D., 2016. Development and validation of a new HPLC method for the determination of biphenyl and dibenzofuran phytoalexins in Rosaceae. *J. Chromatogr. Sci.* 54, 918–922. doi:10.1093/chromsci/bmw019.
152. Termentzi, A., Kefalas, P., Kokkalou, E., 2008. LC–DAD–MS (ESI+) analysis of the phenolic content of *Sorbus domestica* fruits in relation to their maturity stage. *Food Chem.* 106, 1234–1245. doi:10.1016/j.foodchem.2007.07.021.
153. Thakur, A., Dalal, R.P.S., Navjot, 2008. Micropropagation of pear (*Pyrus* spp.): a review. *Agric. Rev.* 29, 260–270.

154. Turkoglu, A., Duru, M.E., Mercan, N., Kivrak, I., Gezer, K., 2007. Antioxidant and antimicrobial activities of *Laetiporus sulphureus* (Bull.) Murrill. Food Chem. 101, 267–273. doi:10.1016/j.foodchem.2006.01.025.
155. USDA, National Agriculture Library, “National Nutrient Database for Standard Reference,” 2012, <http://ndb.nal.usda.gov>.
156. Van Moerkercke, A., Schauvinhold, I., Pichersky, E., Haring, M.A., Schuurink, R.C., 2009. A plant thiolase involved in benzoic acid biosynthesis and volatile benzenoid production. Plant J. 60, 292–302. doi:10.1111/j.1365-313X.2009.03953.x.
157. Vasco, C., Riihinen, K., Ruales, J., Kamal-Eldin, A., 2009. Phenolic compounds in Rosaceae fruits from Ecuador. J. Agric. Food Chem. 57, 1204–12. doi:10.1021/jf802656r.
158. Vavilov, N.I., 1951. The origin, variation, immunity and breeding of cultivated plants. Soil Sci. 72.
159. Vernon, D.M., Bohnert, H.J., 1992. A novel methyl transferase induced by osmotic stress in the facultative halophyte *Mesembryanthemum crystallinum*. EMBO J. 11, 2077–85.
160. Verberne, M. C., Hoekstra, J., Bol, J. F., Linthorst, H. J. M., 2003. Signaling of systemic acquired resistance in tobacco depends on ethylene perception. The Plant Journal: For Cell and Molecular Biology, 35(1), 27–32. Retrieved from <http://www.ncbi.nlm.nih.gov/pubmed/12834399>
161. Verpoorte, R., van der Heijden, R., Hoge, J.H.C., Ten Hoopen, H.J.G., 1994. Plant cell biotechnology for the production of secondary metabolites. Pure Appl. Chem. 66. doi:10.1351/pac199466102307.
162. Villarino, M., Sandín-España, P., Melgarejo, P., De Cal, A., 2011. High chlorogenic and neochlorogenic acid levels in immature peaches reduce *Monilinia laxa* infection by interfering with fungal melanin biosynthesis. J. Agric. Food Chem. 59, 3205–3213. doi:10.1021/jf104251z.
163. Villalta, O.N., Washington, W.S., McGregor, G., 2004. Susceptibility of European and Asian pears to pear scab. Plant Protection Quarterly 19: 2-4

164. Visweswari, G., Christopher, R., Rajendra, W., 2013. Phytochemical screening of active secondary metabolites present in *Withania somnifera* root: role in traditional medicine. *Int. J. Pharm. Sci. Res.* 4, 2770–2776. doi:10.13040/IJPSR.0975-8232.4(7).2770-76.
165. Vrancken, K., Holtappels, M., Schoofs, H., Deckers, T., Treutter, D., Valcke, R., 2013. *Erwinia amylovora* affects the phenylpropanoid-flavonoid pathway in mature leaves of *Pyrus communis* cv. Conférence. *Plant Physiol. Biochem.* PPB 72, 134–44. doi:10.1016/j.plaphy.2013.03.010.
166. Wagner, C., Sefkow, M., Kopka, J., 2003. Construction and application of a mass spectral and retention time index database generated from plant GC/EI-TOF-MS metabolite profiles. *Phytochemistry* 62, 887–900.
167. Walters, D., Raynor, L., Mitchell, A., Walker, R., Walker, K., 2004. Antifungal activities of four fatty acids against plant pathogenic fungi. *Mycopathologia* 157, 87–90.
168. Weeden, N.F., Lamb, R.C., (1987). Genetics and linkage analysis of 19 isozyme loci in apple. *J. Am. Soc. Hortic. Sci.*
169. Widhalm, J.R., Dudareva, N., 2015. A familiar ring to It: biosynthesis of plant benzoic acids. *Mol. Plant* 8, 83–97. doi:10.1016/j.molp.2014.12.001.
170. Wildermuth, M.C., 2006. Variations on a theme: synthesis and modification of plant benzoic acids. *Curr. Opin. Plant Biol.* 9, 288–96. doi:10.1016/j.pbi.2006.03.006.
171. Wolska, K.I., Grudniak, A.M., Fiecek, B., Kraczkiewicz-Dowjat, A., Kurek, A., 2010. Antibacterial activity of oleanolic and ursolic acids and their derivatives. *Cent. Eur. J. Biol.* 5, 543–553. doi:10.2478/s11535-010-0045-x.
172. Yazaki, K., Heide, L., Tabata, M., 1991. Formation of p-hydroxybenzoic acid from p-coumaric acid by cell free extract of *Lithospermum erythrorhizon* cell cultures. *Phytochemistry* 30, 2233–2236. doi:10.1016/0031-9422(91)83620-Z.
173. Zbigniew, S., Beata, Ż., Kamil, J., Roman, F., Barbara, K., Andrzej, D., 2014. Antimicrobial and antiradical activity of extracts obtained from leaves of three species of the genus *Pyrus*. *Microb. Drug Resist.* 20, 337–43. doi:10.1089/mdr.2013.0155.
174. Zhang, Y., Mao, L., Wang, H., Brocker, C., Yin, X., Vasiliou, V., Fei, Z., Wang, X., 2012. Genome-wide identification and analysis of grape aldehyde dehydrogenase (ALDH) gene superfamily. *PLoS One* 7, e32153. doi:10.1371/journal.pone.0032153.

7. Publications

A. Research papers

1. **Saini, S.S.**, Teotia, D., Gaid, M., Thakur, A., Beerhues, L., Sircar, D., 2017. Benzaldehyde dehydrogenase-driven phytoalexin biosynthesis in elicitor-treated *Pyrus pyrifolia* cell cultures. *J. Plant Physiol.* 215, 154–162. doi:10.1016/j.jplph.2017.06.004.
2. Teotia, D., **Saini, S.S.**, Gaid, M., Beuerle, T., Beerhues, L., Sircar, D., 2016. Development and validation of a new HPLC method for the determination of biphenyl and dibenzofuran phytoalexins in Rosaceae. *J. Chromatogr. Sci.* 54, 918–922. doi:10.1093/chromsci/bmw019.

B. Book Chapter:

1. Juneja, K., **Saini, S.S.**, Gaid, M., Beerhues, L., Sircar, D., 2016. Production of life-saving drugs from Himalayan herbs. In: P. Mandal and A.K. Dalai (Eds). *Sustainable utilization of natural resources*, CRC Press, ISBN 9781498761833.

C. Conference Paper/Poster:

1. Sircar, D., **Saini, S.S.**, 2015. Metabolomics and functional genomics approach to decipher disease resistance mechanism in apple against scab disease. International Conference on Molecular Signalling- Recent Trends in Biosciences, Department of Zoology, Shilong, Guwahati (India), November 2015, IL-II-4. [Oral Presentation]
2. Sircar, D., **Saini, S.S.**, 2016. Development of plant natural product –based topical haemostatic agents for rapid wound sealing and healing. XV Annual convention of ISVPT, NDRI, Karnal, Haryana (India) January 2016.[Oral Presentation].
3. **Saini, S.S.**, Sircar, D., 2015. Metabolomics approach for novel drug discovery against metabolic disorder from in vitro plant of *Swertia chirata*. International Conference on

Molecular Signaling- Recent Trends in Biosciences, Department of Zoology, NEHU, Shilong, Guwahati(India).November2015, PP-62.[Poster Presentation].

- 4. Saini, S.S.,** Sircar, D., Thakur, A., 2014. Secondary metabolite contents and antioxidant capacities of *Pyrus pyrifolia* (Asian pear) callus. International Conference on Molecular Signaling– Recent Trends in Biomedical and Translational Research, Department of Biotechnology, IIT Roorkee, Roorkee (India), December 2014, PP- 57.[Poster Presentation]

